Gene Editing for Duchenne Muscular Dystrophy

by

Jacqueline Robinson-Hamm

Department of Biomedical Engineering
Duke University

Date: 3 July 2018
Approved:

_____
Charles Gersbach, Supervisor

_____
Nenad Bursac

_____
Dwight Koeberl

_____
Barry Myers

_____
George Truskey

Dissertation submitted in partial fulfillment of
the requirements for the degree of Doctor
of Philosophy in the Department of
Biomedical Engineering in the Graduate School
of Duke University

2018

ABSTRACT

Gene Editing for Duchenne Muscular Dystrophy

by

Jacqueline Robinson-Hamm

Department of Biomedical Engineering
Duke University

Date: 3 July 2018
Approved:

_____
Charles Gersbach, Supervisor

_____
Nenad Bursac

_____
Dwight Koeberl

_____
Barry Myers

_____
George Truskey

An abstract of a dissertation submitted in partial fulfillment of the requirements for the degree of Doctor of Philosophy in the Department of Biomedical Engineering in the Graduate School of Duke University

2018

Abstract

Duchenne muscular dystrophy (DMD) is a muscle wasting disease that results from a lack of dystrophin protein, which is an essential musculoskeletal protein. Patients are typically non-ambulatory by their teenage years and suffer prematurely fatal respiratory and/or cardiac complications by the third decade of life. DMD is caused by deleterious mutations in the dystrophin gene, which creates an out-of-frame shift leading to a lack of dystrophin protein and manifestation of DMD. Although scientists have had an understanding of the genetic basis of DMD for decades there has been only modest advancement in improving quality of life for these patients.

Becker muscular dystrophy (BMD) is an allelic disease; BMD is also caused by mutations in the dystrophin gene, although these mutations maintain the translational reading frame and thus a truncated, partially functional dystrophin protein is created. BMD patients have a wide range of symptoms, but BMD typically has much less severe symptoms than DMD. Thus, a common approach to creating a therapy for DMD is to shift the DMD genotype to a BMD genotype. One therapy targeting the genetic cause of the DMD by shifting the messenger RNA (mRNA) and thus protein product to one of BMD has been conditionally approved by the US Food and Drug Administration (FDA), but the treatment is transient and thus far has not demonstrated reliable clinical benefit. DMD presents some unique challenges for developing gene therapies. First, the full-

length gene is so large that exogenous delivery in size restricted viral vectors is not an option. Second, popular strategies being explored are transient and would require lifelong administration. The work presented in this dissertation utilized gene editing technology. Building on prior proof-of-concept studies, we show a CRISPR-Cas9 system utilizing *Staphylococcus aureus* Cas9 (SaCas9) can be used to create permanent changes to the dystrophin gene. This technique overcomes the main challenges presented, as editing the native locus does not require delivering the gene exogenously, and CRISPR-Cas9 mediated DNA double stranded breaks result in permanent changes of the genome. Here we further the proof-of-concept body of work for utilizing CRISPR-Cas9 to treat DMD by targeting exon 51 for excision in a humanized mouse model.

Initially, we recognized the need for a relevant small animal model. A majority of DMD *in vivo* work is done in the *mdx* mouse or variants of the *mdx* mouse, which contains a mutated mouse dystrophin gene such that it does not produce dystrophin protein and displays a mild dystrophic phenotype. While this is a useful research tool, in order to move genome editing closer to the clinic we need to be able to test guide RNAs (gRNAs) that target the human dystrophin gene in a small animal model. As the gRNAs target exact sequences of the genome they must be designed to the human *DMD* gene. These human *DMD* targeting gRNAs would not match the mouse *Dmd* gene, and thus there was a clear need for a preclinical humanized small animal model of DMD. We obtained an hDMD/*mdx* mouse that contains the full-length, healthy, wild type human

DMD gene on mouse chromosome 5. Although this mouse has the human *DMD* gene, it is ultimately a healthy mouse. Thus, we utilized *Streptococcus pyogenes* CRISPR-Cas9 (SpCas9) to excise exon 52 of the human *DMD* gene in the mouse zygotes. We identified a founder mouse that lacked exon 52 in the genomic DNA (gDNA) and bred that mouse with the *mdx* mouse line. Thus, using genome editing, we created the hDMDΔ52/*mdx* mouse, which lacks both human and mouse dystrophin protein expression. We confirmed this biochemically by sequencing the gDNA to ensure lack of exon 52 between the gRNA targeted sites, lack of exon 52 in the cDNA, and lack of dystrophin protein by both immunohistochemistry (IHC) staining and Western blot. The hDMDΔ52/*mdx* mouse also displayed a mild dystrophic phenotype compared to its healthy counterpart, the hDMD/*mdx* mouse. We have characterized this hDMDΔ52/*mdx* mouse and shown it lacks dystrophin and has a mild dystrophic phenotype, and this mouse will be a meaningful tool for testing potential DMD therapies.

Next, we created a CRISPR-SaCas9 system that would target the human *DMD* gene for exon 51 excision. While our lab has previously shown efficacy of this method utilizing SpCas9, we switched to the smaller SaCas9 in order to better accommodate the small packaging limit of adeno-associated virus (AAV). gRNAs were designed to target conserved regions in the intronic area flanking exon 51 of dystrophin in both humans and rhesus macaques. gRNAs were tested individually for on-target activity in HEK293T cells and those with on-target activity were assessed for off-target activity *in*

silico. One gRNA upstream of human dystrophin exon 51 and one gRNA downstream of exon 51 were selected based on distance from the exon, percent modification measured by the Surveyor nuclease assay, and potential for off-target activity in humans and rhesus macaques. Those chosen two gRNAs were tested as a deletion pair in both HEK293T cells and immortalized myoblasts from a DMD patient, lacking exons 48 through exon 50 that is correctable by removing exon 51, and shown to create the desired deletion. Currently there is a lack of rules about what makes an effective gRNA, and in particular even the length of the gRNA protospacer sequence for SaCas9 can have effects on on-target activity. Thus, the two chosen gRNAs were tested with protospacer lengths varying from 19 to 23 base pairs (bp) both individually and as deletion pairs in HEK293T cells. The most effective on-target pair was with both gRNA protospacer sequences at 23 bp long. These 23 bp length gRNAs were re-tested in HEK293T cells and DMD patient immortalized myoblasts and shown to be effective at creating deletions in the genome, having that edit carry over in the mRNA of differentiated myoblasts resulting in the loss of exon 51 and the junction of exon 47 to exon 52 when Sanger sequenced, and restored dystrophin protein expression in the differentiated myoblasts by Western blot. Off-target sequences of these 23 bp length protospacers were assessed *in silico* and ten of the predicted off-target sites for each gRNA were tested *in vitro* in HEK293T cells by deep sequencing. Although the upstream gRNA did have two off-target sites that had notable small insertion or deletion (indel) rates measured by treated

gDNA/untreated gDNA, ultimately all measurable off-target activity was at least two orders of magnitude lower than the on-target rate of indel formation.

Finally, we created a CRISPR-SaCas9 system with gRNAs that target human *DMD* for exon 51 removal, and these exact gRNAs tested *in vitro* were tested *in vivo* in our previously characterized hDMDΔ52/*mdx* mouse. Initially we did a small proof-of-concept study by packaging our system in AAV8 and performed local injections into the tibialis anterior (TA) muscle of adult hDMDΔ52/*mdx* mice. 8 weeks after treatment the TA was analyzed. We noted deletion of exon 51 between the gRNA targeted sites in the gDNA, as well as dystrophin protein restoration by IHC and Western blot. While promising, DMD is a systemic disease that affects all skeletal and cardiac muscles. Thus, we next delivered our CRISPR-SaCas9 system using AAV9 systemically by tail vein injections in adult hDMDΔ52/*mdx* mice or temporal vein injections in neonatal hDMDΔ52/*mdx* mice. At 16 weeks of age mice were sacrificed for biochemical analysis. Deep sequencing of gDNA at each gRNA target site showed measurable indel formation above the limit of detection in all tissues assayed in mice treated as both adults and neonates. There were a few trends that emerged in this data and hold true throughout analysis of on-target editing: the upstream gRNA is generally more effective at on-target activity than the downstream gRNA, the mice treated as neonates show more on-target activity than mice treated as adults, and there is much more on-target activity in the heart than in the skeletal muscles. Indels are a measure of on-target activity, but we

delivered a system to create a deletion and not just individual cuts. Thus, gDNA from the heart and TA of mice treated as adults was assayed by linear amplification sequencing, which revealed approximately 4% deletions of exon 51 in gDNA from the heart and about 1% deletions of exon 51 in gDNA from the TA. Through this method we are also investigated inversions of the targeted sequence and AAV integrations into the targeted cut site, both of which were much more prominently present in the heart gDNA than the TA gDNA. Confident we were able to edit the genome at low, although measurable, levels, we examined changes in mRNA. In the mRNA from hearts of both mice treated as adults and neonates we see clear deletions of exon 51 by endpoint polymerase chain reaction (PCR). Sanger sequencing the deletion band revealed the exact junction of exon 50 to exon 53 as expected. We performed quantitative droplet digital PCR (ddPCR) on cDNA from the heart, TA, diaphragm, and gastrocnemius, and similar to the indel formation we saw the highest amount of exon 51 deletions in the heart cDNA at about 20% in both mice treated as adults and neonates. The deletions in skeletal muscles varied from about 0.15% to about 1.5% and were all measurable above the limit of detection as defined by the average of samples from untreated mice. Lastly, we examined dystrophin protein expression. By Western blot we saw mouse to mouse variability in intensity, but largely some degree of dystrophin protein expression restoration in protein extracted from hearts and gastrocnemius muscles from mice treated as both adults and neonates, although qualitatively the mice treated as neonates

have more dystrophin protein expression than those treated as adults. IHC on hearts and TA muscle sections similarly showed variable but nonetheless present dystrophin protein expression restoration in both mice treated as adults and neonates. Consistent with prior data, we saw more dystrophin expression in the heart than in the TA, and this difference is exacerbated in the mice treated as adults.

In sum, the objective of this dissertation was to create a clinically relevant CRISPR-SaCas9 system and test it *in vitro* and *in vivo* in a diseased humanized mouse model. This work is an incremental step to propel forward methods to permanently correct the dystrophin gene by gene editing technology to treat DMD. We created a useful mouse model for the field to test preclinical therapies *in vivo* and make the most of the rapidly advancing gene editing tools. Collectively this work is significant in extending early proof-of-principle studies to a translational strategy for gene editing as a potential treatment for DMD.

Dedication

To all of those who could do better than I if only given the opportunity: may society recognize your value and serve you better with each passing day.

"Everybody knows that you'd break your neck to keep your chin up" ~ Copeland

Contents

List of Tables

List of Figures

List of Abbreviations

6MWT, 6MWD	Six-minute walk text, six-minute walk distance
AAV	Adeno-associated virus
AONs	Antisense oligonucleotides
BMD	Becker muscular dystrophy
bp	Base pair (of DNA)
Cas9	CRISPR associated protein 9
cDNA	Complementary DNA
CIP	Alkaline phosphatase, calf intestinal
CK	Creatine kinase
CRISPR	Clustered Regularly Interspaced Short Palindromic Repeat
ddPCR	Droplet digital PCR
DMD	Duchenne muscular dystrophy
DMD	The human dystrophin gene
Dmd	The mouse dystrophin gene
FDA	United States Food and Drug Administration
gDNA	Genomic DNA
gRNA	Guide RNA
hCas9	Human codon optimized SpCas9

HDAC	Histone deacetylase
IHC	Immunohistochemistry
Indel	Insertion or deletion of bps in the genome
kb	Kilobase
LAM-HTGTS	Linear Amplification-Mediated High-Throughput Genome-wide Translocation Sequencing
mRNA	Messenger RNA
NHEJ	Non-homologous end joining
nNOS	Neuronal nitric oxide synthase
PAM	Protospacer adjacent motif
PCR	Polymerase chain reaction
SaCas9	*Staphylococcus aureus* Cas9
SpCas9	*Streptococcus pyogenes* Cas9
TA	Tibialis anterior, a muscle in the hindlimb

Acknowledgements

To my committee: Dr. Charlie Gersbach, Dr. Nenad Bursac, Dr. Barry Myers, Dr. Dwight Koeberl, and Dr. George Truskey, thank you for expanding the multitude of ways in which I think about this work and for your scientific guidance throughout the years. Further thanks to Dr. Annemieke Aartsma-Rus who was also very generous in her scientific help, always answering questions without hesitation.

Dr. Dave Ousterout: very simply put I would not be here without you. Knowing I would likely be paired with you if I were to attend Duke, I took great stock in your personality during my interview weekend. I knew we'd get along swimmingly and I am so grateful for all of your mentorship and support over the years. This past year you have been especially vital for my sanity and navigating the end phase of my PhD. I don't really understand why you don't like Harry Potter as much as you should, and your sports teams loyalties are borderline atrocious, but you are the big brother I always wish I had and I hope we share a lifetime of borderline rude jabs at each other.

Drs. Pratiksha Thakore, Ami Kabadi, Lauren Toth, and Tyler Gibson: you created a lab culture that was easy to enjoy. I looked forward to coming in and working those long hours (most days). You all, Dave, and Dewran really fostered something special and I am glad to have taken part. I cannot put enough emphasis on how vital it was to have such a supportive group around during my early grad school years. I knew you

were always there for me scientifically and personally, and I still feel that way today. Some of my fondest Durham memories are centered around you. Girls night at Lauren's, dating woes, hair dyeing talks, and adult night at the museum with Ami, the best puns and sad kid holidays hosted and organized by Pratiksha, and daily reminders to be engaged in the world outside of lab with the best desk buddy Tyler. You all shared such great perspective and wisdom with me and I truly missed your presence in lab after you all kicked butt and went on to bigger and better things. I miss you all dearly, but am so thrilled to watch your lives continue to blossom.

Josh and Tyler, the best bay mates. Josh "JBaby" "Grumbles" Black: I could not have picked a better cohort-mate to share this journey with if I tried (except maybe Brian… just kidding!). We balance each other perfectly and your calm but determined attitude is inspiring. Hopefully you will resume participation in yearly hockey trip as that would be very cute. Have fun in your math class—can't wait to hear about how terrible that is. You are brilliant and level-headed and you will succeed in any realm you choose – I can't wait to see where your future takes you, perhaps back to being a Flyers fan. Tyler Klann: Please never stop sending me amazing animal videos/gifs. You have a wicked sense of humor that always made our bay the place to be. Stop working so much, get a pupper, and let me know when you want to play Super Mario Party together. You are such a hard worker and have such great intuition about how to make

things work; I know your future holds big ups for you and I can't wait to see where your life takes you.

Dr. Chris Nelson: You are so kind, capable, and hard-working. We have worked very closely together for four years and every day I thank my lucky stars that I got to work with someone as easy going and exceptionally bright as you. Apologies for leaving so many loose ends untied for you to inevitably end up dealing with. You are going to be a great professor at Arkansas and I will try to usher any bright students I meet your way. More or less anything that Dave didn't teach me you did, I am happy to have gone on this journey with you so very present.

The rest of the Gersbach lab: thanks for making lab so weird; sometimes that was great, occasionally it was awful, but it always gave me something to talk about to my friends outside of academia. Dewran: I will miss our weird eye sessions, also bless you. Veronica: You are a talented scientist and a wonderful person. I am glad to leave DMD in your capable hands.

Dr. Cristina Fernandez and Dr. Katie Glass: you both welcome me into your friend group with open arms and mentored me in uncountable ways. I am so thankful for all the social outings and text messages where you reminded me to keep my cool. You're both wise beyond your years and have such a calmness in the way you tackle problems. It is inspirational, and I look up to you more than you know. In struggles and

happiness you are both always there to answer my call, and I can't even begin to explain how much that is worth to me.

Dr. Brian Crouch: I did not come to grad school looking or expecting to make a best friend, yet here we are. I could write pages about you, but I will settle for sentences instead. I can't wait for continued yearly hockey trip (with more money to spend!), and after we conquer all the arenas surely, we'll find another adventure to go on. You have saved me so many times… I stopped counting long ago. I don't know how I would've done this grad school journey without you, and I certainly am not going to even bother trying to imagine such a horrid scenario. The island is going to be amazing and remember that you are the sun. *"Together we're unlimited" ~ Wicked.*

While lab and the biomedical engineering department is where I spent most of my time at Duke, I found my home outside of this in organizations full of people who want to bring change to the world. Women in Science and Engineering (WiSE) has truly been my home at Duke. Dr. Brittany Morgan and Caroline Amoroso: for three years we've kept in constant touch through all the chaos. Multiple times you've stopped me from rage quitting and hugged me through tears. Fate put us together (really Caroline did I think, ha!) and I never want to be without you fierce women. Dr. Julia Johnson, Paige Daniel, Dr. Candise Henry, Dr. Emily Boehm, and Dr. Katie Bitting: you have all also provided immeasurable support. Having a network of wonderful women like you has gotten me through the tough times, and it's been a bigger pleasure to celebrate the

great times. I would really like to have yearly(-ish) "Doctorettes" where we all get together for a weekend and celebrate our accomplishments, as amongst this talented and caring group those accomplishments are many and will continue to grow over the years. *"To my galaxy of women – thank you for the nurture" – Orphan Black.*

To all of those trying to make Duke and the world a better place: thank you for all of your time and effort you put into causes much bigger than yourselves. As individuals or as groups, such as the Duke Graduate Students Union and the active folks in GPSC, I know you are making incremental progress that will result in lasting change. To those students willing to speak their mind, even if it's unpopular opinion, to the folks with power – keep on keeping on. In particular to Colleen McClean who is an inspiration. We are quite different, but in the best of ways, and you always challenge me to be my best. Keep fighting the good fight, your hard work and dedication to movements bigger than just your dissertation will shape the future.

I started my scientific career at the University of Washington and I owe a lot of my success to folks in the Department of Bioengineering there. Dr. Sarah Chamberlain: you were an excellent mentor and set me down this path with realistic expectations. Drs. Mike Regnier, Dave Marcinek, and Glen Banks: thank you for taking me under your wing, teaching me how to think critically, and teaching me a lot about mice as that proved very useful in my PhD. Dr. Dan Ratner and Dr. Alyssa Taylor: you both taught me so much about teaching, mentoring, and critical thinking and have always been so

generous with your advice regarding my PhD or life. You deserve so much credit for the person I am today. Beth Gay, Greg Carey-Medlock, and Will Lykins: you are genuinely all outstanding people, and I feel lucky to have ever mentored you in any small way. You're all going to go on to do amazing things and I hope to continue to catch snippets of your success.

While I owe much credit to the scientific and emotional support I've gained from the above folks, credit is also due to a wealth of potentially unexpected sources. To Katie Swore, Barbara DeFlaviis, and Misty Pidgeon, and the entire team at the North Carolina Center for Physical Therapy: thank you for literally helping me walk again… twice! As well as for making PT an enjoyable, albeit usually painful, place to come anywhere from 1 to 3 times a week. Bubble graduation was a highlight I will never forget. To Jack in Twinnies for always having a raspberry crunch bar ready when I'm having one of those days, and to NanaTaco for the nourishment and never judging my need for double rice, no beans, and extra chips.

To my trauma therapist: without you I don't know if I would be here today. You have helped me process so much, most importantly that I matter. I am still working on that, but that seed you planted grows a bit every day.

To my best friends: Kyla Williams, Kaylee Royer, Katie Spence, and Katie Truong: thank you for always being there through the mundane to the intense times. You mean the world to me.

xxx

Finally, to Adam and the Bush and Schwartz families for taking me in so generously. Mostly for not asking "when are you going to graduate?" or "what classes are you taking?" too often. Adam – thank you for the endless laughs, 95% of my meals, adventures (Pokemon related or otherwise), and magic. I don't understand how you put up with dating a grad student for four years, but I am so thankful and lucky you did. Thank you for driving me to and from lab for all the late-night cultures and vivarium checks, and for that one time you help me aliquot some reagents and learned to pipette you can have 0.0001% credit for this dissertation. Thank you for bringing Growlie into our lives, as the knee licks and snuggles surely have healing properties. And while you couldn't help me scientifically, you always help me emotionally. You keep me stable, sane, and fed. I love you.

I do not possess rose-colored glasses. I don't look back fondly on times that were brutal. This chapter in my life has easily been the worst, but I know the only reason I am able to end this chapter and start a new one is due to the outpouring of love and support from my friends and colleagues. Graduate school is extremely isolating, and at a time where my mental health was at its worst I was fortunate enough to have loved ones who would check up on me. It makes the world of difference to know you have people you can count on, who are always in your corner, and who will not only answer your call for help but actively check on you to see if you need help without having to ask. I know I

would not have my PhD if my support network didn't reach out and offer encouragement. For these little daily acts of kindness, I am truly grateful to you all.

Chapter 1. Introduction

1.1 Rationale and Significance

Duchenne muscular dystrophy is a prematurely fatal disease with no curative treatment. This X-linked disease affects about 1 in 5000 male births and is the result of deleterious mutation(s) in the *DMD* gene that was uncovered thirty years ago[1, 2]. These mutations lead to an absence of the dystrophin protein, which results in progressive muscle wasting that ultimately leads to death in the third decade of life typically from respiratory and/or cardiac complications. The current standard of care, while it has progressed over the years and been shown to elongate life, is largely palliative as it does not focus on the genetic cause of the disease. An allelic disease, Becker muscular dystrophy, often displays significantly less severe phenotypes, and thus it is a common strategy to try to shift the DMD genotype to a BMD genotype in order to in theory also shift symptoms to be less acute and improve expected lifetime and quality of life.

Many therapies are in development to treat DMD. Although the lead candidate for a DMD treatment is exon skipping, clinical trial results from these treatments still lead to an overall decline in ambulation[3, 4]. Partial dystrophin restoration is promising, but there are several limitations such as poor delivery of oligonucleotides to the heart and the need for lifetime re-administration[5-7]. The FDA Advisory Committee advised for rejected approval for both lead exon skipping candidates, drisapersen and eteplirsen,

based on lack of efficacy, although eteplirsen was eventually granted conditional approval. *Ex vivo* gene therapy approaches show promise, but may be limited therapeutically due to poor *in vivo* engraftment, survival of genetically modified cells, and the systemic nature of DMD[8-16]. Plasmid-mediated gene transfer is being investigated, but low efficiency of delivery and transient expression are of concern[17-19]. Efficiency can be improved by viral delivery[20]. Adenovirus can package the entire dystrophin cDNA, however the potent immune response *in vivo* to adenovirus is troublesome and will likely limit the widespread use of adenovirus in a systemic gene therapy context. Delivering the complete dystrophin gene, as in classical gene therapy, with size-restricted viral vectors is not currently feasible as the full-length dystrophin cDNA is 14 kb[21]. Thus, various truncated dystrophin cDNAs, coined minidystrophin and microdystrophin, have been tested using AAV and result in improved force generation[22-30]. There is evidence that truncated dystrophins improve cardiomyopathy in the *mdx* mouse[31-33], however this treatment may not mitigate myocardial fibrosis[31]. Thus, while proven successful in various animal models for restoring function in skeletal muscle, it is unclear whether these truncated versions of dystrophin will be effective in treating DMD-related cardiomyopathy in humans as they do not possess the full wild type functionality. Further, vector loss over time may be problematic for AAV-delivered minidystrophin and microdystrophin. However, AAV is a promising delivery method

as many muscle-tropic serotypes exist[34-39] and the first FDA approved gene therapy, Spark Therapeutics' Luxturna, utilizes AAV[40]. Current strategies to treat DMD with gene therapy rely on exogenous transgene delivery or require re-administration of a transient treatment, and thus have safety and practicality concerns. Our approach aims to correct the endogenous *DMD* gene permanently after one treatment utilizing the gene editing tool CRSIPR-Cas9 and this method is potentially curative. The overall objective of this work was to develop a CRISPR-Cas9 system suitable to be translated to humans to remove exon 51 in the *DMD* gene by creating and characterizing a humanized mouse model of DMD and testing a CRISPR-Cas9 system both *in vitro* and *in vivo* for excision of exon 51.

1.2 Specific Aims

Aim 1: Creation and Characterization of a Humanized Diseased Mouse Model of Duchenne Muscular Dystrophy

The hDMD/*mdx* mouse[41], which contains full-length wild type human *DMD* on mouse chromosome 5, was obtained from the Leiden University Medical Center. This mouse was mated, and the zygotes were injected with a CRISPR-SpCas9 system with two gRNAs targeted to the intronic region flaking human *DMD* exon 52. Resulting founder pups that lacked exon 52 were identified by PCR genotyping and bred to *mdx* mice. hDMDΔ52/*mdx* (het;hemi) mice were confirmed to have a loss of exon 52 in both gDNA and cDNA, as well as a loss of dystrophin protein in the heart and TA muscle by

IHC staining and loss of dystrophin protein expression in the TA by Western blot. The phenotype of the mice was assessed by *in vivo* motor function tests and hDMDΔ52/*mdx* mouse has decreased overall activity in an open field as measured by distance moved and rearing postures, as well as decreased grip strength compared to the hDMD/*mdx* mouse. This mouse model contains the human dystrophin gene, which we have mutated to be a relevant DMD genotype. CRISPR-Cas9 systems with gRNAs specific for the human dystrophin gene can now be tested *in vivo* in a diseased small animal model of DMD.

Aim 2: Validation of a CRISPR-SaCas9 System for Deletion of Exon 51 *In Vitro*

Prior work has shown feasibility of removing an exon using two gRNAs and CRISPR-Cas9[42]. Our group and others have demonstrated *in vivo* success when delivering a CRISPR-Cas9 system utilizing AAV[43-47], but these studies were conducted in classic mouse models of DMD. Thus, the gRNAs previously used *in vivo* delivered by AAV target the mouse *Dmd* gene. As gRNAs are specific to exact DNA sequences, further tests for the human gene are required. Our lab has previously shown success excising human dystrophin exon 51 *in vitro* as well as cell implantation of edited cells *in vivo*, but this was achieved utilizing SpCas9[48]. SaCas9 is approximately 1 kb smaller than SpCas9[49], thus looking to the future of creating an all-in-one AAV vector system, as opposed to delivery using two viral vectors, a new CRISPR-SaCas9 system needed to be

tested. Here we show selection and screening of SaCas9 gRNAs that target conserved sequences in the human genome and rhesus macaque genome at the intronic sequences flanking exon 51 of *DMD*. On-target efficacy was evaluated *in vitro* of individual gRNAs by the Surveyor assay, and exon 51 deletion potential was evaluated by endpoint PCR of gDNA and cDNA. gRNAs were tested in both HEK293T cells and immortalized DMD patient myoblasts. After initial gRNA screening, the gRNA protospacer length was varied and re-tested. In this specific genomic context, we found 23 bp gRNAs to be more effective by individual on-target activity and deletion pair efficacy, and thus moved forward with 23 bp length gRNAs. Off-target potential was assessed *in silico* with Cas-OFFinder[50] and investigated with deep sequencing, where there were no major concerns found. In this work we have created a CRISPR-SaCas9 system for deletion of exon 51 and showed on-target efficacy *in vitro* with limited off-target potential.

Aim 3: *In Vivo* Gene Correction of Duchenne Muscular Dystrophy by Deletion of Exon 51 Using CRISPR-SaCas9

Following the work of the first two aims, we have gRNAs that target the human *DMD* gene to excise exon 51 as well as a relevant humanized diseased mouse model. Thus, we packaged our CRISPR-SaCas9 system into AAV and delivered it *in vivo* to hDMDΔ52/*mdx* mice as both neonates and adults. Lack of exon 52 in this mouse shifts the reading frame to out of frame and the mouse produces no dystrophin protein; treatment to remove exon 51, leading to the junction of exon 50 to exon 53, restores the

reading frame and creates a BMD genotype. We first showed proof-of-concept of *in vivo* excision of exon 51 by CRISPR-SaCas9 delivered by AAV8 through local injection into the TA muscle of adult mice. After 8 weeks the TA muscle was analyzed and found to have deletion of exon 51 in the gDNA as well as restored dystrophin protein expression by IHC and Western blot. Next, we aimed for systemic treatment as DMD is a systemic disease. We systemically treated neonatal and adult mice with our AAV9 CRISPR-SaCas9 system. At 16 weeks of age we saw indel formation at both gRNA on-target locations as well as deletions of exon 51 in the cDNA in various muscle tissues. Deletions of exon 51 in the heart were most prevalent, and measurable deletions occurred in skeletal muscles tested. Western blot and IHC confirmed restoration of dystrophin protein expression. Overall, we see higher levels of editing in the heart than skeletal muscle, and in mice treated as neonates compared to those treated as adults. The *in vivo* gene editing rates leave room for improvement, but we do see dystrophin restoration and thus a promising start to a potential therapeutic for DMD.

Chapter 2. Literature Review

2.1 Duchenne and Becker Muscular Dystrophy

2.1.1 Pathology

Duchenne muscular dystrophy and Becker muscular dystrophy are allelic X-linked muscle wasting diseases that are caused by mutations in the dystrophin gene. Mutations in the *DMD* gene in DMD patients lead to a lack of the essential musculoskeletal dystrophin protein, whereas mutations the *DMD* gene in BMD patients maintain the reading frame and thus a truncated but partially functional protein is created (see Figure 1[51]).

DMD affects about 1 in 5000 live male births[52], making it the most common form of muscular dystrophy[53]. DMD is the most severe form of muscular dystrophy[54] and is the most common fatal genetic disease[55]. DMD is diagnosed in early childhood, with a historical mean age of diagnosis of 4 years and eleven months for families without a history of DMD[56]. This average age of diagnosis seems to be dropping after observation of delayed motor milestones such as walking and standing up from sitting[57]. Children also often have a waddling gait and trouble with daily activities such as climbing stairs, jumping, and running. The muscle wasting is progressive, and patients are usually bound to a wheelchair by the age of 12. Muscle wasting continues to progress ultimately leading to premature death due usually due to cardiac and/or respiratory complications

in the third decade of life. A retrospective study of 835 DMD patients showed cardiac related deaths have a mean age of 19.6 years, whereas respiratory related deaths for patients who benefitted from mechanical ventilation was 27.9 years[58].

In contrast, BMD is about 3 times less prevalent than DMD[59] and very mild BMD phenotypes can be as minor as asymptomatic increase in concentration of creatine kinase, a marker of muscle damage, in blood serum, muscle cramps, and presence of myoglobin in the urine[54]. BMD patients lose ambulation anywhere between the late teenage years to mid-life years[60], but may preserve ambulation until after age 60[61]. Cardiomyopathy is the cause of death for about half of all BMD patients[62, 63]. Clinically the distinction between BMD and DMD is defined by ambulation past 16 years of age, which all BMD patients' display. BMD has a later onset of muscle weakness and symptoms may not onset until after age 30. Sometimes weakness of the quadriceps femoris is the only initial sign of muscle weakness. The mean age of death for BMD patients is in the mid-40s[54].

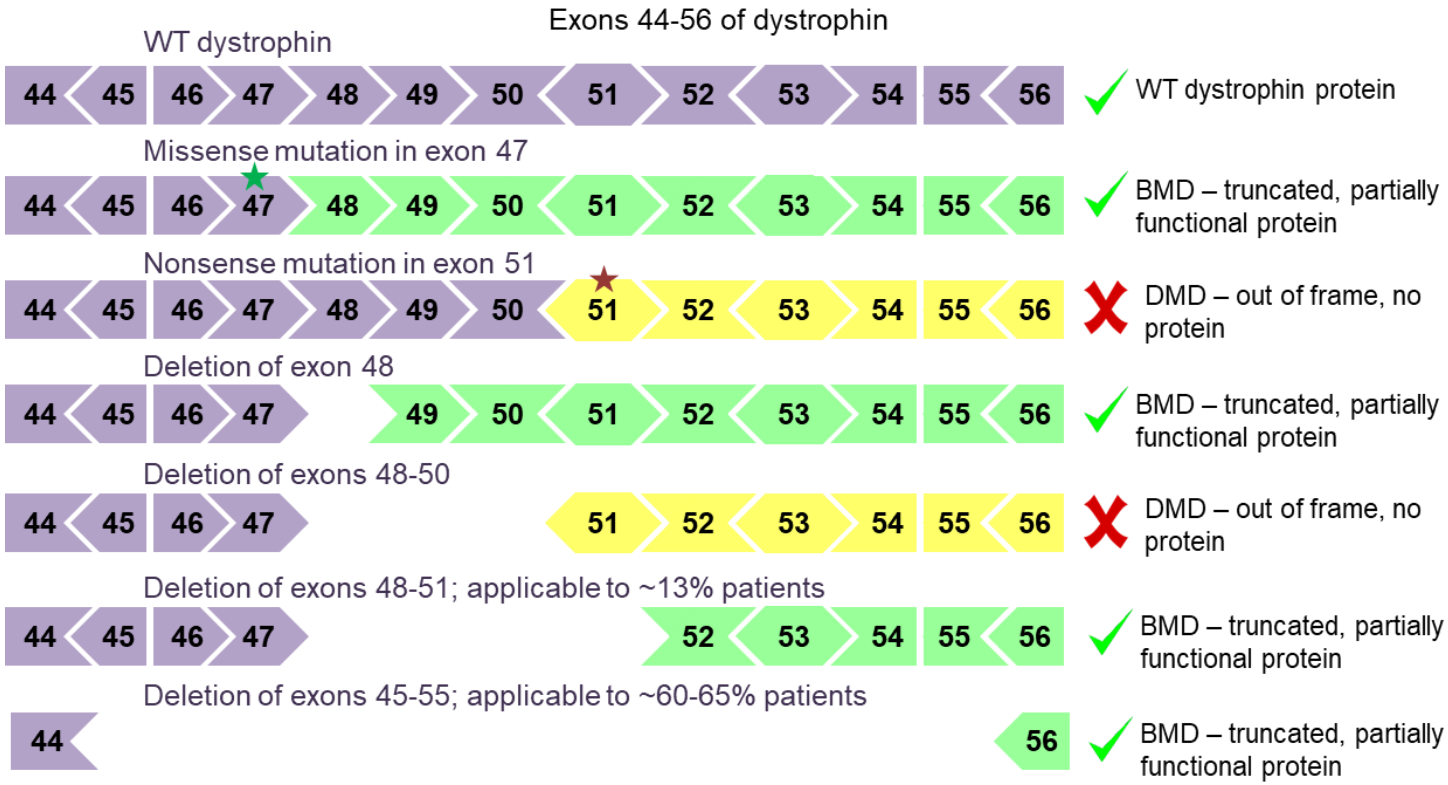

Figure 1: Overview of dystrophin mutations and the BMD or DMD genotypes in the exons 45-55 mutational hotspot region of dystrophin.

2.1.2 The Dystrophin Gene

DMD is the largest known naturally occurring gene made of up about 2.5 million bp of genomic sequence on the X chromosome[64]. Approximately 99% of the gene is made up of introns[64], and the gene contains 79 exons[65]. These exons encode 14,000 bp of messenger RNA. *DMD* can be mutated in an afflicted patient by carrier mothers passing on their mutated DNA or by spontaneous mutation, which occurs in about one-third of cases likely due to the large size of the gene[66] and particularly the large introns[67]. There are many types of mutations possible: deletions of one or more exons are most common, making up about 61% of cases, whereas duplications of exons (9%), nonsense nucleotide changes (16%), nucleotide changes disrupting a splice site (5%), and small insertion or deletion mutations (8%) are generally less common[68]. A majority of exon deletions occur in two mutational "hot spot" regions, exons 45-55 and exons 2-20. If these mutations maintain the reading frame the genotype is one of BMD. However, if the mutations disrupt the reading frame the genotype is that of DMD.

2.1.3 The Dystrophin Protein

The wild type *DMD* gene produces the 427 kilodalton dystrophin protein. Dystrophin is found at the plasma membrane of skeletal and cardiac muscle and some neurons[67]. This protein links the internal cytoskeleton of a cell to the extracellular matrix, and thus plays a structural role. This membrane-spanning protein is essential for membrane stabilization[69] and likely protects the sarcolemma from excessive force during

muscle contraction and relaxation[70]. The protein is organized into four general regions: the actin-binding domain at the N-terminus, the central rod domain, the cysteine-rich domain, and the carboxyl terminal domain. The C-terminus of the dystrophin protein associates with numerous other proteins to create the dystrophin glycoprotein complex. Mutations that cause DMD result in completely absent or extremely reduced levels of dystrophin protein to be produced. When dystrophin is absent the dystrophin glycoprotein complex is destabilized resulting in progressive fiber damage and membrane leakage. The rod domain contains 24 repeating units, called spectrin-like repeats, which account for most of the protein[69]. Loss of exons in the 45-55 hotspot remove part of the repetitive rod domain, whereas loss of exons in the 2-20 hot spot can remove all or some of the actin-binding site with part of the rod domain. Loss of exons in the rod domain have been found to be tolerable without severe pathology, as seen in some BMD patients[69]. BMD patients produce some level of internally truncated, but partially functional dystrophin protein. In particular if the protein created is truncated in the rod region patients can display quite mild phenotypes even with 46% of the coding sequence deleted (exons 17-48)[61]. This specific individual was still ambulatory at 61 years old despite missing almost half of the dystrophin protein.

Dystrophic muscle tissue undergoes continuous cycles of necrosis and regeneration, leading to fibers with centrally located nuclei, increased permeability, and high fibrotic and adipose tissue content. The regenerative capacity of the cell is

eventually lost, likely due to loss of muscle fibers occurring faster than the regenerative ability of the satellite cells, which ultimately leads to muscle necrosis, fibrosis, and loss of muscle function[71]. This process is severe in DMD patients, whereas BMD patients exhibit a wide range of severity of loss of muscle function, but they are typically less acutely impacted than DMD patients.

2.1.4 Standard of Care

Preventative and interventional care for DMD patients has largely been poorly standardized until the past decade[72], although there are some basic measure that have historically been taken. Following initial diagnosis both DMD and BMD patients typically undergo a physical therapy assessment, developmental evaluation to design an individual education plan if needed, cardiomyopathy evaluation, and consultation with a genetic counselor[54]. Generally, both DMD and BMD patients are prescribed ACE inhibitors and/or beta blockers for cardiomyopathy to improve left ventricular function[73-75]. Scoliosis, which is prevalent in non-ambulatory patients, is managed as appropriate, including bracing and surgery[76]. Patients often undergo nutritional assessment, and physical therapy and gentle exercise if possible to promote mobility and prevent contractures. Bone and cardiac health are closely monitored, with a complete cardiac evaluation occurring at least every two years[75]. For DMD patients in particular, respiratory management has been shown to extend life[77-79], and thus respiratory

evaluations during clinic visits are conducted at least every 6 months in non-ambulatory patients[80].

Corticosteroids are often prescribed to DMD patients, whereas the effectiveness in BMD patients is less well understood[54]. Treatment typically begins once motor function plateaus or begins to decline, usually between 4-8 years old in DMD patients. For DMD patients it is thought that prednisone has a stabilizing effect on membranes as well as an anti-inflammatory effect that may be beneficial[81-83]. However, side effects are almost universal including weight gain and behavioral changes[84]. Thus, the dose and frequency with which prednisone is given is often changing. Deflazacort, which has only been available in the United States since 2017, is thought to have fewer side effects, especially weight gain, and may help to decrease the decline of muscle function[85] including helping to preserve pulmonary function[86].

While some interventions and treatments have been shown to prolong life, none of the described standard of care offers hope of a cure. There is a plethora of therapies for DMD, and to a lesser extent for BMD, being investigated including gene therapies that aim to compensate for a lack of dystrophin, and gene and molecular therapies based on restoring dystrophin protein production including cell therapies, exogenous gene delivery, exon skipping, and gene editing.

2.2 Therapies that Compensate for Lack of Dystrophin

2.2.1 Myostatin Inhibition

Myostatin is a member of the transforming growth factor-beta family and a regulator of muscle growth. Inhibition of the myostatin pathway leads to increase in muscle size and strength. Hypertrophy and hyperplasia of the muscle have been shown in mice[87-91], rats[92, 93], dogs[94, 95], cows[96], and non-human primates[91, 97], after myostatin inhibition or knock-out. A recombinant human antibody that binds to myostatin and inhibits its activity[98] is currently being tested in an open-label phase 2 clinical trial (NCT02907619), as well as a phase 2/3 trial testing an anti-myostatin adnectin (NCT03039686). Follistatin is a myostatin antagonist, and thus can also be used to inhibit the myostatin pathway. A modified follistatin can be delivered via AAV; in a phase 1/2a clinical trial for BMD no adverse effects were encountered and 2 out of 3 patients in both the low and high dose cohorts showed improvements in the six-minute walk test (6MWT)[60]. The same treatment is currently being evaluated in 6 DMD patients as a phase 1/2 clinical trial (NCT02354781).

2.2.2 Green Tea Extract

Addition of green tea extract, or specific components of the green tea extract, has been studied in mice and shown to decrease serum creatine kinase levels and preserve some muscle fiber morphology and function[99, 100]. (+)- Epicatechin, an antioxidant that reduces NF-κB pathway signaling[101], is being tested in a phase 1/2 clinical trial

(NCT02964377) for cardioprotective properties[102] and is currently recruiting. Epigallocatechin-Gallate has also been shown to be neuroprotective and is currently being tested in a phase 2/3 clinical trial (NCT01183767).

2.2.3 GALGT2 Gene Transfer

The *GALGT2* gene is known to glycosylate α dystroglycan in skeletal muscle[103, 104] and can induce overexpression of dystroglycan-binding proteins[105] as well as strengthen the extracellular matrix to prevent eccentric contraction-induced muscle injury[106]. Gene transfer of GALGT2 has shown prevention of muscle damage in the *mdx* mouse model of DMD[106]. Further, rhesus macaques treated with an AAV-delivered GALGT2 showed increase expression of dystrophin and laminim α2 surrogate proteins, such as utrophin, plectin1, agrin, and laminin α5[107]. A phase 1/2 clinical trial utilizing AAV delivered GALGT2 is currently recruiting (NCT03333590).

2.2.4 Steroids

Steroid use is generally accepted as part of the standard of care for DMD patients, although the side effects leave vast room for improvement. As previously detailed, breakthrough steroids like deflazacort can have meaningful impact on patient lives. A myriad of improved steroids are being investigated, including vamorolone, which is a glucocorticoid receptor with strong anti-inflammatory activity that may limit negative side effects such as stunted growth, insulin resistance, and weight gain[108]. In a

phase 1 study vamorolone was shown to be safe[108], and a phase 2 study is set to begin shortly (NCT03439670).

Steroid antagonists are also being investigated. Eplerenone, which blocks aldosterone that acts to raise blood pressure, has been shown to be both safe and effective for cardioprotection particularly when started at a young age (NCT01521546)[109]. A phase 3 clinical trial assessing eplerenone to preserve cardiac and pulmonary function in DMD patients is ongoing (NCT02354352).

2.2.5 Inflammation

Muscles from DMD patients show infiltration of inflammatory cells, mostly macrophages and lymphocytes[110]. A study utilizing the *mdx* mouse model depleted the macrophages from the mice and showed reduced muscle pathology[111]. An inhibitor of hematopoietic prostaglandin D synthase, which plays a role in the production of prostanoids and mast cells, is being tested in a phase 2 clinical trial (NCT02752048) with the primary outcome measured being change in the 6MWT.

NF-κB drives inflammation and muscle degeneration while also inhibiting muscle regeneration[101, 112]. Edasalonexent, a small molecule inhibitor of NF-κB, has reduced inflammation and fibrosis as well as increased diaphragm function in mouse and dog models of DMD[113]. It has also proven to be safe in a phase 1 clinical trial[114], and is currently being tested in a phase 1/2 clinical trial (NCT02439216) for further safety and

efficacy studies. Primary outcomes of safety and tolerability and muscle composition and inflammation measured by MRI will assessed.

2.2.6 nNOS Pathway Enhancement

A lack of dystrophin disrupts the recruitment of neuronal nitric oxide synthase (nNOS) to the sarcolemma[115], which affects production of nitric oxide[116]. The loss of nNOS from the sarcolemma versus the total loss in dystrophic muscle is not well understood, but generally nNOS deficiency plays a role in misregulation of muscle development, blood flow, fatigue, inflammation, and fibrosis[117]. Hence many therapies aim to enhance the nNOS pathway. Tadalafil, a phosphodiesterase type 5 inhibitor that boosts defective NO-cGMP signaling in skeletal muscle microvessels, has proven effective in preventing muscle ischemia, injury, and fatigue in *mdx* mice[118, 119]. Short-term dosing also showed forearm muscle ischemia was ameliorated when tested with handgrip exercise in patients with DMD[120] and BMD[121]. In a phase 3 clinical trial daily dosing of tadalafil at a high and low dose both failed to improve 6MWT change from baseline compared to control groups (NCT01865084)[122]. A phase 1 study testing tadalafil and sildenafil, which reduces respiratory weakness and fibrosis in the *mdx* mouse model[123], proved safe as well and improved functional ischemia and exercise-induced muscle blood flow in 10 DMD patients[120]. Sildenafil alone, in a phase 2 clinical trial for DMD and BMD patients, failed to show improvements in cardiomyopathy (NCT01168908)[124].

2.2.7 HDAC Inhibition

Histone deacetylase (HDAC) activity is constitutively active in DMD muscles[125]. Dosing of HDAC inhibitors has been shown to prevent fibrosis and promote regeneration in the *mdx* mouse model[126, 127]. A phase 1/2 study of Givinostat (NCT01761292), an HDAC inhibitor, showed histological evidence of reduced fibrotic tissue[128]. While this study was not designed to test efficacy through assessments like the 6MWT, a phase 3 study is currently recruiting (NCT02851797) and functional benefit results will be evaluated over the next few years.

2.2.8 Utrophin

Utrophin is an autosomal paralogue of dystrophin. Upregulation of utrophin has been proposed as a potential therapy for DMD[129]. When utrophin is upregulated functional improvement is seen in mice[130] and dogs[131]. Small molecules can be used to modulate utrophin levels and have been shown to be well tolerated in patients in a phase 1 clinical trial[132], and a phase 2 clinical trial is ongoing (NCT02858362). While promising there is concern that utrophin does not anchor nNOS to the sarcolemma, thus blood flow relating to metabolic needs may remain in DMD patients treated with utrophin upregulation therapies[133].

2.2.9 Complementary and Alternative Medicines

While largely not covered in this literature review, the rise of complementary and alternative medicines has not escaped potential for treating muscular dystrophy.

Nutraceuticals being investigated include coenzyme Q10, melatonin, traditional Chinese herbal supplements and acupuncture, active compounds from soybeans and turmeric for inflammation, resveratrol, increasing nitric oxide availability by use of beetroot juice, L-arginine, taurine, and vitamin D[134]. While some of these show potential, largely many produce only anecdotal evidence and none address the genetic cause of the disease.

2.3 Therapies that Restore Dystrophin Expression

Many strategies to treat DMD rely on shifting the DMD genotype to one of BMD. While this is ultimately not a cure in the classical sense, as the gene would not be returned to the wild type sequence, the generally much milder symptoms of BMD as shown by natural history make this a promising therapeutic strategy.

2.3.1 Cell-Based Therapies

Cell therapies for DMD aim to introduce functional dystrophin into patient muscle by isolating healthy cells that can then be used to repopulate and replace dystrophic tissue. Early work included clinical trials exploring transplantation of healthy donor muscle progenitors directly into DMD patient muscles, as well as combining methods of immunosuppression with the injection. However, engraftment success was low and few patients showed meaningful dystrophin expression restoration[135]. Along with insufficient donor engraftment, other challenges include immune rejection and poor migration from the injection site[136-138]. While in theory replacing dystrophic cells and muscle with healthy versions seems simple, there are a multitude of challenges. In

particular, body wide delivery would be necessary to treat DMD. DMD affects all skeletal muscles and the heart, so significant migration and an extremely large amount of cells would be needed. As muscle makes up approximately 40% of body weight[139], it is unlikely at this time that a cell therapy will prove efficacious for a systemic disease like DMD.

2.3.2 Exon Skipping

Antisense oligonucleotides (AONs) are small single-stranded chemically modified DNAs or RNAs that are designed to target specific gene transcripts. The small size is crucial for delivery. For treatment of DMD AONs are used to alter pre-mRNA splicing, such that specific exons in dystrophin are skipped during the splicing process[140]. The targeted sequence is spliced out with its flanking introns as the modifications essentially hide the exon from the splicing machinery. By skipping exons the reading frame can be restored, and may be applicable to up to 83% of all DMD mutations[141]. Exon skipping is a mutation-specific approach, such that every patient would need to be genotyped and matched to a therapy that will correct their specific reading frame mutations to return to in-frame. Currently there is a focus on skipping single exons as a proof-of-principle for the overall approach. However, this approach may prove challenging for the patients with duplications of one or more exons; AONs target both the original and duplicated copies, which will generally result in an out-of-frame transcript. Thus, more than 1 exon will need to be targeted for these patients. This

approach requires a combination of several AONs being delivered as a 'cocktail' of drugs in order to skip larger regions of the transcript. If a cocktail for exons 45-55 were effective, this could treat a large cohort of DMD patients to produce functional dystrophin.

2.3.2.1 Eteplirsen

Eteplirsen, brand name Exondys 51, is the first exon skipping therapy to be conditionally approved by the FDA for treatment of DMD patients who would benefit from skipping of exon 51. Skipping of exon 51 is applicable to approximately 13% of patients, which represents the largest patient population for skipping of a single exon[142]. Sarepta Therapeutics eteplirsen, a phosphorodiamidate morpholino oligomer (PMO), remains uncharged at physiological pH[143] and targets exon 51 in dystrophin[144]. A primary outcome assessed in DMD clinical trials is the 6MWT, a validated outcome measure used in a variety of clinical trials[145]. The test essentially consists of seeing how far a person can walk over the time of six minutes. This test aims to measure the systems involved in walking as a measure of disease progression[146]. However, the voluntary nature of this test a well as the duration have been questioned[147]. Treatment with eteplirsen resulted in a slower rate of decline in the 6MWT compared to historical controls, but not maintenance or improvement of function measured by the 6MWT[3].

The FDA cited concerns in their briefing document for the Advisory Committee about how immunofluorescence images were collected, particularly because the primary

outcome evaluation was dystrophin expression. The Western blot data from patient muscle biopsies shows a relative increase of dystrophin about 3-fold higher compared to DMD patients. The FDA also had concerns comparing the treatment groups to historical controls, particularly because the open-label study introduces bias to all participants. Furthermore, the treated patients were receiving intensive physical therapy and steroid treatments and it is unclear if the historical controls were treated similarly. Lastly, at the time of submission only 12 patients had been treated with eteplirsen for one year or longer, and the FDA cited that this small group does not have the power to assess frequency of infrequent but potentially very serious adverse side effects. While the current safety profile of eteplirsen is promising, the lack of data for long-term treatment is notable. The FDA Advisory Committee voted to reject the approval of eteplirsen, however the FDA ultimately did not follow the Advisory Committee's suggestion and granted conditional approval of eteplirsen. The FDA did note in the letter of accelerated approval that "clinical benefit of Exondys 51, including improved motor function, has not been established" and that the clinical benefit of eteplirsen needs to be verified in a 2-year randomized, double-blind, controlled trial with the primary endpoint being the North Star Ambulatory Assessment[148] rather than the 6MWT[149, 150].

2.3.2.2 Ongoing Development of Exon Skipping Therapies

While the first exon skipping drug has been conditionally approved, that drug only targets exon 51. Further clinical trial investigation for exon 51 skipping is ongoing

(NCT03508947), as well as clinical trials to establish AONs for skipping exon 45 (NCT02667483, NCT02530905, NCT03532542), exon 53[151] (NCT02081625, NCT03167255, NCT03532542), and exon 44[152] (NCT02329769) . The impressive preclinical animal data supports the concept of therapeutic AON-mediated exon skipping, but the modest clinical trial results suggest that improvements to delivery, pharmacodynamics, and pharmacokinetics are necessary to significantly improve patient outcomes. More recent AON formulations, such as the tricyclo-DNA oligomers, show improved uptake in multiple tissues after systemic administration, including therapeutic benefit in the heart[153]. Additionally, the incorporation of cell-penetrating peptides into AONs can similarly assist in tissue penetration, particularly facilitating delivery to the heart[154]. Finally, the expression of exon skipping AONs linked to small nuclear RNAs such as U7 enables the efficient delivery and prolonged expression of AONs in skeletal and cardiac muscle by AAV vectors[155, 156]. The success of this approach in dog models of DMD is promising for its continued development[157-159].

2.3.3 Readthrough Therapy

Stop codons are responsible for 13% to 15% of mutations in DMD patients[160, 161]. Being able to readthrough these stop codons and continue to produce the dystrophin protein has potential to impact as many patients as treatment for skipping exon 51. Aminoglycosides have been used to induce readthrough in *mdx* mice, which showed restoration of dystrophin protein expression and protection against contraction induced

injury[162]. Early clinical trials using gentamicin to treat DMD and BMD patients showed the treatment was well tolerated but lacked consistent restored expression of full-length dystrophin across patients[163, 164], which fueled further studies with increased dose and treatment period time. In a later clinical trial dystrophin levels did significantly increase and there was a slight increase in forced vital capacity[165]. However, use of gentamicin as a therapy had potential for severe negative side effects such as renal toxicity, so novel compounds were pursued instead[166]. Ataluren, which induces ribosomal readthrough of premature stop codons, was effective at promoting dystrophin expression in the *mdx* mouse model and human and mouse muscle cells[167]. A phase 2a clinical trial showed dystrophin expression in 23 of 38 patients[168], and a phase 2b clinical trial did not see significant results in the 6MWT, although there were non-statistically significant improvements[169]. A phase 3 study also failed to achieve statistical significance in the 6MWT, but did show a 15 meter improvement in the overall study population as well as all patients in the treated group remained ambulatory whereas 4 of 52 control patients lost ambulation[170]. Ataluren, brand name Translarna developed by PTC Therapeutics, has been approved in Europe to treat some patients with DMD and BMD, and further readthrough compounds are being investigated[171].

2.3.4 Minidystrophin and Microdystrophin

The entire dystrophin gene is too large to deliver, however many variations of delivering the dystrophin complementary DNA (cDNA) are ongoing. The mouse

dystrophin cDNA has been delivered as naked plasmid to the *mdx* mouse and resulted in stably expressed dystrophin in 1-5% of myofibers[172]. This principle was applied in clinical trial where 6 out of 9 patients had low but present levels of dystrophin[18]. However, this plasmid-mediated gene delivery approach is ultimately transient, which presents an array of issues such as patient compliance and cost.

Efficiency of gene transfer and expression levels can be increased by using a viral delivery system rather than plasmid DNA. However, the full-length dystrophin cDNA exceeds packaging limits of many viral vectors. The cDNA can be split up into three parts and delivered through co-injection of three viruses, where the expression cassette is reconstituted *in vivo*; although the efficiency of reconstitution is low, this study suggests that with optimization co-injection may be a viable way to express the full-length dystrophin cDNA[173]. A therapeutic utilizing AAV is particularly compelling as AAV has been shown to have high levels of *in vivo* transduction to achieve long-term gene expression[174], and the virus remains predominantly episomal so it does not pose risk of nonspecific integration like lentivirus[175, 176].

In order to utilize AAV, truncated versions of the dystrophin cDNA have been created termed minidystrophin and microdystrophin. The dystrophin gene contains repetitive domains that can seemingly be removed to truncate the size of the dystrophin cDNA to achieve functionality. This approach has shown improved cardiac performance and preserved muscle function in a variety of mouse models, as well as emphasizing

that dystrophin expression in a relatively small amount of myofibers can result in considerable recovery of contractile force[23-29, 31-33, 177-179]. This promising method was taken to clinical trial where patients were injected intramuscularly with various doses of AAV expressing minidystrophin. Unfortunately, efficacy proved problematic as there were very few dystrophin-positive fibers in some patients even though the viral genomes were easily detectable in muscle biopsies[180]. It appears the immune system played a role in the lackluster results; T cells targeting dystrophin epitopes were detected in the blood of many patients. This likely represents an immune response to the foreign epitope[180]. However, some patients were found to have these T cells before injection of the AAV-minidystrophin. There is no mechanistic explanation for the antidystrophin immune response. Additionally, it is unclear if the delivered minidystrophin played a part. This immune response will also be of utmost concern for future approaches for dystrophin restoration in DMD patients. Clinical trials utilizing AAV now routinely screen patients for pre-existing immunity[181]. Past failure has not deterred hope for minidystrophin and microdystrophin treatments. A phase 1 clinical trial for systemic dosing of AAV9-minidystrophin driven by a muscle specific promoter is currently recruiting (NCT03362502), and a phase 1/2 clinical trial for systemic administration of microdystrophin is also recruiting (NCT03362502).

2.3.5 Gene Editing

Completion of the human genome project enabled diseases with clear genetic causes to have treatments with a genetics-based approach[182]; recent advances in genome engineering have shown considerable promise for addressing the genetic basis of diseases[183-186]. Classical gene therapy has been focused on delivering exogenous DNA to supplement the endogenous gene expression[187]. However, recent developments of sequence-specific DNA-binding proteins, and their nuclease forms, such as zinc finger proteins and nucleases[188, 189], transcription activator-like effectors and nucleases[190-192], meganucleases[193, 194], and CRISPR-Cas9[195, 196] have allowed a variety of DNA targeting methods. These engineered proteins facilitate new opportunities for gene therapy by designing these proteins to bind to nearly any target site in the human genome. The zinc finger protein and transcription activator-like effectors can be fused to the FokI endonuclease domain to enable targeting cleaving of DNA; Cas9 is a nuclease itself and can be utilized in the same fashion. When a DNA break is created, naturally occurring DNA-repair mechanisms are triggered. Non-homologous end joining can occur, leading to a scar in the DNA. This scar is a result of the error-prone repair process that results in small insertions or deletions where the double-stranded break was made, referred to as indels. These indels can be used to shift or mutate a reading frame in the targeted sequence. Two nuclease systems can also be introduced in order to delete the sequence between the two double stranded breaks. Alternatively, the user can provide a donor

template with the nuclease to introduce specific changes at the targeted genomic site. The CRISPR-Cas9 system in particular combines a nuclease that cleaves double-stranded DNA with a gRNA that contains a constant region the Cas9 binds and a variable sequence the user designs to target a complementary genomic sequence. The relative ease of designing and testing this tool along with the efficacy of the system has created excitement around the potential of rewriting the human genome. However, all of these tools have shown preliminary success. These technologies have been used to correct genetic mutations associated with a plethora of diseases such as sickle cell anemia, X-linked severe combined immunodeficiency, and hemophilia[192, 193, 197-200].

CRISPR sequences, the hallmark of a bacterial defense system[201-204], are present in more than 40% of bacteria and 90% of archaea[205]. These repeating elements are adjacent to well-conserved CRISPR-associated genes[206], and the non-repeating spacer sequence was found naturally to match DNA sequencing belonging to viruses and other various mobile genetic elements[204, 207]. The activity of the Cas enzyme is guided by small CRISPR RNAs, which are transcribed from spacer sequences[208]. These spacer sequences have highly similar sequences at regions denoted the protospacer adjacent motif, which is critical for the CRISPR system to function[209]. Particularly important was the discovery that not only can CRISPR systems from one bacterium be transferrable to other bacterial strains[210], but also that these Cas enzymes, specifically Cas9, can be reprogrammed to target a specific DNA sequence in bacteria[211, 212] and eukaryotic cells[213, 214]. The

endogenous CRISPR system requires two RNAs to form the CRISPR-Cas9 complex in order to created DNA double stranded breaks, but a single chimeric RNA can be used in place of these two RNAs termed a single guide RNA[211]. Use of CRISPR-Cas9 in eukaryotic systems allows for ease of design and testing with this extremely flexible tool for a variety of genome-targeting purposes, including gene editing for therapeutic applications[215].

A majority of DMD-causing mutations are deletions that push the translational reading frame out of frame, thus deleting targeted exons of the DNA can restore the reading frame. Frameshifts can also be created with targeted nucleases to create indels. Meganucleases were used to show insertions and deletions could be utilized to restore the reading frame of the dystrophin gene, successfully restoring dystrophin in myoblasts *in vitro* and in muscle fibers through electroporation *in vivo*[216]. ZFNs, TALENs and the CRISPR-Cas9 system have also been used for dystrophin repair[42-44, 48, 217-224]. Exon 51 has been targeted as removal of this exon would address about 13% of the patient population, which represents the largest segment for a single exon[141, 225]. A large deletion of exons 45-55 has also been studied, as this would address mutations for about 60-65% of DMD patients and this naturally occurring deletion often presents as a very mild BMD phenotype[5, 226, 227]. *Ex vivo* editing of patient derived myoblasts[42, 221] and hIPSCs[222, 224] followed by cell transplantation or injection has been shown to restore functional

dystrophin protein expression of the *mdx* mouse *in vivo*. There has also been demonstration of knocking in exon 44 to restore a region of the dystrophin gene[228].

Recently, several groups showed efficacy of true *in vivo* gene editing[43-45, 47, 218]. Adenovirus and AAV have been utilized to deliver CRISPR-Cas9 systems to restore dystrophin expression in skeletal and cardiac muscle in the *mdx* mouse or variants of the *mdx* mouse model. Furthermore, groups have shown both local and systemic delivery of these viral systems in adult and neonatal mice result in increased muscle force. Systemic delivery is of particular interest as treatment of DMD clinically requires systemic application. For the first time, these labs have produced a phenotypic change in a model of muscular dystrophy utilizing CRISPR-Cas9. These results also emphasize findings that relatively few dystrophin positive fibers are required for dramatic protein expression change[229]. Furthermore, Tabebordbar *et al* show that the satellite cells, the stem cells of muscle, are edited via AAV delivered CRISPR-Cas9, meaning that the cells that repopulate muscle will no longer create cells with a DMD genotype[45]. Recently, groups have also shown editing of human dystrophin in a humanized mouse model by CRISPR-Cas9 plasmid delivery[223] and by exon skipping[230]. These recent findings show great promise for the future of genome engineering to address DMD.

Chapter 3. Creation and Characterization of a Humanized Diseased Mouse Model of Duchenne Muscular Dystrophy

This work was done in collaboration with Christopher Nelson, Annemieke Aartsma-Rus, and Charles Gersbach.

3.1 Synopsis

CRISPR-Cas9 has recently been described as a useful tool for creating new animal models[231]. The increased efficiency compared to the traditional route to creating transgenic animals is highly attractive. Further, CRISPR-Cas9 can be targeted to precise loci, enabling the ability to make exact changes to genomic DNA. Here we utilized CRISPR-SpCas9 to target the human *DMD* gene in a transgenic mouse model. By removing exon 52 we created a mouse model with the diseased human DMD genotype and assessed the phenotype. The mouse lacks dystrophin protein expression and displays a mild dystrophic phenotype measured by distance moved and rearing postures in an open field and front paw grip strength. The phenotype is comparable to the *mdx* mouse and shows deficits compared to the unedited healthy hDMD/*mdx* mouse model. Our hDMDΔ52/*mdx* is a useful tool for testing gene therapy strategies for DMD *in vivo* in a small animal model.

3.2 Introduction

Although humans and mice have about 80% of identical DNA in protein coding regions, only about 40% of nucleotides overall[232], including non-coding intronic regions,

are identical. Even in species where greater than 90% of the DNA sequence is conserved, such as the rhesus macaque that has 93.5% identity to humans[233], just a 1% different can result in approximately 30 million different bp. Genome editing tools target precise DNA loci, so these differences across species can have a large effect. For CRISPR-Cas9 to target a precise DNA locus there must be between 17-24 bp for a gRNA to target along with the required protospacer adjacent motif (PAM) for the species of Cas9. Thus, when designing a CRISPR-Cas9 system to target the human genome it is unlikely that a large amount of perfectly overlapping sequences designed for specific target sites in the human gene will exist in the mouse gene. Majority of previous *in vivo* studies for DMD have been conducted in a mouse model such as the *mdx* or *mdx*^{4cv}. These all rely on the mouse genome, rather than the human genome. While they have been crucial in proving proof-of-concepts for a variety of translational projects, ultimately human-specific gRNAs need to be tested and validated in a small animal model. Targeting the mouse genome will likely use gRNAs not compatible with the human genome.

This hurdle requires the use of a humanized mouse. The hDMD mouse contains the full-length wild type sequence of the human *DMD* gene located on mouse chromosome 5[41]. This hDMD mouse has been bred with the *mdx* mouse such that no mouse dystrophin is expressed, and the human dystrophin protein has previously been shown to express to similar levels as the native mouse dystrophin[41]. Thus, a humanized mouse, much more relevant for specific DNA targeting tools for translational medicine,

provides an excellent opportunity for study. While this does contain the human sequence for the *DMD* gene, it is the full-length and healthy 2.5 million bp. A more relevant model would have the human *DMD* gene, but with a DMD genotype – a diseased mouse model. Hence, we undertook transforming this hDMD/*mdx* mouse, with healthy human dystrophin, into a mouse containing a DMD genotype on the human *DMD* gene.

Removal of exon 51 is applicable to about 13% of the DMD population, which is the largest pool of patients for removal of a single exon. Exon 51 removal rescues a DMD genotype that has an existing loss of exon 52. Exon 52 is 118 bp, and thus a small target for removal from a genome. Loss of exon 52 can also be rescued by removal of exon 53, as well as exons 45-55. Thus, we sought out to delete exon 52 from the human *DMD* gene in the hDMD/*mdx* mouse to create a diseased humanized mouse model of DMD.

3.3 Materials and Methods

3.3.1 Design of gRNA to Delete Exon 52

Approximately 250 bp upstream and downstream of exon 52 were obtained from the NCBI Reference Sequence NG_012232.1. These sequences were submitted to crispr.mit.edu with the human target genome specified. This online tool scores gRNAs and sorts them by score based on DNA targeting specificity[234]. The top 4 gRNAs scored for both upstream and downstream of exon 52 were selected for testing.

3.3.2 Plasmid Constructs

The expression cassettes for *S. pyogenes* gRNA and human codon optimized SpCas9 nuclease were used as previously described[48]. Briefly, SpCas9 expression is driven by a CMV promoter (Addgene #41815) and the gRNA constant region with BbsI cloning sites for the protospacer is driven by the human U6 promoter (Addgene #53188) on a separate plasmid. The gRNA plasmid is digested with BbsI and CIP and gel extracted to prepare for cloning.

3.3.3 Molecular Cloning

gRNA sequences were identified and short sequences compatible with the BbsI cut site overhangs were added on. The oligonucleotides containing the gRNA and BbsI cloning sequences were ordered from IDT DNA, ordering both the forward and reverse oligonucleotide for each gRNA sequence. Oligonucleotides were resuspended in molecular biology grade water, and complimentary oligonucleotides for a single gRNA were annealed together with T4 DNA Ligase Buffer and a thermocycler program slowly decreasing in temperature. The resulting annealed oligonucleotides were diluted 1:100 in molecular grade water. Diluted annealed gRNA oligonucleotides were cloned into the previously digested gRNA constant region backbone using T4 DNA ligase. Ligations were transformed into STBL3 or DH5α bacterial cells and plated on agar with carbenicillin. Plates were incubated overnight at 37°C. Individually colonies were grown up overnight in LB broth at 37°C and centrifuged the following morning. Supernatent

was decanted, and pellets were processed using the QIAprep Spin Miniprep Kit (Qiagen). Plasmid was sent to sequencing (Eton Bioscience) and sequenced with the M13R-reverse primer to verify the gRNA insert. Sequence verified plasmids were transformed, glycerol stocks were made, and further bacterial preps were completed as required.

3.3.4 Cell Culture and Transfection

HEK293T cells were obtained from the American Tissue Collection Center (ATCC) through the Duke Cell Culture Facility. Cells were maintained in DMEM supplemented with 10% fetal bovine calf serum and 1% penicillin/streptomycin. Cells were cultured at 37°C with 5% CO2. Transfection was mediated by Lipofectamine 2000 (Invitrogen) using a total of 800 nanograms (ng) of plasmid DNA. For testing single guide RNAs 400 ng of human codon optimized SpCas9 (hCas9) plasmid DNA and 400 ng of sequence verified gRNA plasmid DNA were combined. For testing deletions mediated by 2 gRNAs, 400 ng of hCas9 plasmid DNA and 200 ng of each sequence verified gRNA plasmid DNA were used. Lipofectamine and DNA were suspended in OptiMEM and placed dropwise on cells in a 24-well plate. 400,000 cells were transfected in suspension in 0.5 mL of media per well. Cells were cultured for 48-72 hours.

3.3.5 Surveyor Assay for Indel Detection

Cells were harvested by adding trypsin and centrifuging the cells at 350 rpm. Supernatant was aspirated and the cell pellet was processed using the DNEasy Blood

and Tissue Kit (Qiagen). gDNA was assayed for indel formation using the Surveyor Mutation Detection Kit (IDT DNA), which detects mutations characteristic of nuclease-mediated non-homologous end joining (NHEJ). The target locus in the genomic DNA isolated from cells was PCR amplified using AccuPrime High Fidelity PCR kit (Invitrogen). The resulting PCR products were randomly melted and annealed in a thermocycler programmed to 95°C for 240 s, 85°C for 60 s, 75°C for 60s, 65°C for 60s, 55°C for 60 s, 45°C for 60 s, 35°C for 60 s, and 25°C for 60s with a -0.3°C/s rate between steps. This melting and annealing allows for small mismatches, from the nuclease activity, in DNA strands to be annealed together. These mismatches were then detected and cut, creating DNA fragments from the PCR amplified regions. This was achieved by incubating 8 μl of the reannealed regions with 1 μl of Surveyor Nuclease S and 1 μl of Enhancer S for 1 hour at 42°C. Next 1.25 μl of SDS and 2 μl of loading buffer were added and the mixture was incubated for 5 minutes at 65°C. 6ul of this product was loaded into a 10% TBE polyacrylamide gel and run at 200V for 30 minutes. The gel was stained in ethidium bromide, followed by 3 washes in deionized water, and imaged on a Bio-Rad Gel Imager. The on-target activity of the gRNA was estimated by quantification of densitometry of cut and uncut bands using the ImageLab software suite (Bio-Rad) as previously described[235].

3.3.6 *In Vitro* Testing of gRNAs to Delete Exon 52

After assessment of individual gRNAs upstream and downstream of exon 52 the two gRNAs with the most on-target activity, as measured by quantification of the results of the Surveyor assay, were transfected as pairs of gRNAs to create a deletion of exon 52. 48-72 hours after transfection cells were harvested by trypsin and centrifuged. Supernatant was aspirated, and the pellet was processed with the DNEasy Blood and Tissue kit. Resulting gDNA was amplified using a primer upstream of the upstream gRNA target site, and downstream of the downstream gRNA target site by PCR utilizing the AccuPrime High Fidelity PCR kit. PCR products were electrophoresed on a 1% agarose gel with ethidium bromide at 130V for 30 minutes. The gel was assessed for deletion of exon 52 using densitometry and the ImageLab software suite. The gRNA pair resulting in the highest amount of deletion of exon 52 was chosen to move forward with.

3.3.7 Creation of the hDMDΔ52/*mdx* Mouse

An overview of the general process for injecting mRNA into mouse zygotes is shown in **Error! Reference source not found.**. Briefly, mRNA of 2 gRNAs for exon 52 deletion and hCas9 was generated by the Duke BAC Recombineering Core through *in vitro* transcription. hDMD/*mdx* mice were obtained from Leiden University Medical Center under material-transfer agreement. Mice were mated to each other until we obtained 10 singly-housed hDMD/*mdx* (homo;hemi) males. Female B6SJLF1/J mice (Jackson Laboratories #100012) were superovulated by giving an intraperitoneal

injection of pregnant mare's serum gonadotropin on day 1, followed by an intraperitoneal injection of human chorionic gonadotropin on day 3. 12 hours after hCG injection, female superovaulated mice were mated 1:1 with male hDMD/*mdx* mice. Mice were checked for vaginal plugs, then zygotes were harvested. Pronuclear injection of both gRNAs and hCas9 mRNA was performed into approximately 220 zygotes. Zygotes that survived injection were implanted into pseudo-pregnant CD1 female mice and left to gestate. 7-10 days after birth tails snips were taken from pups. Tail snips were processed using the DNEasy Blood and Tissue kit (Qiagen) and PCR amplified to assess deletion of exon 52. Chimeric mice lacking exon 52 were mated to *mdx* mice to establish a stable line of hDMDΔ52/*mdx* mice.

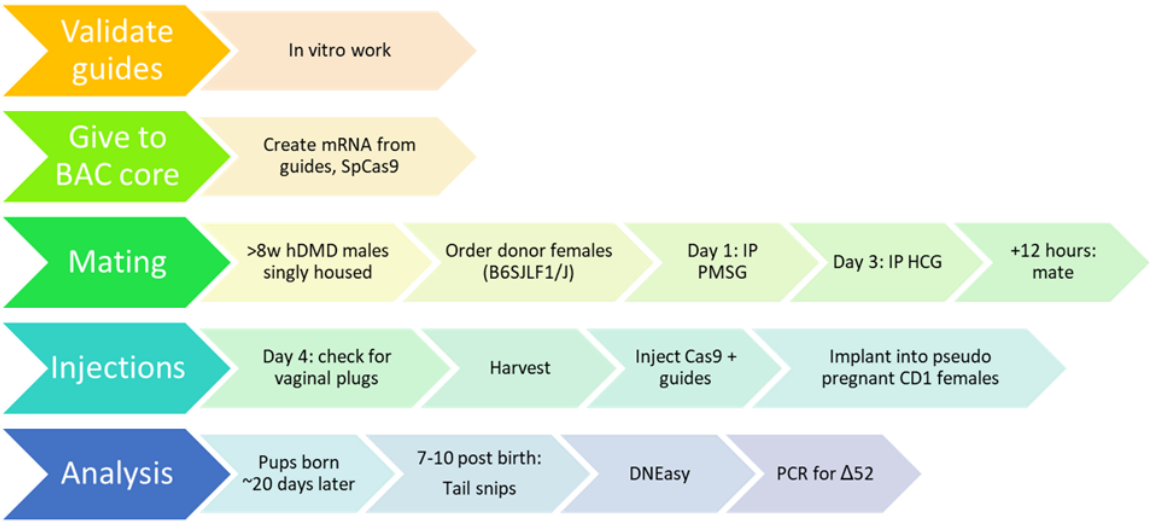

Figure 2: Overview of the process to utilize a CRISPR-Cas9 system to inject into mouse zygotes to create a transgenic mouse with a precise edit.

3.3.8 Biochemical Analysis of the hDMDΔ52/*mdx* Mouse

3.3.8.1 Endpoint PCR Assay to Detect Genomic Deletions

Lack of exon 52 was confirmed by PCR amplification, as described in 3.3.6 *In Vitro* Testing of gRNAs to Delete Exon 52, of gDNA from tail snip and ear punch, and resulting band was extracted using the QIAQuick Gel Extraction Kit (Qiagen) and Sanger sequenced (Eton Biosciences).

3.3.8.2 mRNA Analysis

RNA was extracted from tissue using the RNEasy Universal Plus Mini Kit (Qiagen). RNA was reverse transcribed using SuperScript VILO cDNA Synthesis kit (Thermo Fisher) for 2 hours at 42°C according to the manufacturer's instructions. The target loci was amplified by 35 cycles of PCR with the AccuPrime High Fidelity PCR kit (Invitrogen). PCR products were electrophoresed on 1% TAE-agarose gels and stained with ethidium bromide for analysis. The resolved PCR bands were extracted with the QIAQuick Gel Extraction Kit (Qiagen) and Sanger sequenced (Eton Biosciences) for analysis.

3.3.8.3 Western Blot

Tissues were either snap frozen after harvesting or stored in RNALater, then disrupted with a probe sonicator (Fisher Scientific FB50) or a BioMasherII homogenizer in RIPA buffer (Sigma) with a protease inhibitor cocktail (Roche) and incubated for 30 minutes on ice with intermittent vortexing. Samples were centrifuged at 16000xg for 30

minutes at 4°C and the supernatant was isolated. Total protein amount was quantified using the bicinchronic acid assay according to the manufacturer's instructions (Pierce). Protein isolate was mixed with NuPAGE loading buffer (Invitrogen) and 5% β-mercaptoethanol and boiled at 100°C for 10 minutes. 20-25 μg total protein per lane was loaded into 4-14% NuPAGE Bis-Tris gels (Invitrogen) with MOPS buffer (Invitrogen) and electrophoresed for 30 minutes at 200V. Protein was transferred to nitrocellulose membranes for 1 hour in 1X tris-glycine transfer buffer containing 10% methanol and 0.01% SDS at 4°C at 400mA. The blot was blocked between 1 hour and overnight at 4°C in 5% milk-TBST. Blots were probed with MANDYS8 (1:200, Sigma) for 1 hour in 5% milk-TBST at room temperature or overnight at 4°C. Blots were then incubated with mouse horseradish peroxidase-conjugated secondary antibody (Santa Cruz) for 30 minutes in 5% milk-TBST. Blots were visualized using Western-C ECL substrate (Biorad) on a ChemiDoc chemiluminescent system (Biorad).

3.3.8.4 Immunohistochemical Staining

Muscle biopsies were stored in RNALater or flash frozen in liquid nitrogen, then mounted and frozen in Optimal Cutting Temperature compound. Serial 10 micron sections were obtained by cryosectioning of the embedded tissue at -20°C. Cryosections were washed in PBS and blocked in PBS containing 10% heat-inactivated fetal bovine serum for dystrophin detection for 30-60 minutes. Cryosections were incubated overnight at 4°C with MANDYS8. After primary staining, dystrophin was detected

using a tyramide-based immunofluorescence signal amplification detection kit (Life Technologies). Sections of the heart and tibialis anterior muscle were stained with the MANDYS8 antibody (Sigma) to assess dystrophin expression. Briefly, cryosections were incubated with 1:200 goat anti-mouse biotin-XX secondary (Life Technologies #B2763) in blocking buffer for one hour at room temperature. The signal was then amplified using streptavidin-HRP conjugates (1:100, from TSA Kit) in blocking buffer for one hour at room temperature. Finally, cryosections were incubated with tyramide-AlexaFluor488 conjugates (1:100, TSA kit) in manufacturer-provided amplification buffer for 10 minutes at room temperature. Stained cryosections were then mounted in ProLong AntiFade (Life Technologies #P36934) and visualized with conventional fluorescence microscopy.

3.3.8.5 Serum CK Assay

Blood was drawn by cardiac puncture either while the mouse is under anesthesia or post-mortem. Blood was left at room temperature for 10-30 minutes, or on ice for 15-120 minutes. Blood was centrifuged at 1200 rpm for 25 minutes; the top layer of serum was collected and snap frozen in liquid nitrogen. Serum was diluted 1:5 and tested per manufacturer's instructions using the Liquid Creatine Kinase (CK) Reagent Set (Pointe Scientific). Statistical analysis was a two-tailed t-test.

3.3.9 Phenotype Analysis of the hDMDΔ52/*mdx* Mouse

Mice were assessed for phenotypic changes in four tests: open field, rotarod, foot fault, and grip strength. 11 *mdx* mice were tested, but 1 died between 1 year and 1.5

years of age. 10 hDMD/*mdx* and 10 hDMDΔ52/*mdx* mice were tested. In instances where there is missing data at a time point all mice possible are used for comparisons at one single time point between different mouse strains; for a single mouse strain across different time points mice without all data points are excluded in all time points in order to conduct a repeated measures analysis.

3.3.9.1 Open Field Protocol

In open field mice were allowed exploration of an open field arena (20 x 20 x 30 cm) for 30 minutes (Omnitech Versamax Legacy). Automated monitoring of activity and location of animals was conducted with infrared diodes on the x, y, and z axis interfaced to a computer running Fusion Activity software (version 5.3, Omnitech). Data was output in 5 minute windows, giving 6 data points per mouse for total distance moved and rearing postures exhibited. Data was analyzed first with linear regression to assess the role of time. If time does not have a statistically meaningful role, data was collapsed into one average instead of six data points for each mouse. Averages for comparison between mouse strains were analyzed by one-way ANOVA corrected by Tukey. If the time factor is meaningful data was analyzed by repeated measures two-way ANOVA corrected by Tukey. When comparing time points within the same mouse strain a repeated-measures one-way ANOVA corrected by Tukey was conducted.

3.3.9.2 Rotarod Protocol

In the rotarod (Med Associates) test mice were subjected to two protocols. In both protocols mice were given four 300 second trials separated by an interval of 20-30 minutes and duration on the rod, latency to fall, is recorded. On day one mice were tested on an accelerating rotarod. The rotarod started at 4 RPM and increased to 40 RPM over 300 seconds. The average speed of the rotarod at which the mouse fell off was recorded and rounded to the nearest 4 RPM. This was the speed used on the second day of testing in the steady speed protocol. This speed was typically 24 RPM but declines with mouse age. On the second day of testing mice underwent four trials of 300 seconds each at a steady speed as determined by the first day of testing. The average of the 4 trials was calculated, resulting in one data point per mouse. Data comparing mouse strains at one time point was analyzed by one-way ANOVA corrected by Tukey. Data comparing different time points within one mouse strain were analyzed by repeated measures one-way ANOVA corrected by Tukey.

3.3.9.3 Foot Fault Protocol

In the foot fault test mice were placed onto a platform comprised of parallel rods and allowed free exploration for five minutes. Directly beneath the rods is a platform that records each time the mouse's foot slips between the rods and touches the platform (CleverSys). The total number of foot faults were scored using Foot Fault software

(CleverSys). Mice were given three trials across three consecutive days. Data was analyzed by repeated measures two-way ANOVA corrected by Tukey.

3.3.9.4 Grip Strength Protocol

In grip strength, the instrument bar (San Diego Instruments) was adjusted to the angle which bests suits the mouse's ability to grip and pull. Mice were given 3-5 trials each for front paws and whole body grip strength. The average of the trials was reported as grams-force. Data between strains at one time point was analyzed by one-way ANOVA corrected by Tukey. Data within one strain across time points was analyze by repeated measures one-way ANOVA corrected by Tukey.

3.4 Results

3.4.1 Targeting CRISPR-SpCas to Excise Exon 52 *In Vitro*

After transfection of individual gRNAs with hCas9 into HEK293T cells, on-target activity was assessed by the Surveyor assay. Of the four gRNAs tested upstream of exon 52 in intron 51, labeled 93-96, three of the four showed meaningful activity, with two showing 13-15% modification. Of the four tested downstream of exon 52 in intron 52, labeled 97-100, two of the four showed activity, between 9-11% modifications.

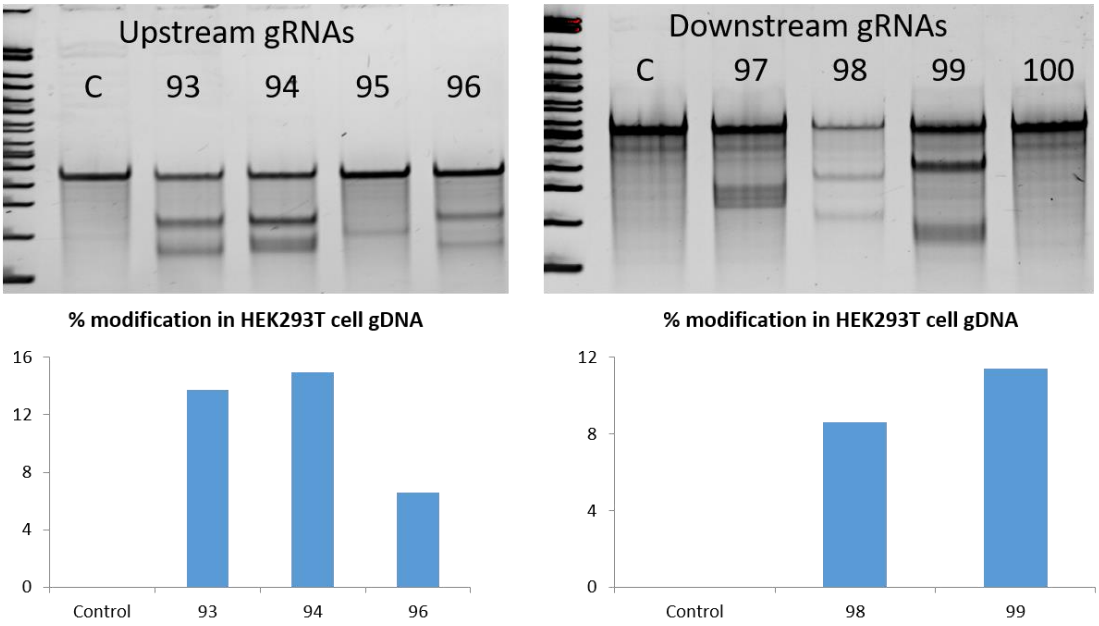

Figure 3: Surveyor assay to assess on-target editing in intronic regions flaking dystrophin exon 52. Left: Surveyor assay of gRNAs (labeled 93-96) and quantification of percent mofidication by densitometry. Right: Surveyor assay of gRNAs downstream of exon 52 (labeled 97-100) and quantification of percent modification by densitometry. "C" is a control lane using gDNA transfected only with Cas9 and with no gRNA.

These four gRNAs, two each upstream and downstream (labels 93, 94, 98, and 99), were tested pairwise together in transfections to delete exon 52. All four pairs of gRNAs tested deleted exon 52 from the genomic DNA, and measurements by densitometry indicated the pair of gRNAs 94 and 99 was most effective at removal of exon 52.

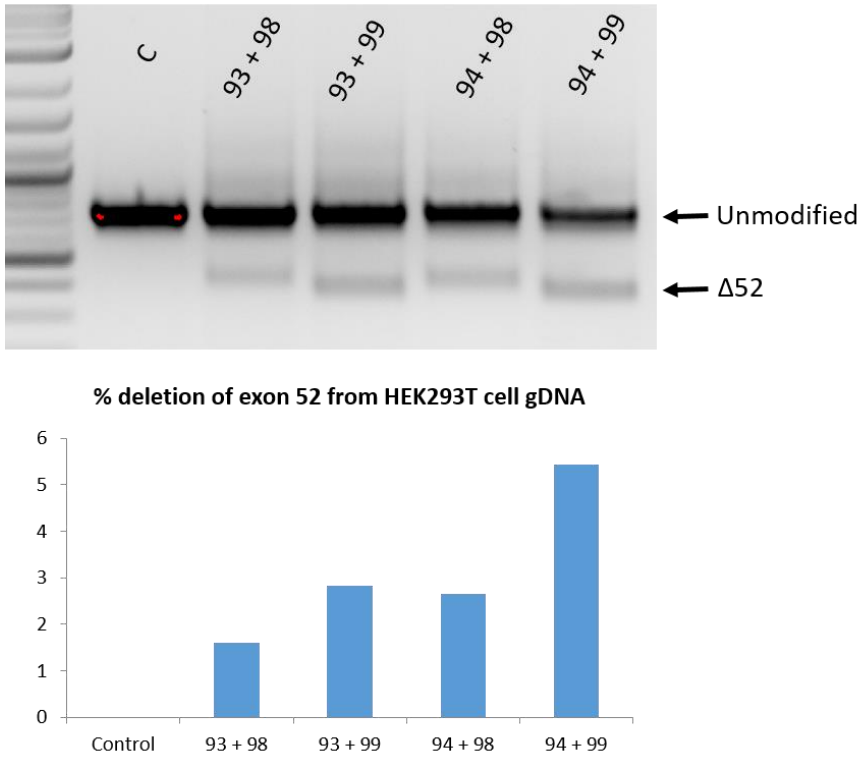

Figure 4: *In vitro* deletion of exon 52. Endpoint PCR electrophoresed on an agarose gel showing a smaller band, indicative of a deletion of exon 52 (top). Quantification of percent deletions by densitometry (bottom).

3.4.2 Injection of the CRISPR-SpCas9 System for Exon 52 Deletion into Zygotes and Resulting Founder Pups

These gRNA plasmids were given to the Duke BAC Recombineering core for creation of mRNA and injection into zygotes. 2 rounds of injections occurred. From the first there were 471 embryos produced from five visible plugs, and 150 fertilized embryos. Of the embryos that survived the pronuclear injection nine pups were born from three surrogate mothers. The second round of injections produced 5 visible plugs, but only 77 usable embryos. Despite the low number of embryos 17 pups were born. Typically, about 300 usable embryos are produced; these low numbers are likely

reflective of the fact that the *mdx* mouse strain is known to be a challenging breeder (The Jackson Laboratory Strain 001801). From the first round of injections, one pup (#7) had a clear deletion of exon 52, and from the second round of injections two pups (#63 and #76) displayed deletion of exon 52.

Founder pup #63 exhibited both the expected unmodified parent band lacking any deletion and the deletion band, whereas founders #7 and #63 displayed only the PCR amplification band lacking exon 52. Founder #7 was qualitatively not a good breeder, whereas founder #76 starting breeding well at the age of sexual maturity.

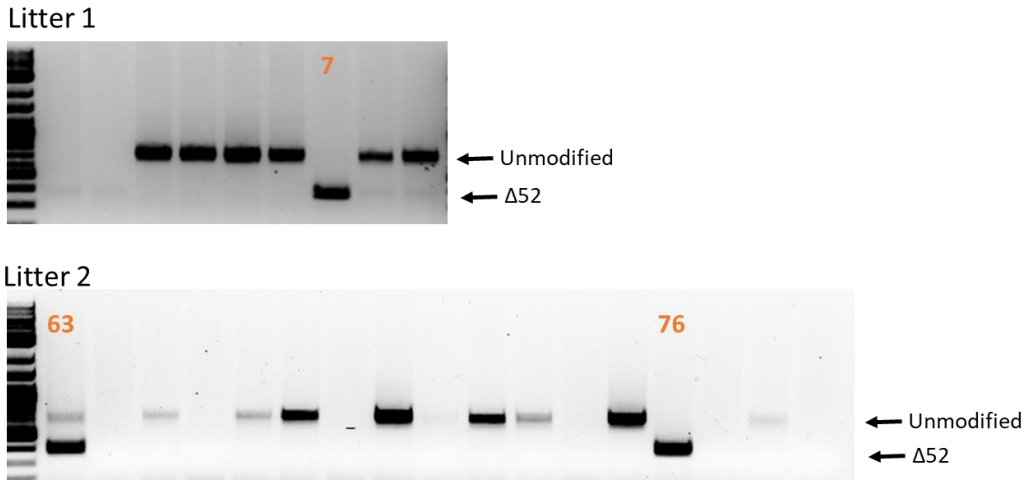

Figure 5: Genotyping founder pups after CRISPR-SpCas9 mRNA zygote injection. Genotyping by PCR amplification of gDNA from tail snips of pups born after zygote injection of our CRISPR-Cas9 system to remove exon 52. Top band is unmodified, smaller band is a lack of exon 52. 7, 63, and 76 are random identifying numbers for the pups; these three show deletions of exon 52.

Pups resulting from breeding with founder #76 consistently lacked exon 52, and thus founder pup #76 was used to create the hDMDΔ52/*mdx* mouse line and the other

founders were euthanized to ensure we were propagating the exact same genomic DNA changes from founder #76.

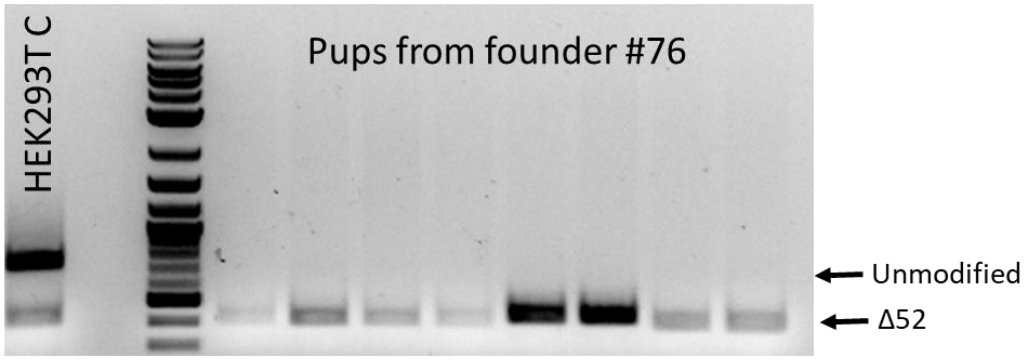

Figure 6: Genotyping results of pups from founder #76. Genotyping by PCR amplification of gDNA from tail snips from a litter with sire 76. Left-most lane is gDNA from treated HEK293T cells, showing the top unmodified band and the smaller band lacking exon 52. All pups sired from founder 76 show only the smaller band lacking exon 52.

Pups from the first litter bred from founder #76 were sacrificed for biochemical analysis. Sequencing of the loci around where our CRISPR-Cas9 system targeted exon 52 removal indicate a 16bp insertion between the predicted cut sites 3bp into the gRNA sequence upstream of the PAM. We expected this insertion to not be problematic as it is in an intronic region.

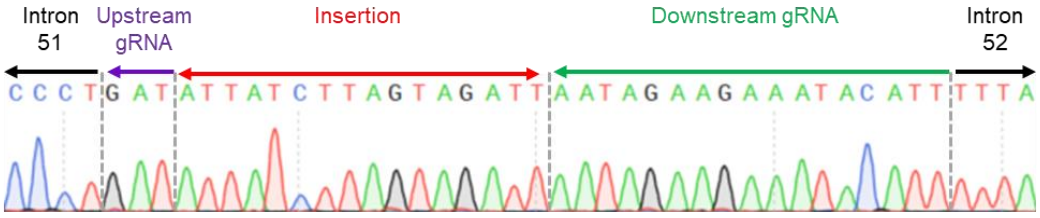

Figure 7: Indel scar between cut sites for removing exon 52. Sanger sequencing of gDNA from an hDMDΔ52/*mdx* mouse. There is an insertion (red) between the expected cut sites of the two gRNAs.

3.4.3 Deletion of Exon 52 in the Genome Results Edited RNA and Protein

Pups from later litters were assessed for modifications in the mRNA by PCR amplification of cDNA. As introns are not transcribed into RNA, we expected to see a loss of exon 52 with no additional bp insertions or deletions as a result of our gRNA targeted scar. We observed the expected perfect ligation of exon 51 to exon 53, indicative that our system to remove exon 52 from the gDNA carries through to the mRNA.

We further characterized the mouse by IHC staining. Immunofluorescence staining for dystrophin on sections from muscle biopsies taken from the heart and TA confirmed a lack of dystrophin expression, with the exception of a few revertant fibers that is consistent with what is seen in the *mdx* mouse.

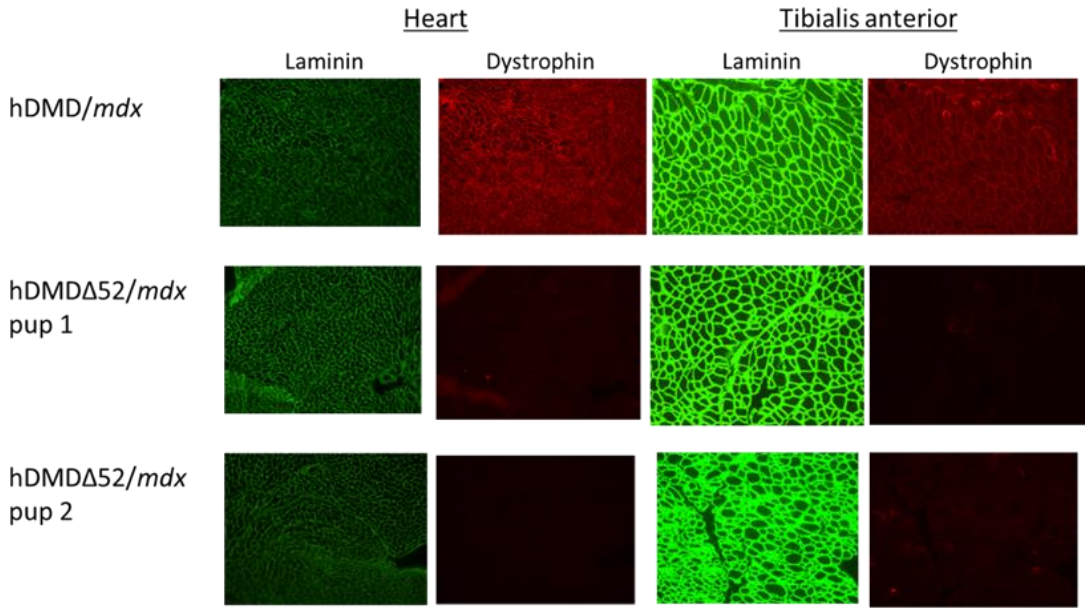

Figure 8: IHC staining for dystrophin on sections of the heart and tibialis anterior muscles. Top row shows the hDMD/*mdx* mouse, which is positive for

dystrophin staining (red) at the cell membrane and overlaps with the laminin staining (green). Rows 2 and 3 show representative hDMDΔ52/*mdx* mice (pup 1 and pup 2) that have consistent laminin staining, but lack dystrophin staining with the exception of a few rare revertant fibers.

We also performed Western blot on protein extracted from the TA muscle and confirmed lack of dystrophin protein expression in our mouse compared to clear dystrophin expression in the hDMD/*mdx* mouse.

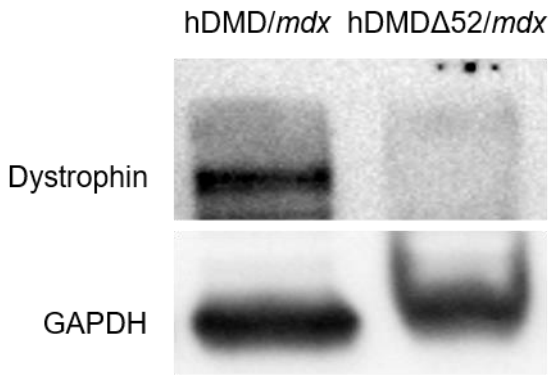

Figure 9: Western blot for dystrophin shows the dystrophin-expressing hDMD/*mdx* mouse in the first column and a lack of dystrophin expression in our hDMDΔ52/*mdx* mouse in the second column.

3.4.4 Deletion of Exon 52 in the Genome Results in Elevated Serum CK Activity

Through a UV assay we also showed an increase in serum CK levels compared to the wild type C57BL/6J mouse strain, consistent with reports for the *mdx* mouse model.

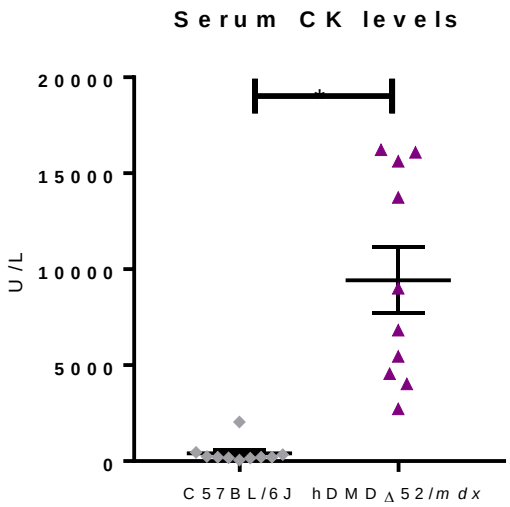

Figure 10: Elevated serum CK activity in hDMDΔ52/*mdx* mice.

3.4.5 Phenotype Analysis of the hDMDΔ52/*mdx* Mouse

hDMDΔ52/*mdx*, hDMD/*mdx*, and *mdx* underwent phenotypic testing at the Duke Mouse Behavioral and Neuroendocrine Core Facility at 8 weeks, 16 weeks, 1 year, and 1.5 years of age. The hDMD/*mdx* mouse serves as a positive control as this mouse has healthy human dystrophin. The *mdx* mouse serves as a benchmark, as we would expect our hDMDΔ52/*mdx* mouse to display a similar phenotype.

3.4.5.1 Open Field Protocol

At 8 weeks of age we saw a dystrophic phenotype in the *mdx* and hDMDΔ52/*mdx* mice compared to the hDMD/*mdx* mice in distance moved in an open field. Both dystrophic mice moved significantly less on average over 6 five-minute periods.

Consistent with less movement in an open field, the two dystrophic mouse lines also displayed less rearing postures measured during the same test.

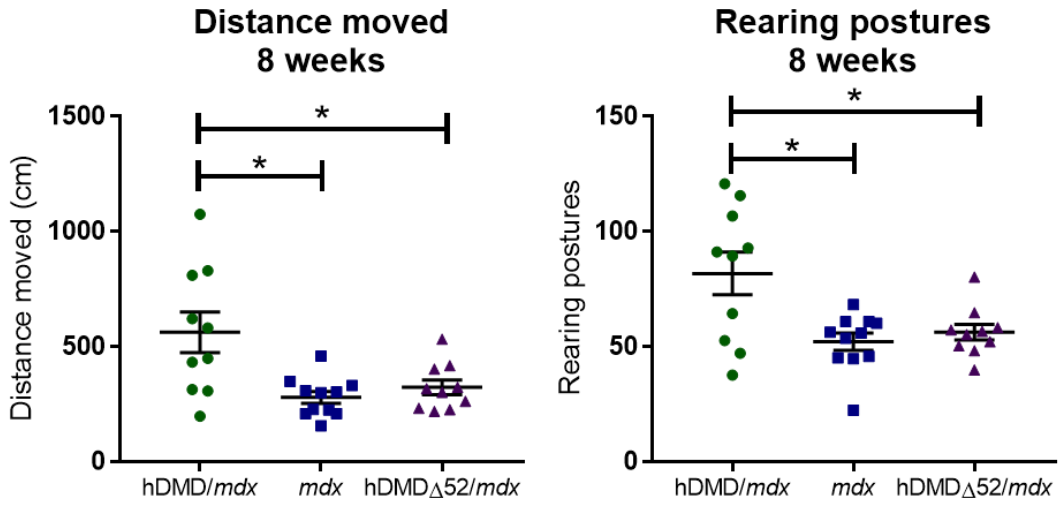

Figure 11: Assessment of total distance moved (left) and rearing postures (right) displayed in an open field at 8 weeks of age. hDMD/*mdx* mice (green circles) serve as the healthy control, *mdx* mice (blue squares) serve as the negative control we expect our hDMDΔ52/*mdx* mice (purple triangles) to be similar to. The hDMD/*mdx* mouse is statistically significantly more active in the open field than both dystrophic mice, which are indistinguishable from each other.

Mice were serially tested to assess the baseline of the phenotype of the mouse over the lifetime. 8 weeks is a relatively early test as the mouse is just now considered a young adult. The *mdx* phenotype is mild, and we expect our hDMDΔ52/*mdx* phenotype to be similar. Thus, further assessments were carried out. Generally, the dystrophic phenotype trends continue through all timepoints. At 16 weeks, 1 year, and 1.5 years we saw the expected statistically significant decrease in overall distance moved by both the *mdx* and hDMDΔ52/*mdx* mice compared to the hDMD/*mdx* mice. Rearing postures

generally continued to trend downward in the dystrophic mice, although it was not always statistically significant.

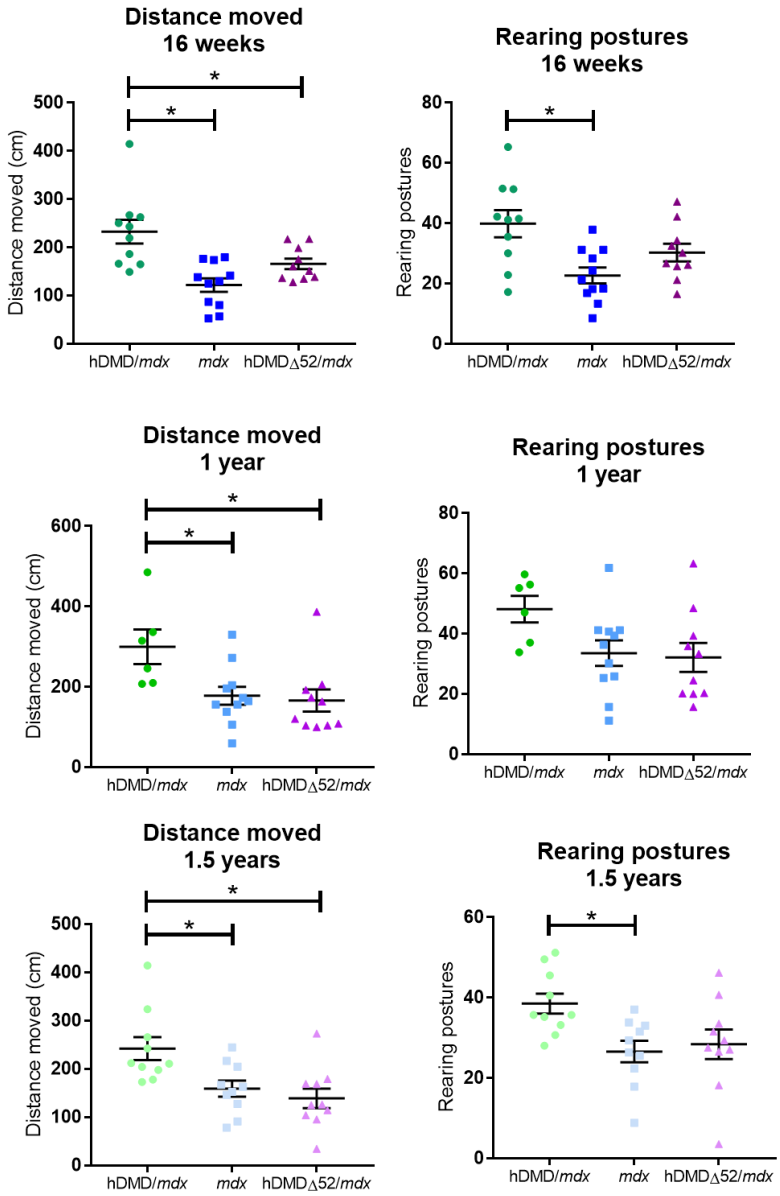

Figure 12: Asessment of total distance moved (left) and rearing postures (right) at 16 weeks, 1 year, and 1.5 years of age. hDMD/*mdx* mice serve as the healthy control, *mdx* mice serve as the negative control we expect our hDMDΔ52/*mdx* mice to be

similar to. The distance traveled measures continues such that the hDMD/*mdx* mouse travels more than both dystrophic mice, which are indistinguishable from each other, across all time points. Rearing postures are generally decreased in both dystrophic mice compared to the hDMD/*mdx* mouse strain, however this difference is not always statistically significant.

Rather than comparing between mice strains at one time point, we have also compared within a mouse strain across time. Notably there is a dramatic drop in total distance moved after the 8-week time point. This is interestingly also true for the healthy control hDMD/*mdx* mouse, although the 8-week value for the hDMD/*mdx* mouse is about twice as much than the dystrophic strains. Thus, even a dramatic drop within the strain over time can still lead to differences across strains. Also, somewhat unexpectedly we saw no difference between the 16-week time point and 1.5 years in any strain, particularly in either dystrophic strain. In general, it is thought that aging mice should exacerbate the dystrophic phenotype. We did not observe this phenomenon in this test at this time point. It may be that 1.5 years is not old enough, as it is not uncommon to see aged *mdx* mice reported at 20+ months old[236].

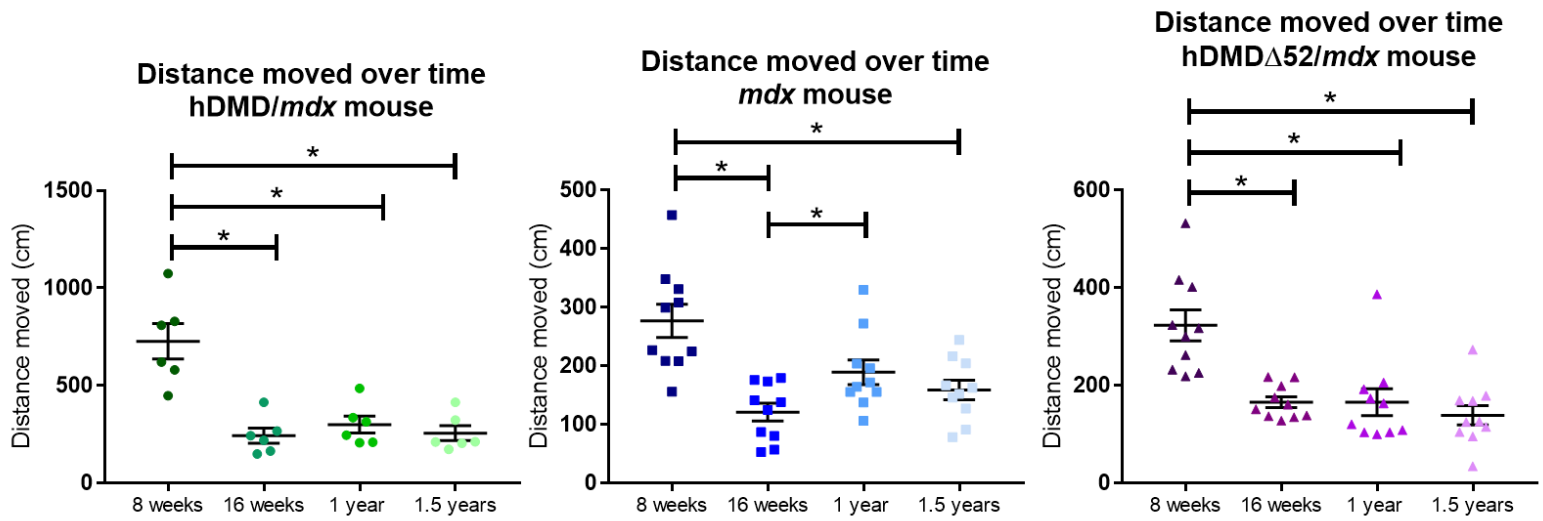

Figure 13: All mice strains decreased their overall distance moved after 8 weeks of age. No strains, including both dystrophic mouse strains, show statistically significant decreases in overall distance moved between 16 weeks and 1.5 years or 1 year and 1.5 years of age.

Rearing postures within each mouse strain over time displays a similar pattern as distance moved: there is a significant decrease between 8 weeks of age and 16 weeks of age, and otherwise the number of rearing postures displayed stayed relatively steady over time in all three genotypes. In both primary outcomes from the open field protocol, distance moved and rearing postures, we did not see a decrease between 16 weeks of age and 1.5 years of age in any strain. This is to be expected for the hDMD/*mdx* mouse but is surprising for the *mdx* and hDMDΔ52/*mdx* dystrophic mouse strains.

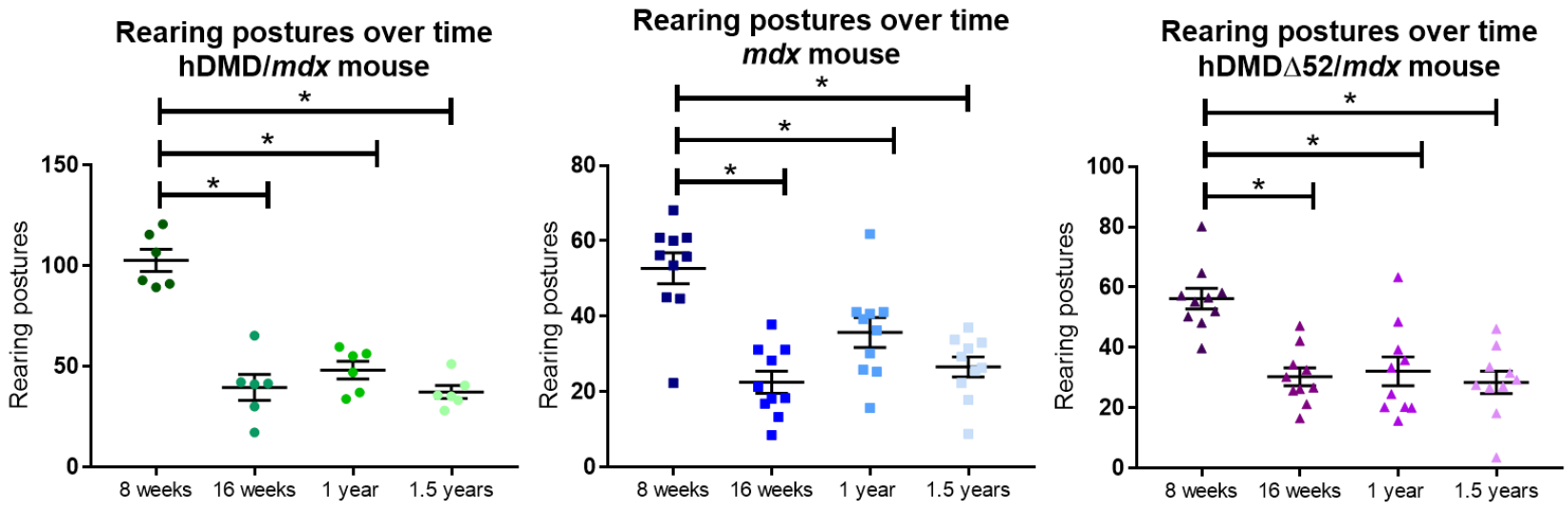

Figure 14: Rearing postures over time within a mouse strain. All three mice strains show a decrease in rearing postures after 8 weeks of age, but none show statistically significant changes between 16 weeks, 1 year, and 1.5 years old.

3.4.5.2 Rotarod Protocol

The accelerating rotarod protocol was conducted at 4 time points as previously specified to test coordination as a proxy for muscle integrity. At all time points we do not see any statistically significant differences between mouse strains.

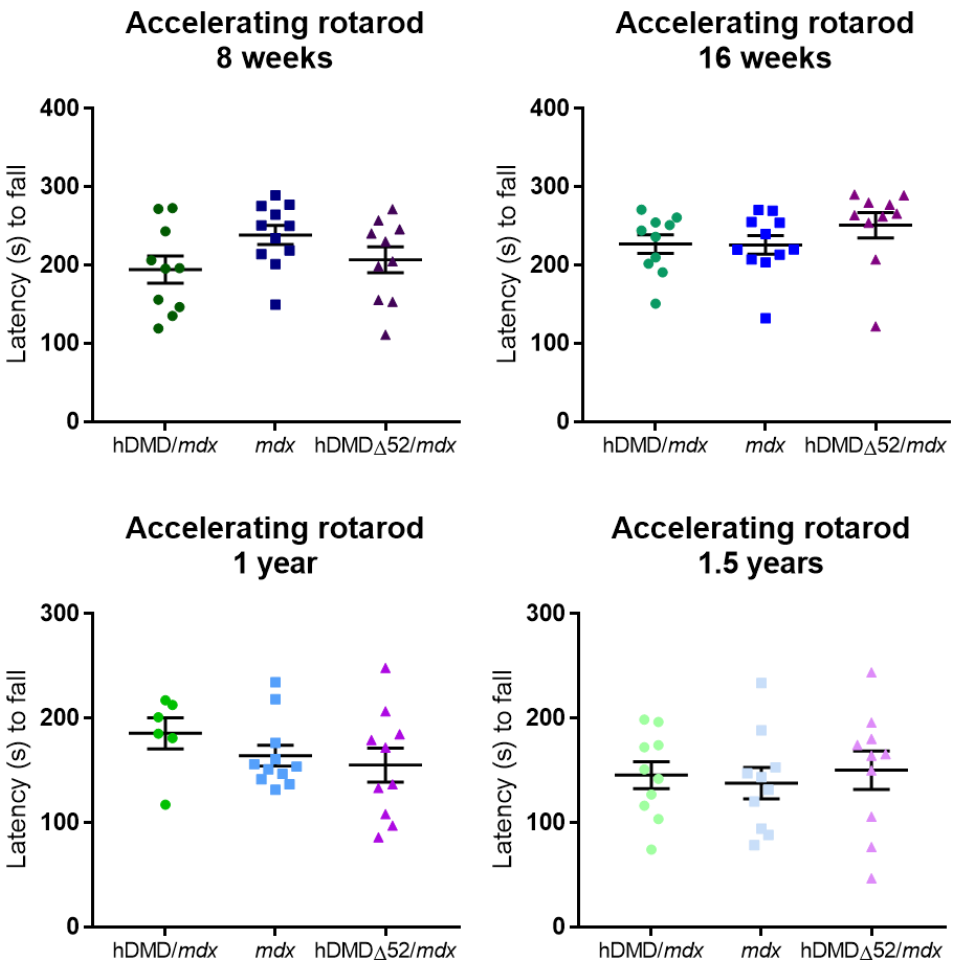

Figure 15: Accelerating rotarod protocol does not show any differences between mouse strains at any of the 4 time points measured.

Within a mouse strain there was a clear effect of aging in the two dystrophic mice. In our healthy control hDMD/*mdx* mouse we do not see any significant differences in latency to fall on an accelerating rotarod over time. The *mdx* mouse shows no distinguishable difference between 8 weeks and 16 weeks of age, but the 1 year and 1.5 year time points show a lack of coordination in comparison to both earlier time points. The hDMDΔ52/*mdx* mice shows no deficit in latency to falling off the accelerating rotarod in the early 8 and 16 week time points, and similarly to the *mdx* mice show a deficit at 1.5 years of age. This protocol clearly demonstrates the effect of aging on coordination in the dystrophic mouse strains, as our healthy h*DMD*/mdx mouse showed no decline, whereas both the *mdx* and hDMDΔ52/*mdx* dystrophic mouse strains fall off of the accelerating rod earlier as they age.

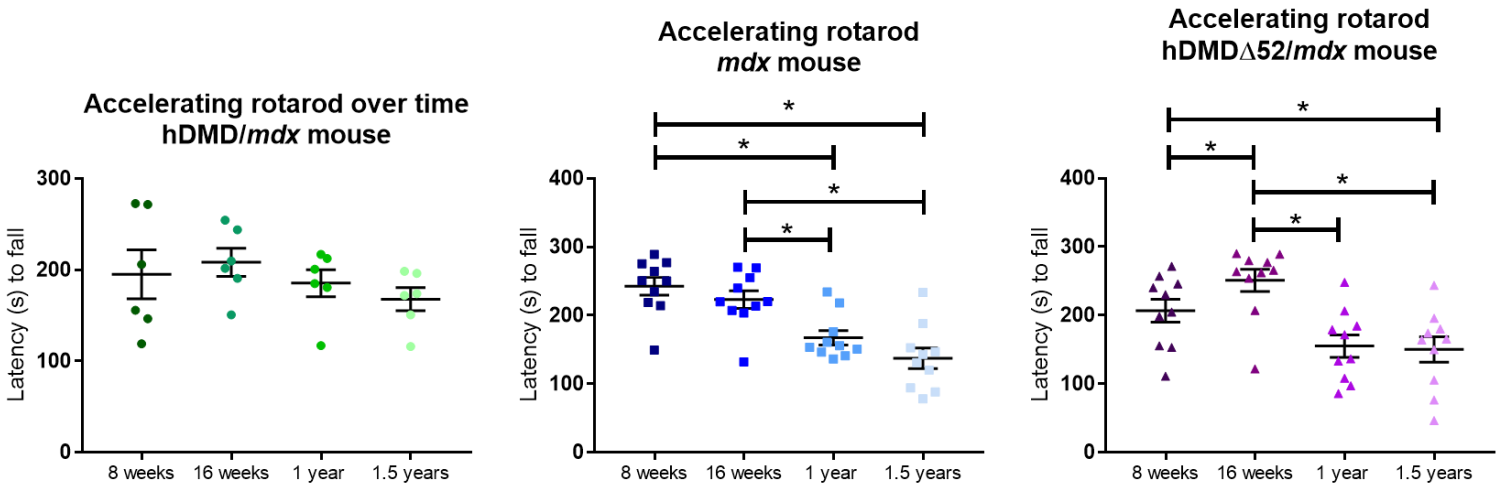

Figure 16: Accelerating rotarod protocol within mouse strains. The hDMD/*mdx* mouse maintains coordination over time, whereas both dystrophic strains see a statistically significant decrease in the latency to fall, and thus a lack of coordination, as they age.

Steady speed rotarod tests were conducted at all 4 time points as previously specified. Generally, over the trials or taking an average of all the trials we saw little to no appreciable difference. At 8 weeks the trend of the dystrophic mouse strains falling off the rod sooner than the hDMD/*mdx* mouse strain was present, but not statistically significant. At 16 weeks of age, the *mdx* mouse and hDMD/*mdx* mouse showed similar time to latency, whereas the hDMDΔ52/*mdx* mouse displayed an increased ability to stay on the rod. At 1 year and 1.5 years of age the expected trend, the hDMD/*mdx* mouse having a higher time to latency compared to the two dystrophic mouse strains, returns but is not statistically significant.

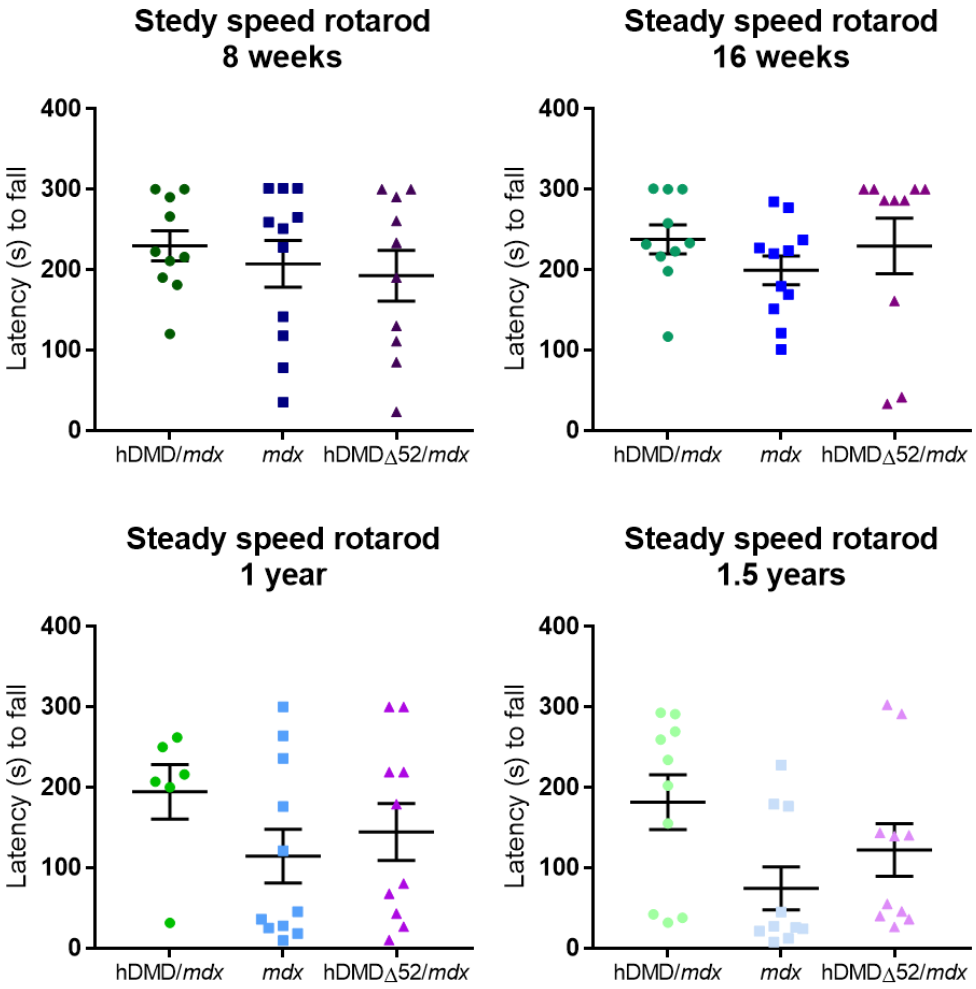

Figure 17: Steady speed rotarod protocol between mouse strains at four time points. Generally, we see a trend of the two dystrophic mouse strains falling off the rod earlier than the healthy hDMD/*mdx* mouse strain, however these trends are not statistically significant.

Within a single mouse strain over time we observed a general decrease in latency to falling off of the rod in the two dystrophic phenotypes. The healthy hDMD/*mdx* mouse strain showed very little loss in coordination on a rotarod at steady speed such that there is no significant difference in these time points.

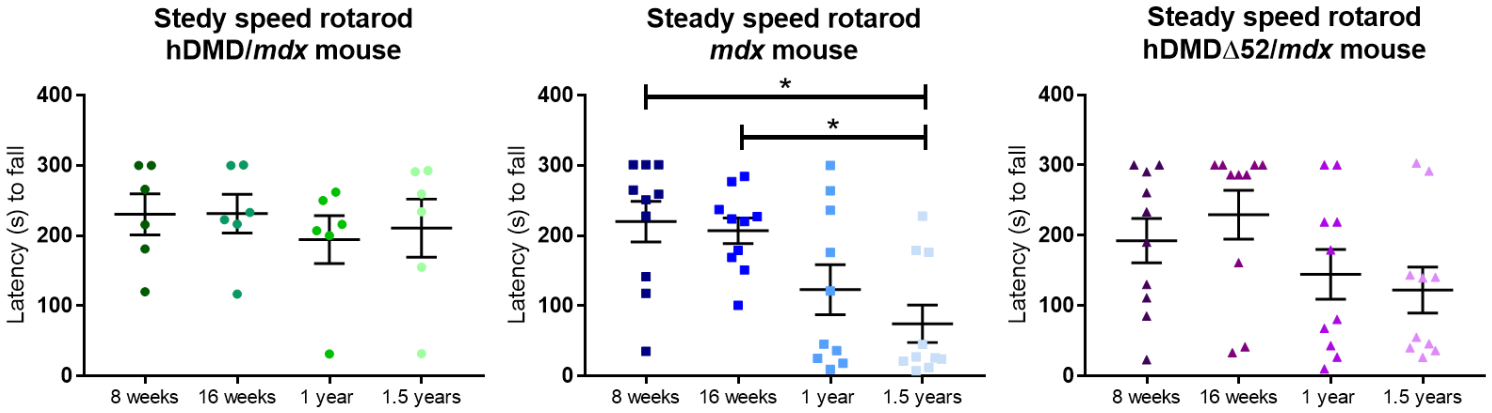

Figure 18: Steady speed protocol within a mouse strain over time. The hDMD/*mdx* mouse maintains coordination and displays no statistically significant differences in latency to fall over the four time points. The *mdx* mouse shows statistically significant decreases at 1.5 years of age, and the hDMDΔ52/*mdx* mouse strain trends downward with time but without a statistically significant change in latency to fall.

3.4.5.3 Foot Fault Protocol

Similar to the rotarod tests, we see little differences in foot fault. Surprisingly, the *mdx* mouse performed well in the foot fault assessment, as fewer faults is indicative of increased coordination. At 8 weeks and 16 weeks of age the *mdx* mouse displays significant coordination compared to both the hDMD/*mdx* and hDMDΔ52/*mdx* mouse, which are indistinguishable from each other.

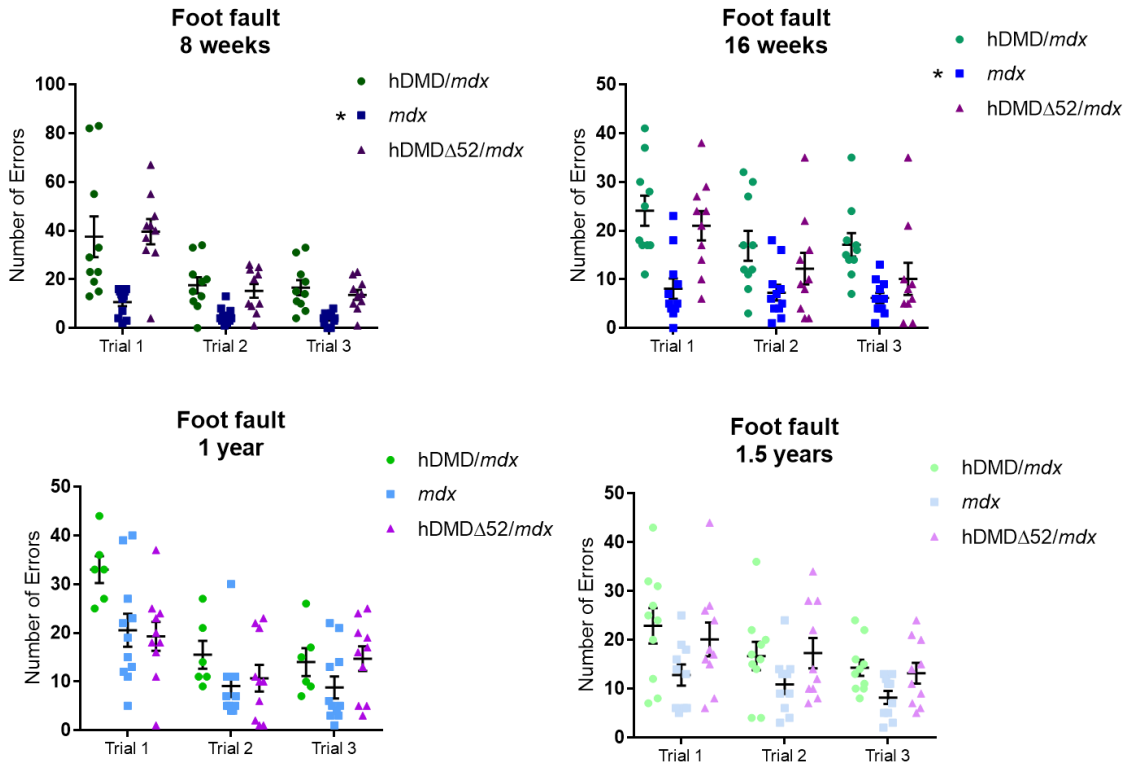

Figure 19: Foot fault protocol between mouse strains at a given time. Overall the *mdx* mouse strain consistently shows the least amount of foot faults, making it the most coordinated strain. The hDMD/*mdx* and hDMDΔ52/*mdx* mouse strains are indistinguishable.

Within the *mdx* mouse strain we see no statistically significant change in increased number of errors committed over time. In both the hDMD/*mdx* and hDMDΔ52/*mdx* mice we see decreases in numbers of errors over time, but this is likely due to the high amount of errors in the first trial at 8 weeks of age for both mouse strains. While there is statistically significant changes in both dystrophic mouse strains over time, we did not see a strong trend of increasing number of errors as expected.

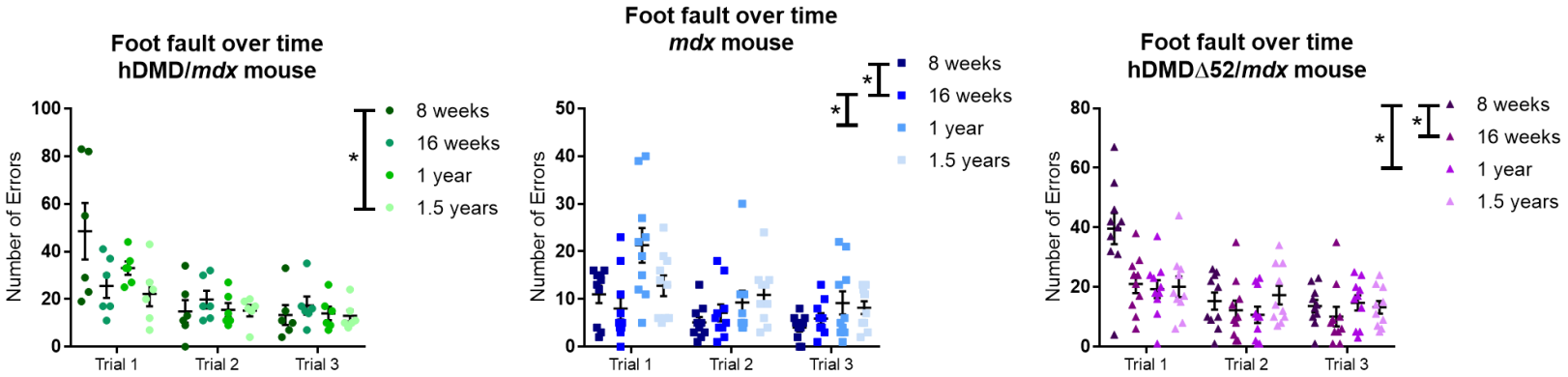

Figure 20: Foot fault protocol within a mouse strain over time. The hDMD/*mdx* mouse displays less faults overall at 1.5 years of age compared to 8 weeks of age, indicative of improved coordination on this test, likely from learning. The *mdx* and hDMDΔ52/*mdx* mouse strains are largely unchanged over time and do not display a loss of coordination with age as expected.

3.4.5.4 Grip Strength Protocol

Front paw grip strength and whole body grip strength were measured directly, with rear paw grip strength being inferred from the subtraction of the front paw average from the whole body average. Similar to the rotarod tests, at 8 weeks and 16 weeks of age we unexpectedly observed increase front paw grip strength in the *mdx* mouse compared to both the hDMD/*mdx* and hDMDΔ52/*mdx* mouse strains. The hDMDΔ52/*mdx* was significantly weaker than the healthy hDMD/*mdx* mouse. By 1 year of age the *mdx* front paw grip strength measurement suggested dystrophy, as it was statistically weaker than the hDMD/*mdx* line. Similarly, our hDMDΔ52/*mdx* mouse was weaker than the healthy hDMD/*mdx* line at 1 year of age. However, at 1.5 years this trend was abolished as the hDMD/*mdx* mouse line appears to have lost some strength.

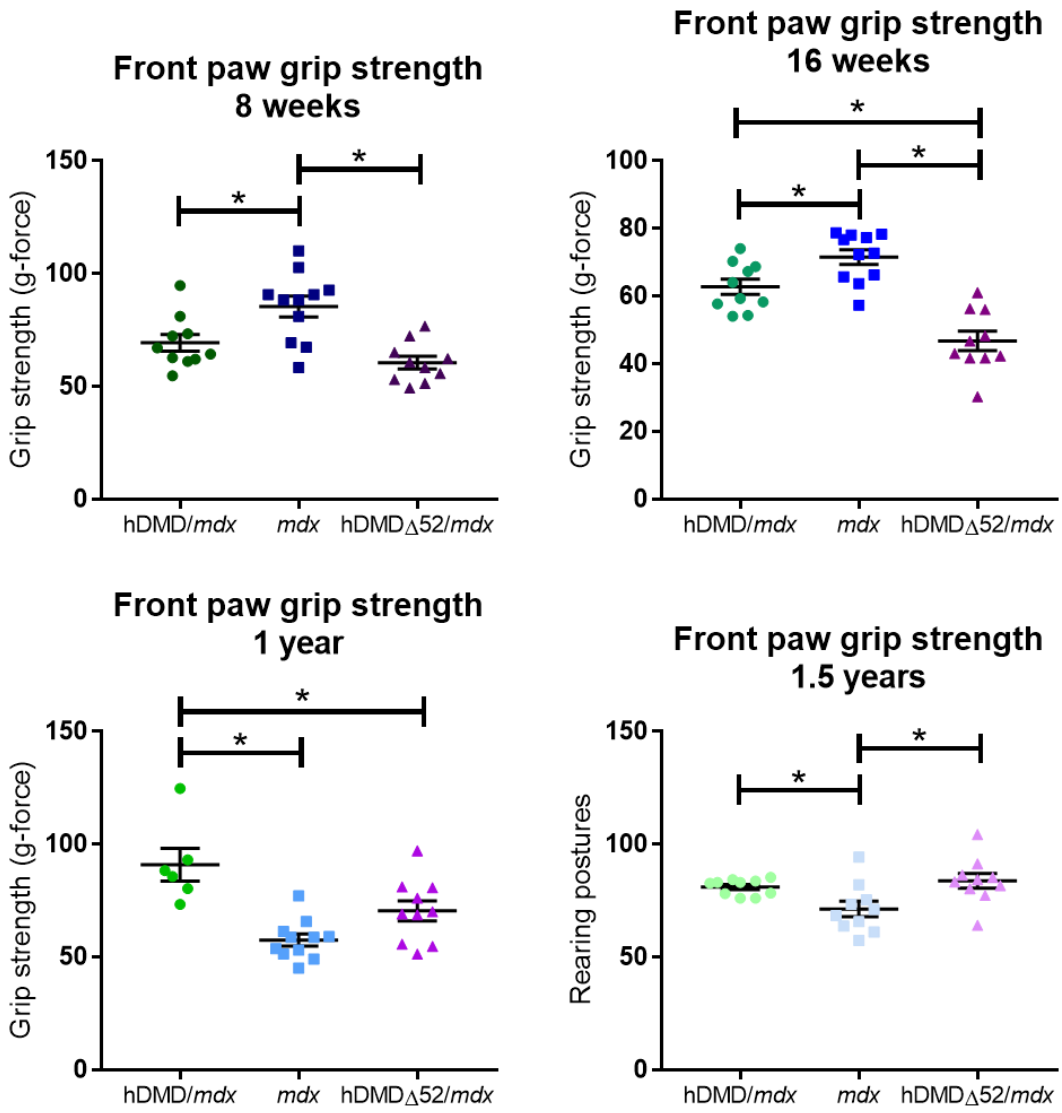

Figure 21: Front paw grip strength between strains over time. The hDMDΔ52/*mdx* mouse strain shows decreased strength compared to the hDMD/*mdx* mouse strain at the first three time points. The *mdx* strain shows significant strength at 8 and 16 weeks of age, but displays significant dystrophy beginning at 1 year of age.

Front paw grip strength compared within a mouse strain measured across time shows little differences in the hDMD/*mdx* mouse line, a general decrease over time in the *mdx* line, and an initial decrease followed by a rise in the hDMDΔ52/*mdx* line.

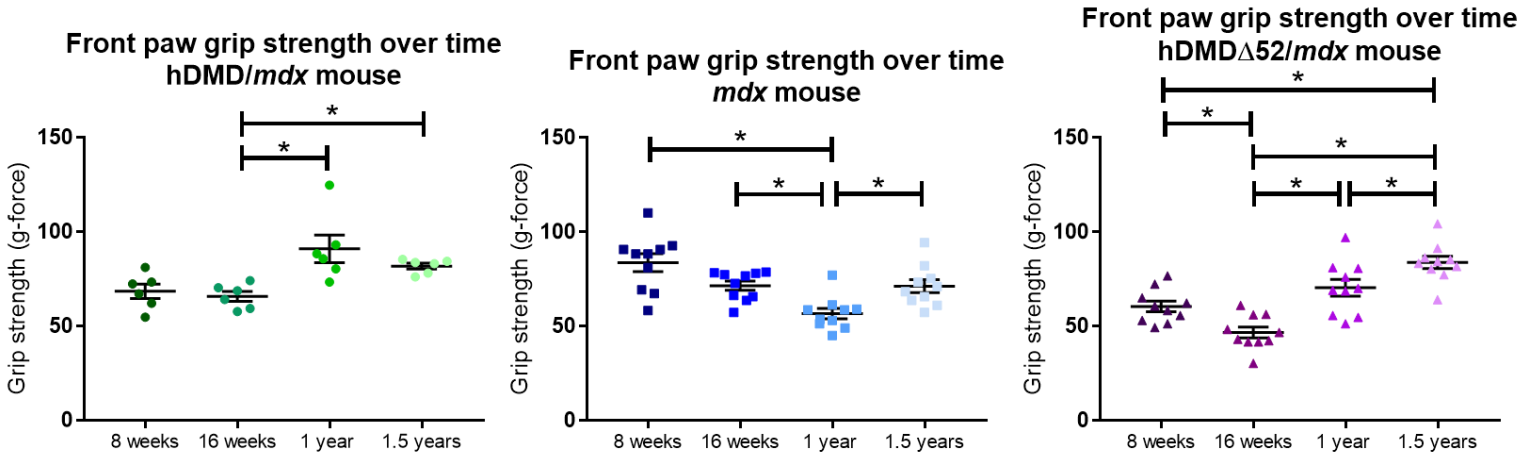

Figure 22: Front paw grip strength within a mouse strain over time. The healthy hDMD/*mdx* mouse shows relatively constant grip strength measures over time as expected. Both dystrophic strains display an unexpected increase in strength at 1.5 years of age after having shown initial signs of decrease.

Whole body grip strength shows little difference in the first year, but at 1.5 years the expected trend emerges of the dystrophic mouse lines being indistinguishable from one another and significantly weaker from the healthy control hDMD/*mdx* mouse.

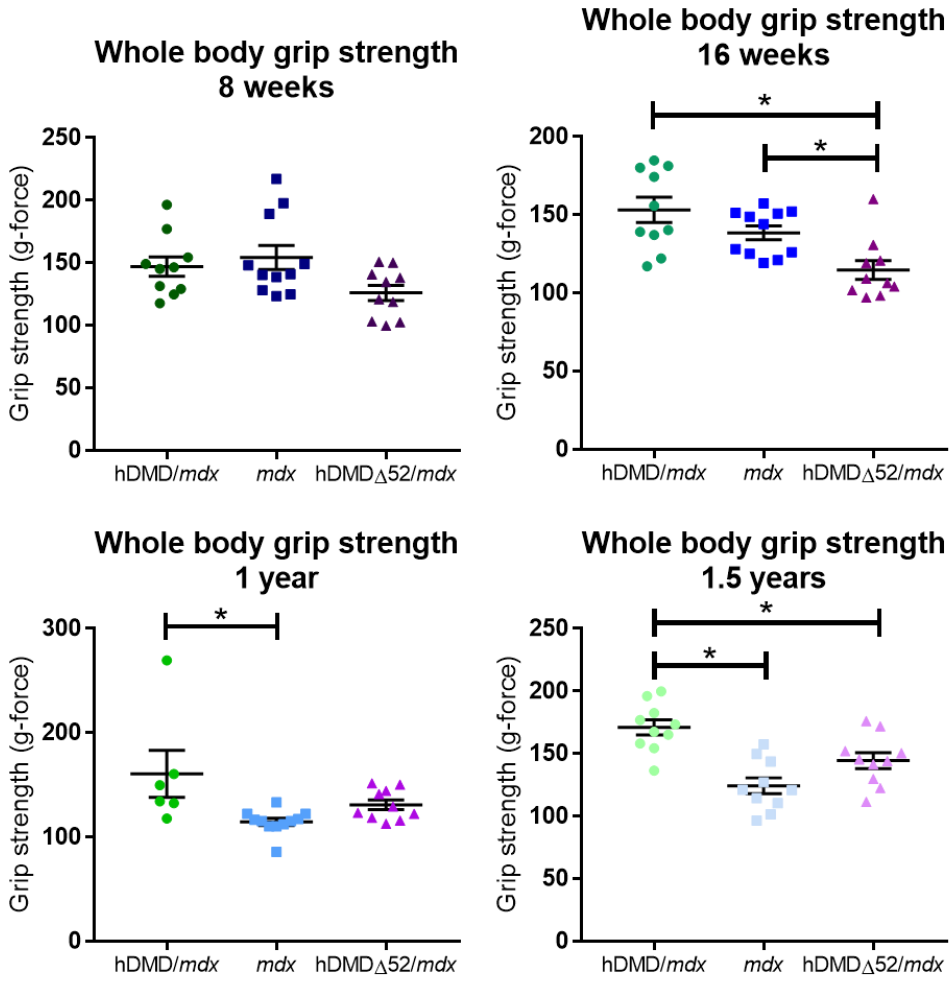

Figure 23: Whole body grip strength between mouse strains over time. Whole body grip strength is largely indistinguishable between mouse strains until the mice have aged significantly, to 1.5 years old, at which time the two dystrophic mouse lines show statistically significantly decreased whole body grip strength compared to the hDMD/*mdx* mouse line.

Whole body grip strength within each mouse strain over time showed few differences. The hDMD/*mdx* mouse did not change over time as expected in this healthy mouse model. The *mdx* mouse did see a decrease at 1 year compared to 8 weeks and 16 weeks, but this decrease was no longer statistically significant by the 1.5 year measurement. The hDMDΔ52/*mdx* mouse had an overall P-value < 0.05, but when comparing the mean of each column to the mean of every other column there was no statistical significance.

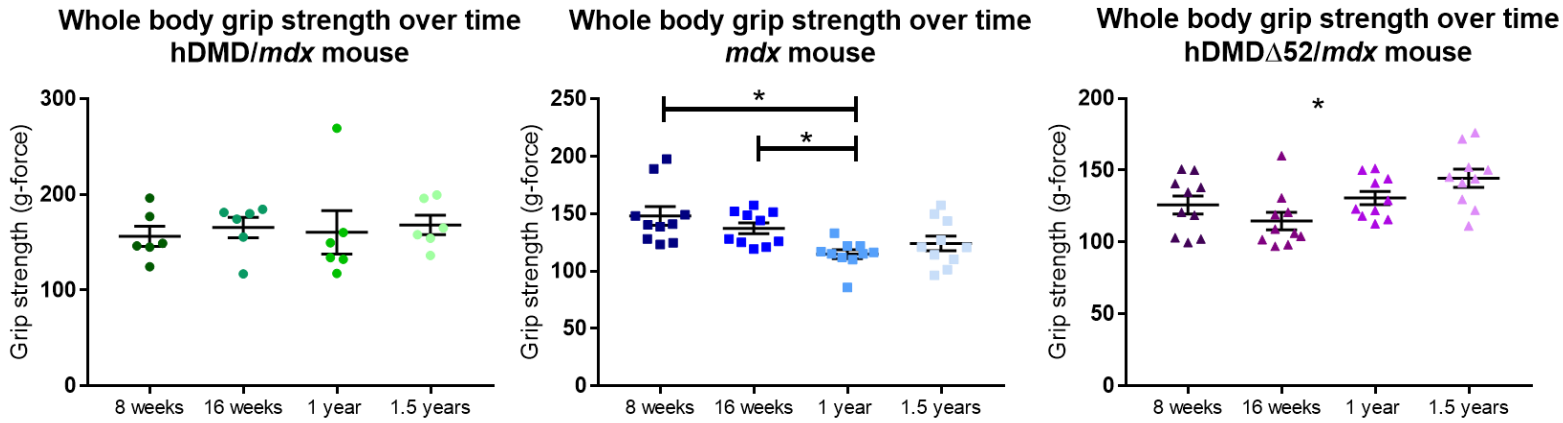

Figure 24: Whole body grip strength within a mouse strain over time. Comparing time points within each mouse strain reveals little to no difference. Interestingly, the two dystrophic mouse strains are not statistically weaker at 1.5 years of age compared to 8 weeks of age.

Rear paw grip strength, as a subtractive measure of front paw grip strength from whole body grip strength, shows similar trends to the whole body grip strength. We see the expected pattern of a stronger hDMD/*mdx* mouse at 16 weeks and 1.5 years, just as in the whole body grip strength.

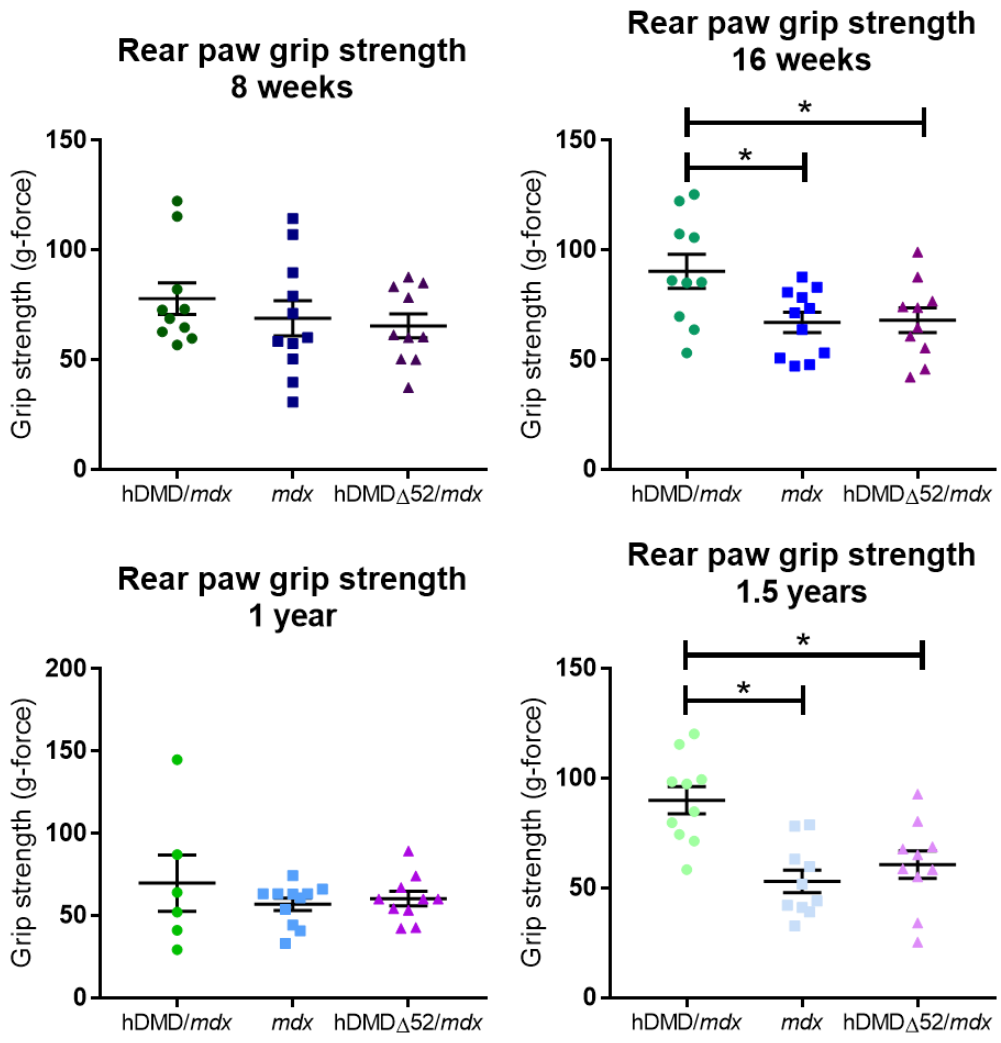

Figure 25: Rear paw grip strength between strains. The expected decreased rear paw grip strength of both dystrophic strains is observed at 16 weeks and 1.5 years of age.

Within mouse strains we see no statistically significant changes over time of rear paw grip strength, mirroring the data we see within strains over time of whole body grip strength. As this measure is subtractive and not measured directly it is not surprising to see the whole body grip strength trends mimicked.

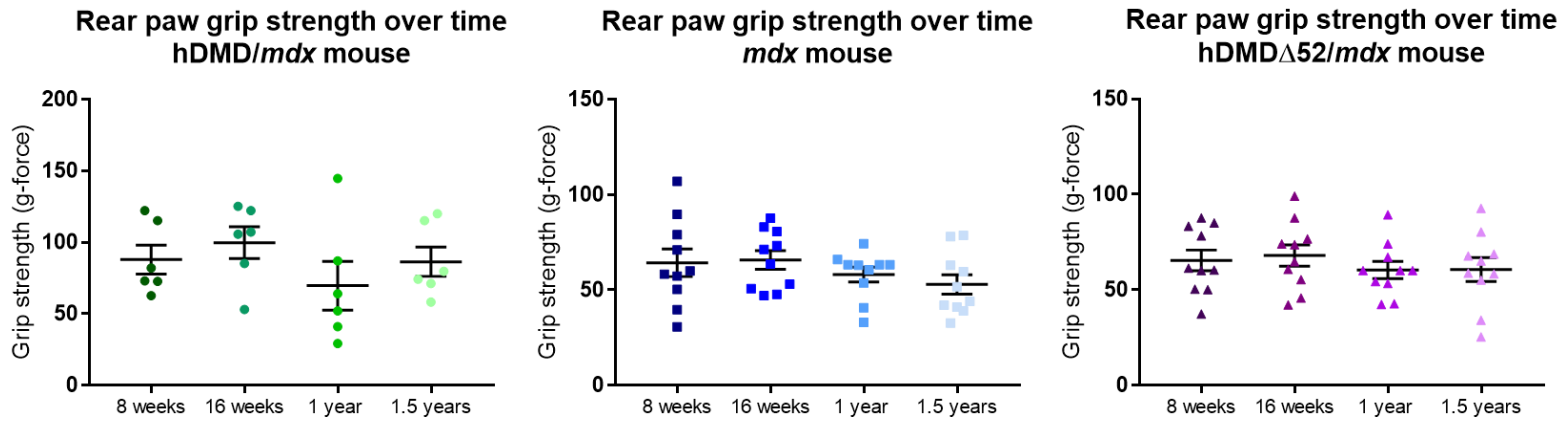

Figure 26: Rear paw grip strength within a mouse strain over time. We observed no statistically significant changes in rear paw grip strength within any of the three mouse strains over the four time points assessed.

3.5 Discussion

3.5.1 Exon 52 Removal in Zygotes

After successful screening of SpCas9 gRNAs for exon 52 deletion *in vitro*, the gRNAs and SpCas9 were transcribed into mRNA for injection into zygotes for creating a transgenic animal utilizing CRISPR-Cas9. Here, we demonstrated modest rates of successful gene editing in a zygote, 3 out of 26 pups born following mRNA injection. While this is only an 11% success rate, this proved much more efficient than another groups attempt at targeting ES cells by homologous recombination with a targeting vector where over 1000 colonies were screened and negative for the deletion of exon 52[230]. When using TALENs to mediate the homologous recombination they showed a 3.2% success rate and again screened 1000 colonies. CRISPR-Cas9 mRNA injection into zygotes appears to be a significantly simpler process, less laborious, and has increased success rates.

3.5.2 Biochemical Analysis to Characterize the hDMDΔ52/*mdx* Mouse

The founder mouse we chose to carry out the linage did not have the perfect ligation 3 base pairs into the PAM, however the 16 base pair insertion scar proved to have no consequence in the removal of exon 52 in the mRNA. Subsequently, we saw a lack of dystrophin protein expression by Western blot and staining regardless of the 16 base pair insertion. We also observed increase serum CK levels compared to wild-type

mice, a hallmark sign of damaged muscle fibers, indicative of the dystrophic genotype and phenotype.

3.5.3 Dystrophic Phenotype of the hDMDΔ52/*mdx* Mouse

The expected dystrophic phenotype of our mouse is mild, like that of the *mdx* mouse. Interestingly, we generally see this to be true in the open field tests and the front paw grip strength tests, but lack to see a difference in the foot fault and rotarod tests. In particular the rotarod tests had high variability and increased sample size may be required. In the future we plan to conduct the grip strength tests with a larger number of pulls/trials for each mouse in order to also test fatigue, as well as assess the mouse by the two limb and four limb hanging protocols[237]. Alternatively, a more severe mouse model can be utilized. For example, we are currently breeding our hDMDΔ52/*mdx* mouse with a utrophin null line, which has a considerably more severe phenotype.

3.5.4 Conclusions

Importantly, we have created a mouse model that may be a relevant tool for the field. It is applicable to tests methods for loss of exon 51, exon 53, and exons 45-55 by genome editing, like CRISPR-Cas9, or RNA modification such as antisense oligonucleotide therapies. Depending on the regulatory landscape, it may be possible to obtain permission for a small phase 1 clinical trial based on efficacy and toxicity of a relevant humanized small animal model, like our hDMDΔ52/*mdx* mouse, alone. This

well-characterized tool presents the field with an exciting new option for pursuing gene therapies for DMD.

Genome editing has proven a powerful tool for creation of new animal models. Compared to the traditional route of creating transgenic animals, use of CRISPR-Cas9 to edit a zygote can be achieved with relative ease. Here, we have shown deletion of a small region in the human *DMD* gene, and other groups have done the same in the hDMD mouse. CRISPR-Cas9 has also been utilized to create various models[238] utilizing single cuts, nicks, knock-ins, and deletions[231]. Precision edits to the genome in an animal model allow for potentially more relevant small animal models to aid in clinical translation. While we have utilized CRISPR-Cas9 to create a more relevant mouse model for DMD, the tool has also been shown to create transgenic larger animal models such as pigs, cows, and nonhuman primates. Thus, this strategy is now being widely applied to a variety of diseases and animal models.

Chapter 4. Validation of a CRISPR-SaCas9 System for Deletion of Exon 51 *In Vitro*

This work was done in collaboration with Christopher Nelson and Charles Gersbach.

4.1 Synopsis

Removal of exon 51 is a common method for shifting a DMD genotype to a BMD genotype. Here we demonstrate feasibility of this using a CRISPR-SaCas9 system with two gRNAs targeted to intronic regions surrounding human dystrophin exon 51. gRNAs were designed to target the human genome as well as conserved sequences in the rhesus macaque genome. We show removal of exon 51 from gDNA, as well as loss of exon 51 in cDNA by PCR amplification. This loss of exon 51 at the genomic level leads to dystrophin protein restoration in immortalized DMD patient myoblasts. We also evaluated potential for off-target cutting in the human genome. These gRNAs can be tested directly in the hDMDΔ52/*mdx* mouse for *in vivo* safety and efficacy and can also be tested in larger animal models such as the rhesus and crab-eating macaques.

4.2 Introduction

Approximately 13% of DMD patients can be treated by removal of exon 51 to shift to a BMD genotype, which represents the largest possible patient population for removal of a single exon. Thus, this is a common method being explored to treat DMD. Our lab has previously used SpCas9 targeted to the intronic region around exon 51 to show viability of this method for removal of exon 51 and dystrophin protein restoration.

While successful, this strategy utilized SpCas9, which is coded by 4104 bp[214]. Packaging SpCas9 in AAV for eventual *in vivo* delivery can be achieved, however the large size of SpCas9 may be a limiting factor. AAV packaging limits are typically reported to be about 4700 bp[239]. Thus, utilization of SpCas9 would require two vectors for packaging both the SpCas9 and the two gRNAs required to create a deletion. A future gene therapy for DMD utilizing AAV would ideally only require one AAV per treatment for manufacturing considerations, both cost and logistics. Thus, rather than continue with the already verified SpCas9 system we set out to create a system utilizing the smaller SaCas9. SaCas9 has been shown to have comparable on-target activity to SpCas9 while creating fewer off-target DNA breaks[240]. SaCas9 is 3156 bp[49], about one kb smaller than SpCas9. This easily allows packaging of SaCas9 and one gRNA into a plasmid ready for AAV production. As our system is a deletion we do require two gRNAs, but future engineering of smaller elements may allow both gRNAs and SaCas9 to fit into the AAV packaging limit. There is a clear need for exploration of potential permanent therapeutics for DMD, thus we investigated a CRISPR-SaCas9 system for exon 51 removal.

4.3 Materials and Methods

4.3.1 Design of gRNAs to Delete Exon 51

Intronic regions directly upstream and downstream of human, rhesus macaque, and crab-eating macaque exon 51 in *DMD* were obtained from NCBI (NC_022292.1,

NC_027913.1, and NC_022292.1 respectively). The human dystrophin genome surrounding exon 51 was annotated for any differences compared to the rhesus macaque genome. Sites with the required PAM (NNGRRT) and at least 18 bp of conserved sequence were marked as eligible sequences. Potential gRNA sequences were run through the Basic Local Alignment Search Tool (NCBI) to ensure the protospacer would only target one site in the human genome, the intended on-target cut site in the intronic regions around exon 51. Eligible sequences were ordered from IDT DNA for cloning.

4.3.2 Plasmid Constructs

A stable SaCas9 expression plasmid without ITRs containing CMV driven SaCas9 was created from the Zhang AAV plasmid containing (Addgene 61592). Similarly, the gRNA cassette was cloned into a plasmid driven by the hU6 promoter with BbsI cloning sites.

4.3.3 Molecular Cloning

Molecular cloning was carried out as described in 3.3.3 Molecular Cloning.

4.3.4 Cell Culture and Transfection

Cell culture and transfection of HEK293T cells was carried out as described in 3.3.4 Cell Culture and Transfection. Immortalized myoblasts from a DMD patient lacking exons 48-50 were maintained in basal skeletal muscle media (PromoCell) supplemented with 20% fetal bovine calf serum (Sigma), 50 μg/mL of fetuin (Sigma), 10

ng/mL of human epidermal growth factor (Sigma), 1 ng/mL of human basic fibroblastic growth factor (Sigma), 10 μg/mL of human insulin (Sigma), 1% GlutaMAX (Invitrogen), and 1% penicillin/streptomycin (ThermoFisher) or antibiotic-antimycotic (ThermoFisher). Cells were maintained at 37°C at 5% CO_2. HEK293T cells were transfected as described in 3.3.4 Cell Culture and Transfection. Immortalized DMD patient myoblasts were electroporated as previously described[48]. Briefly, one million cells were electroporated in PBS using the Gene Pulser XCell (BioRad) with 20-40 μg of DNA in less than 20 μl of volume at 160 volts, a capacitance of 1000, and infinite resistance. Cells were transferred to a 6-well plate after electroporation and allowed to grow undisturbed for 3 days.

4.3.5 Surveyor Assay for Indel Detection

The surveyor assay was carried out as specified in 3.3.5 Surveyor Assay for Indel Detection.

4.3.6 *In Silico* Off-Target Prediction

Off-target analysis was conducted *in silico* using Cas-OFFinder[50]. Initially, the protospacer being evaluated was the query sequence, the PAM type selected was SaCas9 with NNGRRT, up to 4 mismatches were allowed, and the genome specified was either the homo sapiens of macaca mulatta. Bulge size was not considered at this time. Results were sorted by number of mismatches. Further off-target analysis was conducted on final gRNA selection as the query sequence, the PAM type selected was SaCas9 with

NNGRRT, up to 4 mismatches, and up to 2 bp bulge in both DNA and RNA. This was run for homo sapiens, macaca mulatta, and macaca fascicularis. Further, the human off-target analysis was expanded to include up to 9 mismatches rather than 4.

4.3.7 Detection of Exon 51 Deletion

Exon 51 deletion was detected using primers surrounding the gRNA target sites and the AccuPrime High Fidelity PCR kit, with the general protocol following the methods described in 3.3.6 *In Vitro* Testing of gRNAs to Delete Exon 52.

4.3.8 Cell Differentiation

Immortalized DMD patient myoblasts were grown up to confluency in growth media and then maintained in differentiation media consisting of DMEM supplemented with 1% insulin-transferrin-selenium (Invitrogen) and 1% penicillin/streptomycin (Invitrogen) for 6-7 days. After visual inspection to determine differentiation, myofibers were trypsinized for harvested, centrifuged, and media was aspirated away from the cell pellet. The pellet was resuspended in PBS, centrifuged, and the PBS was aspirated. Cell pellets were snap frozen in liquid nitrogen and stored at -80°C.

4.3.9 mRNA Analysis

RNA was isolated from differentiated myofibers using the RNEasy Plus Mini Kit (Qiagen) according to the manufacturer's instructions. RNA was reverse transcribed to cDNA using the VILO cDNA synthesis kit (Life Technologies) for 2 hours at 42°C according to the manufacturer's instructions. PCR amplification, gel analysis, and

sequencing were performed as described in 3.3.8.1 Endpoint PCR Assay to Detect Genomic Deletions.

4.3.10 Western Blot

Detection of dystrophin protein was carried out by Western blot. Differentiated immortalized DMD patient myofibers were collected and lysed in RIPA buffer (Sigma) and supplemented with a protease inhibitor cocktail (Roche). Protein was quantified and processed as specified in 3.3.8.3 Western Blot.

4.3.11 Deep Sequencing of Potential Off-Target Sites

Potential off-target sites for both final gRNA selections were evaluated *in silico* with up to 9 mismatches with 0 bp bulge, and with up to 4 mismatches with up to 2 bp bulge in DNA and RNA. Results were compiled and scored by applying higher weight to genome mismatches distal to the PAM. Bulge location was not taken into account in the weighting. The sequence that had the least amount of mismatches in the genome and no bulge was selected for evaluation regardless of score. The sequences with the 4 highest scores for sequences with no bulge, not including the initial lowest mismatch, were also selected. Sequences with the 5 highest scores including bulges were selected for analysis, but sequences that were effectively repeats of each other with the exception of different bulge location were not included. Thus, each gRNA was analyzed for off-targets at 5 locations with no bulge and 5 locations with 1-2 bp bulges in the DNA or

RNA. Primers were designed to amplify the on-target and off-target regions in amplicons of less than 200 bp in size.

HEK293T cells were transfected with SaCas9 only or SaCas9 and either the upstream or downstream gRNA in triplicate. gDNA from these cells were combined such that the three biological replicates were combined into one. gDNA was PCR amplified around the on-target and 20 off-target regions of interest for 30 cycles using the AccuPrime High Fidelity PCR kit (Invitrogen) and cleaned with Agencourt AMPure XP Beads (Beckman Coulter). A second round of PCR amplification was used to add Illumina flowcell binding sequences and experiment-specific barcodes on the 5′ end of the primer sequence. The PCR products were pooled and sequenced with 150 bp paired-end reads on an Illumina MiSeq instrument. Samples were demultiplexed according to assigned barcode sequences and the added Illumina sequences were trimmed from reads. Because the amplicons are less than 200 bp there was overlap in the paired-end reads. This overlap was used to create a consensus PCR amplicon for each paired-end read using single ungapped alignment. Indel analysis was performed using default CRISPResso settings and a 20 bp window[241].

4.4 Results

4.4.1 On-Target Activity of Individual gRNAs

gRNAs were designed to target intron 50 and intron 51 within 3000 bp of exon 51. Initially all protospacers were designed to be 22 bp long. The deletion product was

designed to be relatively small in size, thus we only designed gRNAs near the exon. These gRNAs target conserved regions in the human and rhesus macaque genome. 6 gRNAs in intron 50 (156, 157, 159, 168, 170, 171) and 3 gRNAs in intron 51 (160, 166, 167) showed on-target activity when tested individually *in vitro*. gRNAs were first tested individually with SaCas9 in HEK293T cells by transfection, and gDNA was assessed for on-target activity by the Surveyor assay.

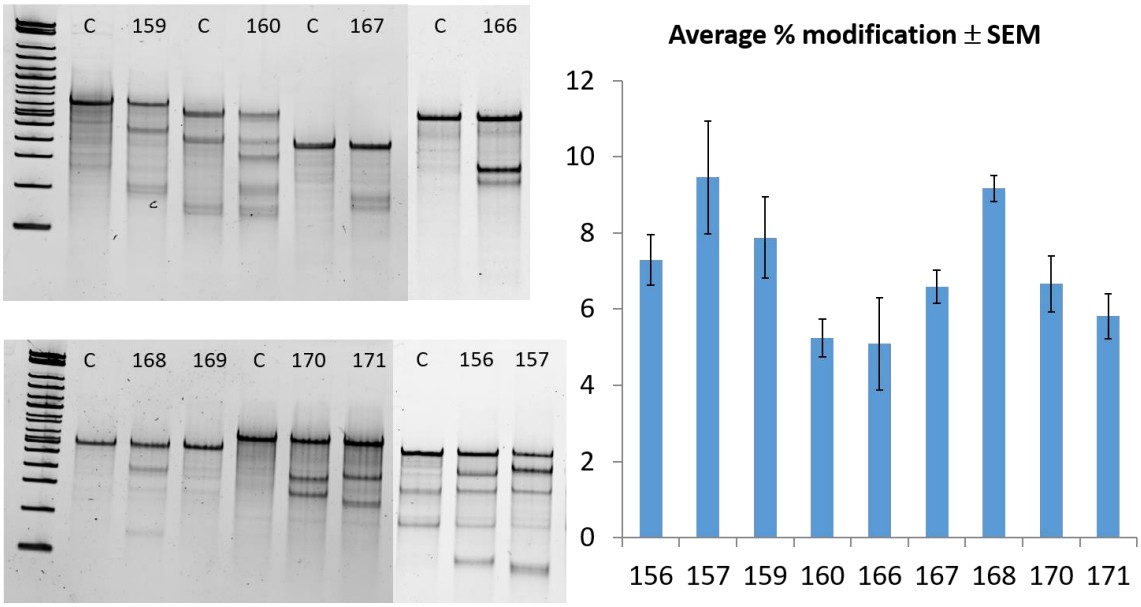

Figure 27: On-target activity of individual gRNAs *in* vitro for exon 51 deletion. The left shows representative on-target activity of individual gRNAs, C is a negative control transfected with only SaCas9. The right shows the average percent modification measured by densitometry of bands on the gel by any given gRNA, n=3, mean ± SEM.

4.4.2 *In Silico* Off-Target Predictions for Individual gRNAs

In silico off target analysis of all nine gRNAs was run using Cas-OFFinder as specified in 4.3.*6 In Silico* Off-Target Prediction. gRNAs were evaluated based on how

far away in the genome they targeted from exon 51, the percent modification as measured by Surveyor in **Error! Reference source not found.**, and how many potential off-targets were found in the human and rhesus macaque genome.

Table 1: *In Silico* off-target analysis for gRNAs flanking exon 51. gRNA column is an arbitrary number used for labeling, where is relative to exon 51 does the gRNA target, how far (nt) is the number of nucleotides the predicted gRNA cut site is from exon 51 in the human genome, human off target is the number of hits in the human genome that contain a certain amount of mismatches from the *in silico* analysis, and the rhesus off target column is the same *in silico* analysis for the rhesus genome.

gRNA	Where	How far (nt)	% mod ± SEM	Human off target	Rhesus off target
JCR156	upstream	1300	7.28% ± 0.66	4 mismatch: 23 3 mismatch: 6 2, 1 mismatch: 0	4 mismatch: 19 3 mismatch: 7 2 mismatch: 1 <2: 0
JCR157	upstream	1284	9.45% ± 1.48	4 mismatch: 6 <4 mismatch: 0	4 mismatch: 5 <4 mismatch: 0
JCR159	upstream	101	7.88% ± 1.07	4 mismatch: 16 <4 mismatch: 0	4 mismatch: 15 3 mismatch: 1 <3 mismatch: 0
JCR168	upstream	1824	9.17% ± 0.35	4 mismatch: 21 3 mismatch: 1 <3 mismatch: 0	4 mismatch: 13 <4 mismatch: 0
JCR170	upstream	2851	6.66% ± 0.74	4 mismatch: 1 3 mismatch: 1 <3 mismatch: 0	4 mismatch: 3 <4 mismatch: 0
JCR171	upstream	2947	5.82% ± 0.59	4 mismatch: 5 3 mismatch: 1 <3 mismatch: 0	4 mismatch: 2 3 mismatch: 1 2 mismatch: 1

					<2 mismatch: 0
JCR160	downstream	78	5.25% ± 0.50	4 mismatch: 2 <4 mismatch: 0	4 mismatch: 4 <4 mismatch: 0
JCR166	downstream	1266	5.09% ± 1.21	4 mismatch: 25 3 mismatch: 5 <3: 0	4 mismatch: 17 3 mismatch: 5 <3 mismatch: 0
JCR167	downstream	1534	6.59% ± 0.44	4 mismatch: 4 3 mismatch: 2 <3 mismatch: 0	4 mismatch: 10 <4 mismatch: 0

gRNAs JCR157 and JCR160 were selected for further evaluation.

4.4.3 Deletion of Exon 51 in Two Cell Types Using CRISPR–SaCas9

gRNAs JCR157 and JCR160, which target the intronic region around exon 51 for deletion of exon 51, were transfected into HEK293T cells and electroporated into immortalized DMD patient myoblasts with SaCas9 to determine compatibility for creating a deletion. gDNA was PCR amplified around the region of interest and electrophoresed on an agarose gel for assessment.

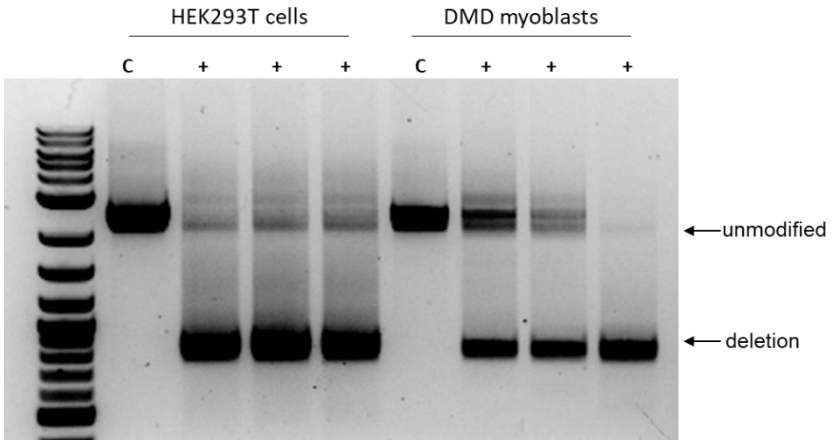

Figure 28: Unmodified parent bands and smaller sized bands indicating the deletion of exon 51 mediated by our CRISPR-SaCas9 and 2 gRNA system. C is control treated with only SaCas9, and + are cells treated with both gRNAs and SaCas9.

4.4.4 Protospacer Length Effects on On-Target Activity

JCR157 and JCR160 protospacers were originally designed to be 22 bp long. The same location was targeted, but with varying lengths of protospacer to investigate if the change in length effected on-target activity. Protospacer length was varied from 19 to 23 nucleotides long and tested for on-target activity in HEK293T cells.

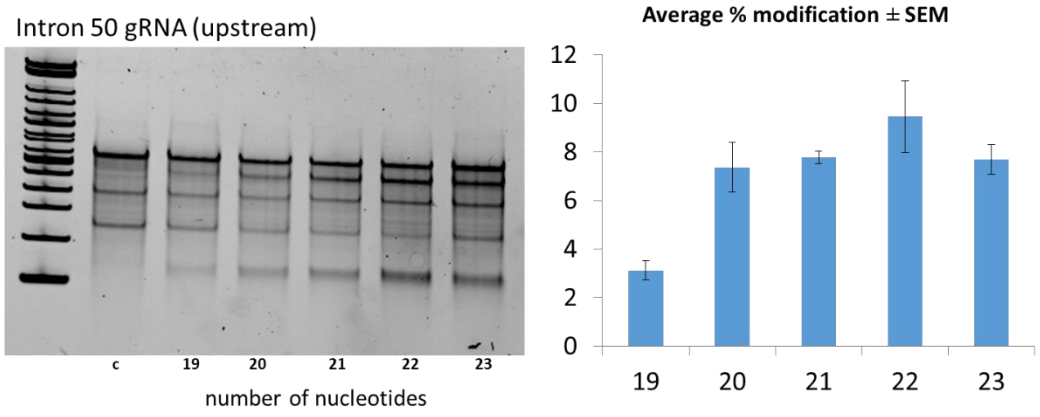

Figure 29: JCR157, originally with a 22 nucleotide length protospacer, modified to have protospacer length between 19 and 23 bp and tested in HEK293T cells. A

representative Surveyor assay is shown. The average percent modification was calculated from n=3, average ± SEM. C is control transfected with only SaCas9.

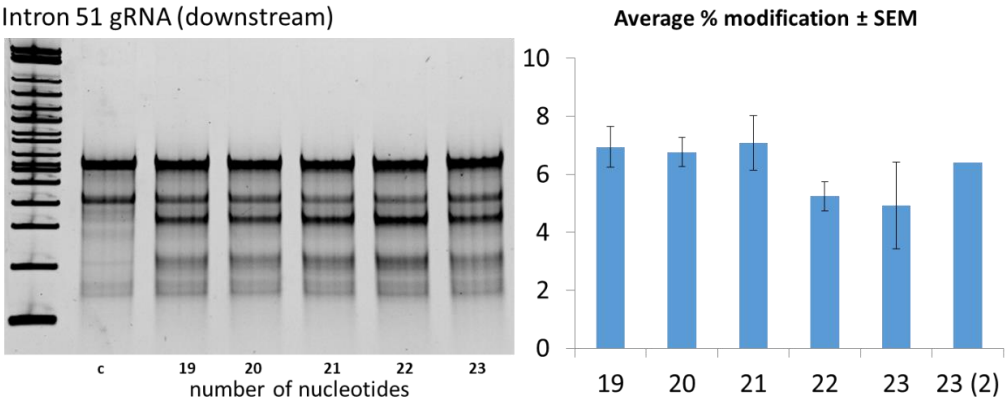

Figure 30: JCR160, originally with a 22 nucleotide length protospacer, modified to have protospacer length between 19 and 23 bp and tested in HEK293T cells. A representative Surveyor assay is shown. The average percent modification was calculated from n=3, average ± SEM. C is control transfected with only SaCas9. The last lane labeled 23 (2) shows the average of percent modification from 2 gels for the 23 length protospacer, as one value was a clear outlier at 1.9%.

4.4.5 Varying Protospacer Length in Combination Mildly Effects Exon 51 Deletion Efficiency

gRNAs with protospacer lengths of 21, 22, and 23 nucleotides both upstream and downstream of exon 51 were assessed for efficacy as a pair to create deletions after transfection of HEK293T cells.

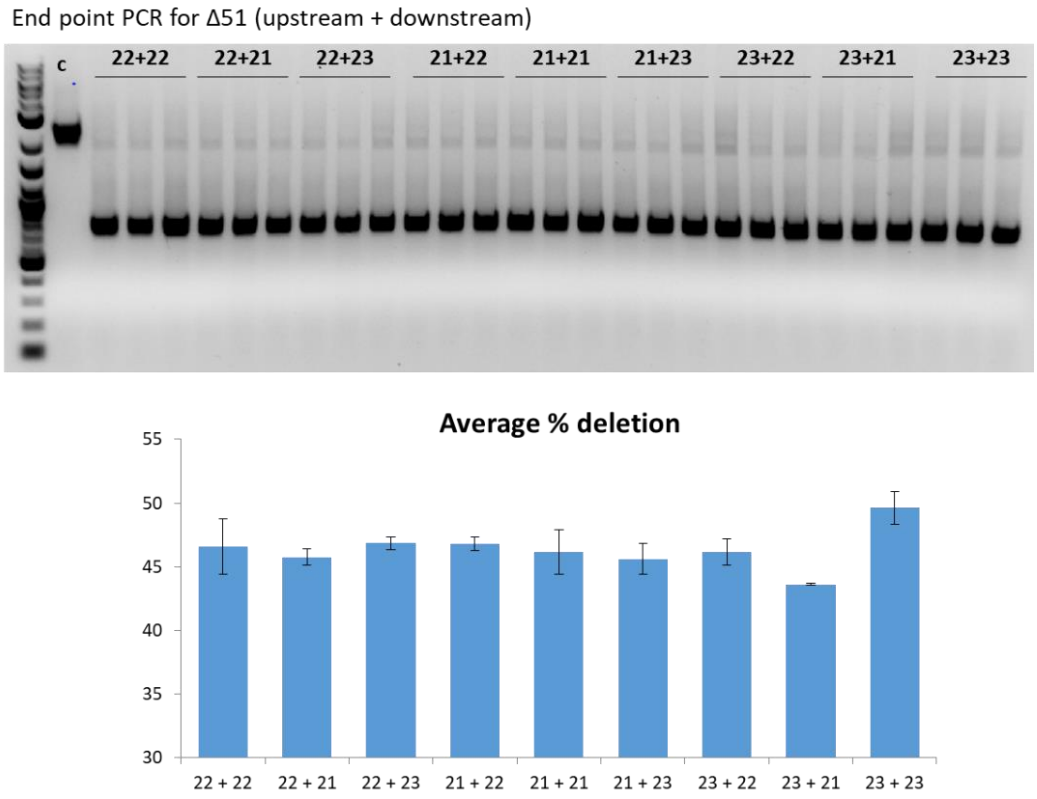

Figure 31: Representative gel image showing deletion of exon 51 in HEK293T cells transfected with SaCas9 and 2 gRNAs flanking the exon of varying lengths. The average ± SEM was calculated from densitometry on n=3.

The gRNA pair using both 23 nucleotide length protospacers was identified as most promising, numbered JCR179 (upstream of exon 51 in intron 50) and JCR183 gRNA (downstream of exon 51 in intron 51).

4.4.6 23 bp Length Protospacers Show Repeatable On-Target Activity

gRNAs JCR179 and JCR183 were tested individually for on-target efficacy in HEK293T cells and DMD immortalized patient myoblasts.

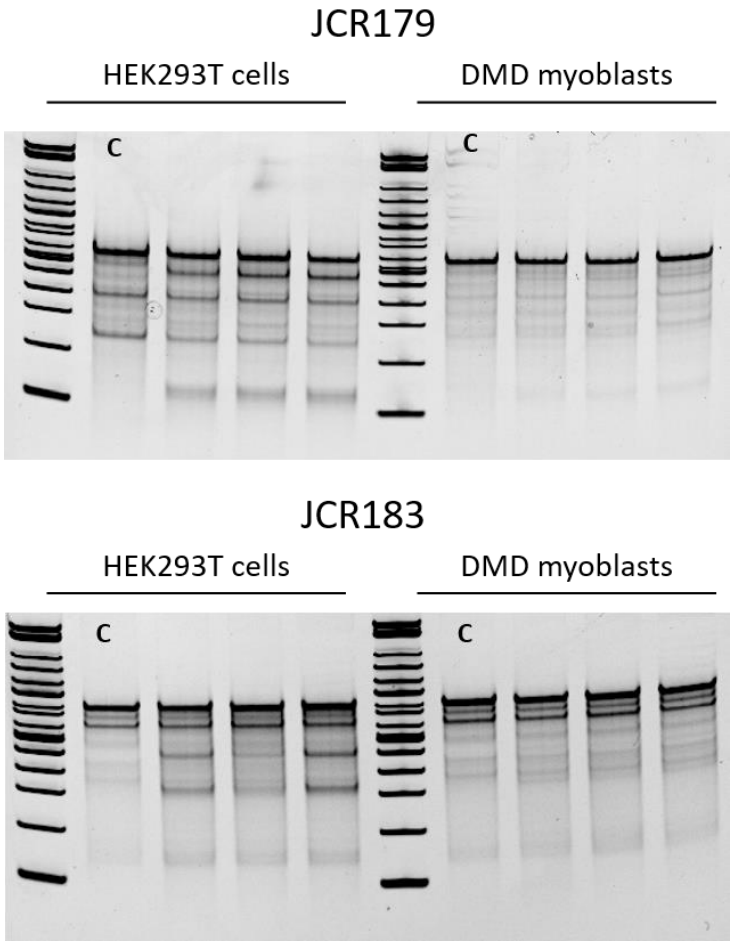

Figure 32: Surveyor assays for both 23 nucleotide length gRNAs in HEK293T cells and immortalized DMD patient myoblasts. C is a control lane with only SaCas9, all other lanes are replicates with the individual gRNA and SaCas9.

Next, JCR179 and JCR183 were transfected together with SaCas9 in HEK293T cells and electroporated into immortalized DMD patient myoblasts to assess potential for creating the desired deletion.

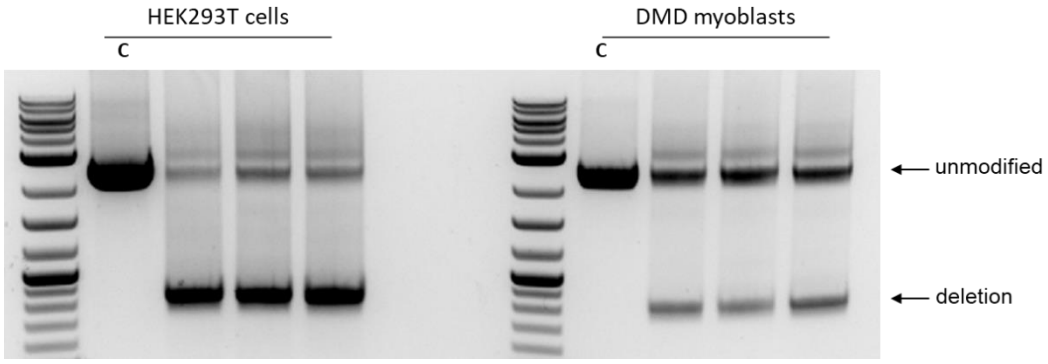

Figure 33: PCR products around exon 51 showing the deletion of exon 51 in the smaller bands on the gel mediated by our CRISPR-SaCas9 system and gRNAs JCR179 and JCR183 in both HEK293T cells and immortalized DMD patient myoblasts. C is a control lane treated only with SaCas9. The following lanes are 3 replicates of the same treatment of both gRNAs and SaCas9.

4.4.7 Deletion of Exon 51 in Genome Leads to Loss of Exon 51 in mRNA

Immortalized DMD patient myoblasts were differentiated and RNA was harvested. RNA was reverse transcribed to cDNA, and the cDNA was amplified by PCR using primers in exon 44 and exon 52. Unmodified parent bands and deletion bands were Sanger sequenced for evaluation of loss of exon 51.

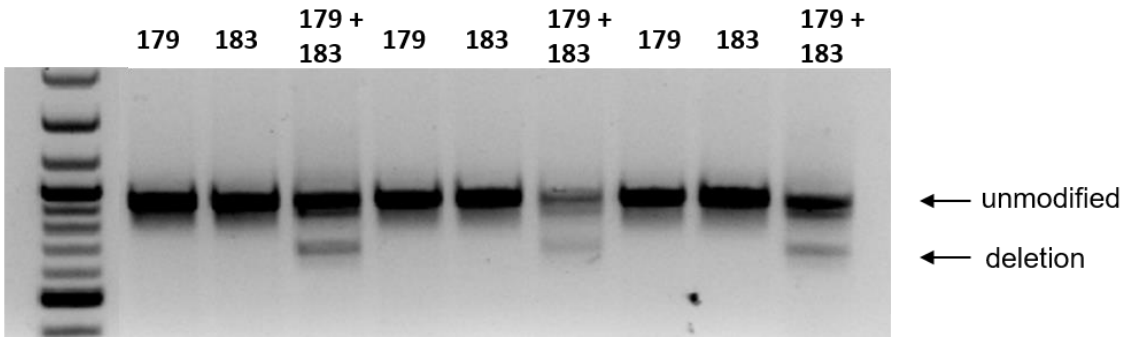

Figure 34: PCR amplification and gel analysis of cDNA shows the smaller deletion band in only cells treated with both gRNAs and SaCas9.

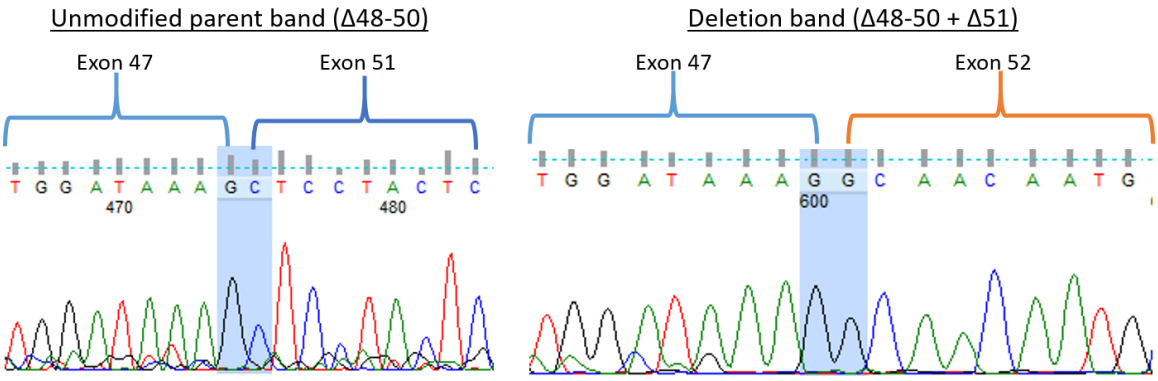

Figure 35: Sanger sequencing of the unmodified and deletion bands from gel extracts in Figure 34 show lack of exon 51 in the deletion band and the exact junction of exon 47 to exon 52 as expected.

4.4.8 Excision of Exon 51 in Genome Leads to Restoration of Dystrophin Protein Expression

Protein was extracted from differentiated myofibers and assessed for dystrophin protein expression by Western blot.

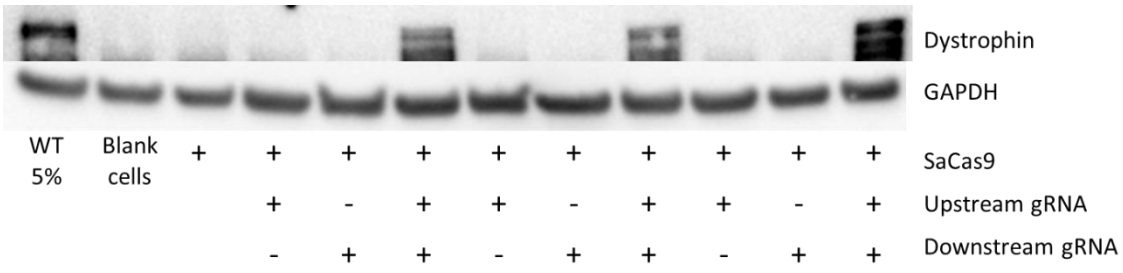

Figure 36: Western blot for dystrophin protein expression from immortalized DMD patient cells. Only cells treated with both the upstream and downstream gRNA and SaCas9 show dystrophin protein restoration expression, indicating that our CRISPR-SaCas9 system is causal.

4.4.9 23 bp Length gRNAs have No Predicted Off-Targets in the Human Genome with 3 or Less Mismatches

gRNAs JCR179 and JCR183 show efficacy individually and as a pair to create a deletion. These gRNAs, now with a 23 bp protospacer, were evaluated *in silico* for

potential off-target activity allowing for up to 4 mismatches in the human, rhesus macaque, and crab-eating macaque genomes.

Table 2: Summary of *in silico* off-target analysis of the upstream gRNA. Number of mismatches refers to the number of nucleotides in the genome that do not match the protospacer. The human, rhesus macaque, and crab-eating macaque genomes were assessed.

gRNA	Human	Rhesus macaque	Crab-eating macaque
JCR179 (upstream)	**1, 2, or 3 mismatches w/0 bulge – 0** 2 mismatches with 1 bulge size – 1, DNA bulge, chr9 3 mismatches with 1 bulge – 6 • Bulge in DNA – 2 in chr9 • Bulge in RNA – 4 in chr3, 6, 12 3 mismatches with 2 bulge size – 7 • Bulge in DNA – 2 in chr6, X • Bulge in RNA – 5 in chr3, 7, 13, 14 4 mismatches – 1 in chr2 4 mismatches with 1 bulge – 122 • Bulge in DNA - 32 • Bulge in RNA – 90	**1 mismatch – 0** 2 mismatches with 2 bulge size – 2, RNA bulge, in chr1, 11 3 mismatch w/0 bulge– 1 in chr18 3 mismatches with 1 bulge – 10 • Bulge in DNA – 4 in chr14, 15, 18 • Bulge in RNA - 6 in chr2, 4, 5, 12 3 mismatches with 2 bulge – 35 • Bulge in DNA – 5 • Bulge in RNA - 30 4 mismatches – 2 in chr1, 3 4 mismatches with 1 bulge – 131 • Bulge in DNA – 47 • Bulge in RNA – 84	**1 mismatch – 0** 2 mismatches with 2 bulge size – 2, RNA bulge, in chr11 3 mismatch w/0 bulge – 1 in chr10 3 mismatch with 1 bulge – 11 • Bulge in DNA – 4 in chr10, 14, 15 • Bulge in RNA – 7 in chr2, 4, 5, 12,13 3 mismatch with 2 bulge – 32 • Bulge in DNA – 4 in chr4, 10, 13 • Bulge in RNA - 28 4 mismatch w/0 bulge – 1 in chr13 4 mismatch with 1 bulge – 120 • Bulge in DNA – 47 • Bulge in RNA - 73

Table 3: Summary of *in silico* off-target analysis of the downstream gRNA. Number of mismatches refers to the number of nucleotides in the genome that do not match the protospacer. The human, rhesus macaque, and crab-eating macaque genomes were assessed.

gRNA	Human	Rhesus macaque	Crab-eating macaque
JCR183 (downstream)	**1, 2, or 3 mismatches w/0 bulge – 0** 3 mismatches with 1 bulge – 10 • Bulge in DNA – 4 in chr9, 11 • Bulge in RNA – 7 off targets in chr2, 15, 18, 11 3 mismatches with 2 bulge – 14 • Bulge in DNA – 0 off targets • Bulge in RNA – 14 off targets in chr12, 3, 1, 2, 21, 17, 6, 14, 9, 18 4 mismatches with 0 bulge – 2 in chr2, 3 4 mismatches with 1 bulge – 121 • Bulge in DNA – 30 • Bulge in RNA – 91	**1 mismatch – 0** 2 mismatches with 2 RNA bulge – 1 (bulge in RNA at chr4) 3 mismatches with 0 bulge – 2 in ChrX 3 mismatches with 1 bulge – 10 • Bulge in RNA – 10 at chr8, 7, 16, 20, 9 3 mismatches with 2 bulge – 21 • Bulge in DNA – 7 in chri8, 17, 11 • Bulge in RNA – 14 in chr8, 4, 10, 6, x, 18 4 mismatches, 0 bulge – 1 in Chr2 4 mismatches with 1 bulge – 92 • Bulge in DNA – 14 • Bulge in RNA – 78	**1 mismatch – 0** 2 mismatches with 2 RNA bulge – 1 (bulge in RNA at chr4) 3 mismatch with 0 bulge – 2 at Chr6, 8 3 mismatch with 1 bulge – 9 • Bulge in RNA – 9 in Chr8, 7, 9, 20 3 mismatch with 2 bulge – 18 • Bulge in DNA – 4 in ch8, 17 • Bulge in RNA – 14 in chr 4, 6, 8, 10, 18, X 4 mismatch with 0 bulge – 1 in Chr2 4 mismatch with 1 bulge – 83 • Bulge in DNA – 15 • Bulge in RNA – 68

4.4.10 Deep Sequencing at Potential Off-Target Sites in the Human Genome Reveals Little Off-Target gRNA Activity

10 off-target sites, shown in Table 4 and

Table 5 in the human genome were identified for each gRNA to be assessed *in vitro*. Lowercase letters in the off-target DNA indicate the nucleotide that is a mismatch from the gRNA sequence.

Table 4: Ten predicted off-target sites for the upstream gRNA.

JCR179: CTAGACCATTTCCCACCAGTTCTNNGRRT Upstream gRNA				
OT #	**Off-target DNA**	**Position**	**# mis match**	**Bulge**
1	aTCTGgcctCCCAGCTGTGTGTTGAGAGT	chr12:107142017, 107142417	5	0
2	aaaTGAaAAgaCAGCTGTGTGTTTGGAAT	chr8:106857602, 106858002	6	0
3	tctgacTAACCCAtCTGTGTGTTCTGGGT	chr9:79943551, 79943951	7	0
4	aTtatggAACgCAGCTGTGTGTTTAGAAT	chr2:163347518, 163347918	7	0
5	CTCTGAgAACaCAGCTaTGTGTcCTGGAT	chr2:156507464, 156507864	4	0
6	aTCcGATt--CCAGCTGTGTGTTCAGAAT	chr7:2370970, 2371370	3	2
7	CaCTGATAACCCtGGACTGTGTGgTAAGAAT	chr6:50926005, 50926405	3	2
8	CTCTGAaAGTAgCCAGCTGTGTGcTTGGAGT	chrX:12401804, 12402204	3	2
9	CcCTGAcAACCCAcCT-TGTGTTATGAGT	chr3:30293153, 30293553	3	1
10	CTCTGActtCCCAGCTGTGTAGTcCTGGGT	chr4:9914904, 9915304	4	1

Table 5: Ten predicted off-target sites for the downstream gRNA.

JCR183: CTAGACCATTTCCCACCAGTTCTNNGRRT Downstream gRNA				
OT #	**Off-target DNA**	**Position**	**# mis match**	**Bulge**
1	tTtGACCATTaaCCACCAGTTCTCAGGGT	chr2:20474819, 20475219	4	0
2	aaAaAggATTTCCCcCCAGTTCTCTGAAT	chr2:229995093, 229995493	6	0
3	CTAccaCATTagCCACCAGTTCTCAGAAT	chr2:122297287, 122297687	5	0
4	aaAaACCATTTCCCctCAGTTCTGCGGAT	chr17:76897040, 76897440	5	0
5	aaAGACCAaTTCaaACCAGTTCTAGGGGT	chr20:4200507, 4200907	5	0
6	acAaAtCATTTCtCtCCAGTTCTTTGAAT	chr12:66496322, 66496722	6	0
7	CcAaAgCATTTCCCA--AGTTCTGTGAAT	chr2:176857782, 176858182	3	2
8	tTgGttCA-TTCCCACCAGTTCTAAGGGT	chr5:3790697, 3791097	4	1
9	CTttACCATTTCtCA-CAGTTCTGTGGGT	chr11:76348972, 76349372	3	1
10	CTtaAagATTTCCCACC-GTTCTTAGAAT	chr6:22928312, 22928712	4	1

Off-target analysis was conducted by targeted PCR amplification of the region of interest and deep sequencing to assess the presence of indels. Results are summarized in Table 6 and Table 7. In a test of one replicate, the downstream gRNA had very little off-target activity in the 10 sites sequenced overall. The upstream gRNA had 2 targets, in chromosomes 6 and 8, with a treated/untreated ratio of >3, but neither fall within a gene

and are potentially inconsequential. Further, both gRNAs had on-target activity 2 orders of magnitude higher than the off-target site with highest treated/untreated ratio.

Table 6: Results of deep sequencing at predicted off-target sites for the upstream gRNA. % Indels is the raw number of indels measured, Treated/Untreated is a ratio of the % Indels for each target site in cells treated or not treated with SaCas9 and the gRNA.

	#	Sequence	Chr	#Mis match	#Bulge	% Indels	Treated/ Untreated
Upstream gRNA	On	CTCTGATAACCCAGCTGTGTGTT	X	0	0	10.32198	541.31914
	OT1	aTCTGgcctCCCAGCTGTGTGTTGAGAGT	12	5	0	0.00599	0.80381
	OT2	aaaTGAaAAgaCAGCTGTGTGTTTGGAAT	8	6	0	0.01219	4.72349
	OT3	tctgacTAACCCAtCTGTGTGTTCTGGGT	9	7	0	0.01077	0.50565
	OT4	aTtatggAACgCAGCTGTGTGTTTAGAAT	2	7	0	0.01829	1.01779
	OT5	CTCTGAgAACaCAGCTaTGTGTcCTGGAT	2	4	0	0.02145	1.15074
	OT6	aTCcGATt--CCAGCTGTGTGTTCAGAAT	7	3	2	0.03847	1.98617
	OT7	CaCTGATAACCCtGGACTGTGTGgTAAGAAT	6	3	2	0.06162	5.12194
	OT8	CTCTGAaAGTAgCCAGCTGTGTGcTTGGAGT	X	3	2	0.08000	1.51824
	OT9	CcCTGAcAACCCAcCT-TGTGTTATGAGT	3	3	1	0.01695	0.59104
	OT10	CTCTGActtCCCAGCTGTGTAGTcCTGGGT	4	4	1	0.03293	2.19131

Table 7: Results of deep sequencing at predicted off-target sites for the downstream gRNA. % Indels is the raw number of indels measured, Treated/Untreated is a ratio of the % Indels for each target site in cells treated or not treated with SaCas9 and the gRNA. Italicized results had less than 10,000 reads and thus were unlikely to pick up rare gene edit activities, thus may not be representative of the true % indel and treated/untreated rates.

	#	Sequence	Chr	#Mis match	#Bulge	% Indels	Treated/ Untreated
Downstream gRNA	On	CTAGACCATTTCCCACCAGTTCT	X	0	0	7.95862	122.50396
	OT1	tTtGACCATTaaCCACCAGTTCTCAGGGT	2	4	0	*0.02095*	*1.70051*
	OT2	aaAaAggATTTCCCcCCAGTTCTCTGAAT	2	6	0	0.49412	1.16700
	OT3	CTAccaCATTagCCACCAGTTCTCAGAAT	2	5	0	0.01741	1.54855
	OT4	aaAaACCATTTCCCctCAGTTCTGCGGAT	17	5	0	*0.03581*	*0.32211*
	OT5	aaAGACCAaTTCaaACCAGTTCTAGGGGT	20	5	0	*0.00000*	*0.00000*
	OT6	acAaAtCATTTCtCtCCAGTTCTTTGAAT	12	6	0	0.01727	2.02953
	OT7	CcAaAgCATTTCCCA--AGTTCTGTGAAT	2	3	2	0.01839	0.66683
	OT8	tTgGttCA-TTCCCACCAGTTCTAAGGGT	5	4	1	0.07263	1.63037
	OT9	CTttACCATTTCtCA-CAGTTCTGTGGGT	11	3	1	0.03695	0.63062
	OT10	CTtaAagATTTCCCACC-GTTCTTAGAAT	6	4	1	0.04533	1.71282

4.5 Discussion

4.5.1 Individual gRNA On-Target Activity, Off-Target Predictions, and Deletion of Exon 51 in gDNA

gRNAs were originally designed starting as close to exon 51 as possible. Of 16 gRNAs tested, 9 gRNAs showed variable levels of on-target activity in HEK293T cells, between approximately 5% and 10%. As we aimed to keep the deletion as small as possible we did not test any other gRNAs further away from the exon. To help determine which two gRNAs, one in intron 50 and one in intron 51, we proceeded with the 22 bp protospacers that were assessed *in silico* for off-target activity.

Currently, there are no definite rules of what makes for a "good" gRNA. We aimed to balance on-target activity, size of the deletion and thus location of the gRNA target relative to the exon, and amount of potential off-targets in the human genome and some consideration for off-target potential in the rhesus macaque genome. Particular weight was given to the potential off-targets in the human genome, as if these gRNAs were to be further developed for clinical use the safety profile for humans must be favorable. Hence, JCR157 and JCR160 were chosen to move forward with as they both had no off-target locations with less than 4 mismatches in the protospacer in the human genome.

4.5.2 Effect of Varying Protospacer Length

As previously discussed, there is no set length for the SaCas9 protospacer. We initially tested all protospacers at a 22 bp length for ease of comparison. After selection

of individual gRNAs to move forward with we decided to test them in varying lengths from 19 to 23 bp. All lengths showed activity with a general trend of increased on-target activity with increased protospacer length as assessed by the Surveyor assay. The 21, 22, and 23 bp length protospacers were tested as deletion pairs, and again all produced clear deletions of exon 51. While all pairs worked well, we moved forward with both 23 bp length protospacers as those created a deletion in 49% of the PCR amplified gDNA as measured by densitometry. This was the most effective pair of gRNAs for creating the desired deletion. However, the least effective pair still created deletions in 43% of gDNA as measured by densitometry, so further investigation into effect of gRNA length in different locations in the human genome warrant study.

The 23 bp gRNAs, JCR179 and JCR183, were evaluated for individual on-target activity in both HEK293Ts and DMD immortalized patient myoblasts. As previously observed we saw robust levels of editing in HEK293T cells. Levels of editing in the immortalized DMD myoblasts were less apparent by the Surveyor nuclease assay, particularly for JCR183. However, when evaluated as a deletion pair we saw clear lack of exon 51 in both HEK293T cells and the immortalized DMD patient myoblasts. These gRNAs proved effective for on-target activity in the genome in two cells types.

4.5.3 Gene Edits are Carried Through Transcription and Translation

JCR179 and JCR183 showed efficacy for individual on-target activity as well as deletion of exon 51 in the genome. Ultimately, we are interested in dystrophin protein

restoration, so further assays were conducted to assess the potential for changes at the genomic level to be carried through transcription and translation. We previously obtained immortalized DMD patient myoblasts as a gift from Vincent Mouly that lack exons 48-50[242]. The loss of exon 48-50 is an out of frame deletion, and thus a DMD genotype and these cells do not produce functional dystrophin protein. This genotype can be shifted to in-frame by deleting exon 51, for a Δ48-51 genotype, restoring the reading frame and creating a BMD genotype. Immortalized DMD patient myoblasts were electroporated with our CRISPR-SaCas9 system and differentiated into myofibers. RNA was extracted, reverse transcribed to cDNA, and PCR amplified. Cells treated with both gRNAs and SaCas9 displayed smaller bands indicative of deletion of exon 51 when electrophoresed on an agarose gel. Cells treated with only 1 gRNA and SaCas9 showed only one unmodified band on a gel, showing that both gRNAs are necessary to create the targeted deletion as expected. Sanger sequencing of the larger and smaller band confirmed that the smaller band is the deletion of exon 51, and exon 47 ligates perfectly to exon 52.

Protein was extracted from myofibers and probed for dystrophin protein expression via Western blot. Similarly, only cells treated with all 3 parts of the system—both the upstream and downstream gRNA and SaCas9—showed dystrophin protein restoration. This confirms that exon 51 deletion is achievable using these gRNAs and

SaCas9, and that the excision of exon 51 utilizing CRISPR-SaCas9 is a viable option to restore dystrophin protein expression.

Prior off-target analysis was conducted on 22 bp length protospacers. As we have shown efficacy of the 23 bp length protospacers and are moving forward with those, further off-target analysis was conducted on JCR179 and JCR183. *In silico* analysis with Cas-OFFinder confirmed that like the 22 bp length protospacer corollaries these 23 bp length protospacers also have no off-target sites with less than 4 mismatches in sequence and 0 bp DNA or RNA bulge. Both gRNAs also do not have any exact matches in either the rhesus macaque or crab-eating macaque genome. 10 off-target sites were selected for each gRNA for evaluation by deep sequencing. Sites with mismatches in the genome with and without DNA or RNA bulge were analyzed. Potential off-target sites were chosen by assigning a weight factor to each DNA position with the highest weight further from the PAM, as mismatches away from the seed sequence are most likely to be tolerated. Off-targets were assessed in HEK293T cells as they are human genome targets and thus cannot be accurately assessed in the hDMDΔ52/*mdx* mouse, which only contains the human *DMD* gene and not the rest of the human genome. Two potential off-target sites, off-target 2 and 7 for the upstream gRNA, showed relatively high levels of indels measured by treated/untreated. However, the on-target showed two orders of magnitude higher indel rates measured by treated/untreated. The downstream gRNA showed no such off-targets with potentially high levels of activity. Upstream OT2 is in a

region of chromosome 8 that is not in a gene, and OT7 is similarly in a region of chromosome 6 that is not located in a gene. Thus, while these off-targets may prove to have significant rates of indel formations they should be of little biologic consequence.

4.5.4 Conclusions

Through this worked we have shown efficacy of a CRISPR-SaCas9 system to target *DMD* for excision of exon 51. On-target activity was shown to be two orders of magnitude more efficacious than off-target activity, and the only off-targets with potentially concerning activity do not reside in genes. The off-target assessment was conducted on only 10 sites per gRNA, thus a genome wide unbiased method for detection of off-targets[243, 244] would bolster the work. The gRNAs selected were tested at several protospacer lengths, furthering the obvious need for thoroughly tested guidelines of what makes an effective gRNA to be standardized. Moreover, the best individual gRNAs may not create the most effective deletion pair, and thus larger screens of gRNAs in pairs would be enlightening to find the best pair for creating deletions. While the chosen gRNAs do have limitations, they show clear on-target activity both individually as well as for creating deletions in two relevant cell types. For this preclinical study the chosen gRNAs display generally desirable characteristics, particularly the high ratio of on-target to off-target activity, but further optimization of gRNA sequence and pairs may help increase the on-target activity.

Chapter 5. *In Vivo* Gene Correction of *DMD* by Deletion of Exon 51 Using CRISPR-SaCas9

This work was done in collaboration with Christopher Nelson, Matthew Gemberling, Veronica Gough, Matthew Oliver, Ruth Castellnos Rivera, Aravind Asokan, Annemieke Aartsma-Rus, and Charles Gersbach.

5.1 Synopsis

Removal of exon 51 utilizing CRISPR-Cas9 shows potential to treat patients in the future. Here, we further the preclinical proof-of-principle body of work by treating a humanized mouse model, with an edited human *DMD* gene that creates a DMD genotype, with a CRISPR-SaCas9 system. We first showed feasibility with a small local injection study, finding that AAV-mediated CRISPR-SaCas9 treatment for excision of exon 51 in the TA results in loss of *DMD* exon 51 in the gDNA and dystrophin protein restoration by IHC and Western blot. We next treated both adult and neonatal mice systemically with AAV9 packaging our CRISPR-SaCas9 human *DMD* exon 51 targeting system. We found measurable indels at both gRNA target sites, upstream and downstream of exon 51, in various skeletal and cardiac muscles from mice treated as adults and neonates. Indel rates were highest in the heart, and generally higher for mice treated as neonates than mice treated as adults. Deletions of exon 51 in cDNA were also present in samples from various skeletal and cardiac muscles measured by ddPCR. The heart cDNA had about 20% deletions of exon 51 in both mice treated as adults and

neonates, whereas the deletion rates in skeletal muscle samples were an order of magnitude lower. IHC staining and Western blot both confirm dystrophin protein expression restoration. There was mouse to mouse variability, and the mice treated as neonates displayed more prominent dystrophin expression restoration, but dystrophin protein expression was visible to some degree in all mice. This work furthers proof-of-principle for CRISPR-Cas9 to be an effective permanent treatment for DMD.

5.2 Introduction

While promising *in vitro* work is exciting, ultimately preclinical therapies must be tested *in vivo* for safety and efficacy. Plasmid delivery of CRISPR-Cas9 systems *in vivo* is possible but not very effective, thus we chose to package our system in muscle-tropic AAV vectors. Due to AAV packaging limit constrains we had to use two viral vectors to deliver both gRNAs and SaCas9, but are pursuing an all-in-one vector system that will be able to package all three essential components of the system. With the characterized hDMDΔ52/*mdx* mouse and our human dystrophin exon 51 targeting CRISPR-SaCas9 system validated *in vitro* in hand, we were able to test those exact human *DMD* targeting guides in our hDMDΔ52/*mdx* mouse. Although *in vivo* off-target potential of these human targeting gRNAs cannot be evaluated effectively, as the mouse has only the human dystrophin gene and otherwise lacks the human genome, we were able to assess on-target editing of the human *DMD* gene for *in vivo* efficacy. This is the first such work

utilizing an AAV-mediated delivery of CRISPR-Cas9 to the human *DMD* gene in a small animal model.

5.3 Materials and Methods

5.3.1 Molecular Cloning and AAV Production

gRNAs identified in 4.4.6 23 bp Length Protospacers Show Repeatable On-Target Activity were cloned into a plasmid containing SaCas9 driven by the CMV promoter with the BsaI restriction enzyme (Addgene plasmid #61591, see Figure 37). SURE 2 supercompetent cells (Agilent Technologies) were used for transformation (see Figure 37). Colonies were prepared, sequence verified, and test digested with the SmaI restriction enzyme to investigate potential recombination events. Verified plasmids were grown up at 32°C overnight for no more than 14 hours in 400-500 mL of Terrific Broth (Thermo Fisher) in 2 L flasks. Bacterial pellets were processed using the EndoFree Plasmid Mega Kit (Qiagen), and resulting plasmid was SmaI test digested and sequence verified. Plasmid was sent to collaborators in Aravind Asokan's laboratory at the University of North Carolina, Chapel Hill, or the Nationwide Children's Hospital Viral Vector Core where AAV was produced.

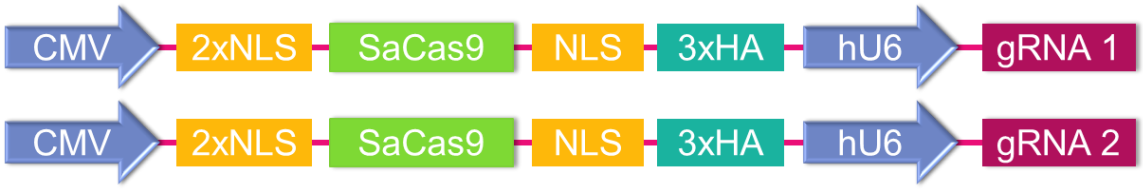

Figure 37: Plasmid design for AAV production where gRNA1 and gRNA2 are JCR179 and JCR183.

5.3.2 Intramuscular Injections of AAV

All animal studies were conducted under protocols approved by the Duke University Institutional Animal Care and Use Committee. 7-8 week old male hDMDΔ52/*mdx* mice were anesthetized and placed on a warming pad. The TA muscle was prepared for injection of 30 μl of AAV8 solution (~5E11 viral genomes/mouse) or saline into the right or left TA, respectively. 8 weeks after treatment mice were euthanized via CO_2 inhalation and tissues were collected into RNALater (Life Technologies) for DNA, RNA, or protein analysis.

5.3.3 Systemic Injection of AAV into Adult and Neonatal Mice

P2 neonatal hDMDΔ52/*mdx* male mice were anesthetized by hypothermia and then injected with 40 μl AAV9 solution (~1.5E12 viral genomes/mouse) into the temporal vein. 7-8 week old adult male hDMDΔ52/*mdx* mice were injected via the tail vein with 200 μl of AAV9 solution (~4E12 – 7.5E12 viral genomes/mouse). At 16 weeks of age mice were euthanized by CO_2 inhalation and tissues were collected into RNALater (Life Technologies) for DNA, RNA, or protein analysis, or embedded in OCT for frozen tissue sections.

5.3.4 Biochemical Analysis to Detect Deletion of Exon 51 and Dystrophin Protein Expression

Endpoint PCR detection of loss of exon 51 in gDNA and cDNA was performed as previously described in 4.3.7 Detection of Exon 51 Deletion. Staining of histological

sections and Western blot probing for dystrophin protein expression was performed as previously described in 3.3.8 Biochemical Analysis of the hDMDΔ52/*mdx* Mouse.

5.3.5 ddPCR for Deletion of Exon 51 in cDNA

Quantitative ddPCR was performed on cDNA samples using a QX200 Droplet Digital PCR System. Exon 51 deletion in cDNA extracted from animal tissues was detected using the QX200 ddPCR Supermix for Probes (BioRad) and Taqman assays with probes designed to bind to the junction of human dystrophin exon 50 and exon 53, as well as a probe for exon 59. ddPCR for deletion of exon 51 in cDNA from animal tissues analysis was conducted by using the same threshold across all wells.

5.3.6 Deep Sequencing for On-Target Activity

Deep sequencing for detection of indels created by genome editing was performed on genomic DNA samples from heart, diaphragm, TA, and gastrocnemius for all mice treated as adults (n=10 except for gastrocnemius n=5) and mice treated as neonates (n=4). PCR of the genomic DNA was completed using two primer pairs designed to flank the two cut sites. A second round of PCR was used to add Illumina flowcell binding sequencing and experiment-specific barcodes on the 5′ end of the primer sequencing. The PCR products were pooled and sequenced with 150 bp paired-end reads on an Illumina MiSeq instrument. Indel analysis was performed using CRISPResso[241] with a window of 5 and default parameters. Deep sequencing to detect deletions of exon 51 was adapted from a previously published method for linear

amplification-mediated high-throughput genome-wide translocation sequencing[245]; n=4 for heart samples and n=7 for TA samples.

5.4 Results

5.4.1 Intramuscular Injection of AAV Packaged CRISPR-SaCas9 System Leads to Loss of Exon 51

The AAV8 packaging our previously *in vitro* validated CRISPR-SaCas9 system was intramuscularly injected into the TA of adult mice to remove exon 51 from the genome. When gDNA was PCR amplified, electrophoresed on an agarose gel, and Sanger sequenced, we observed the dominant product being the expected ligation of the gRNAs 3 bp upstream from the PAM.

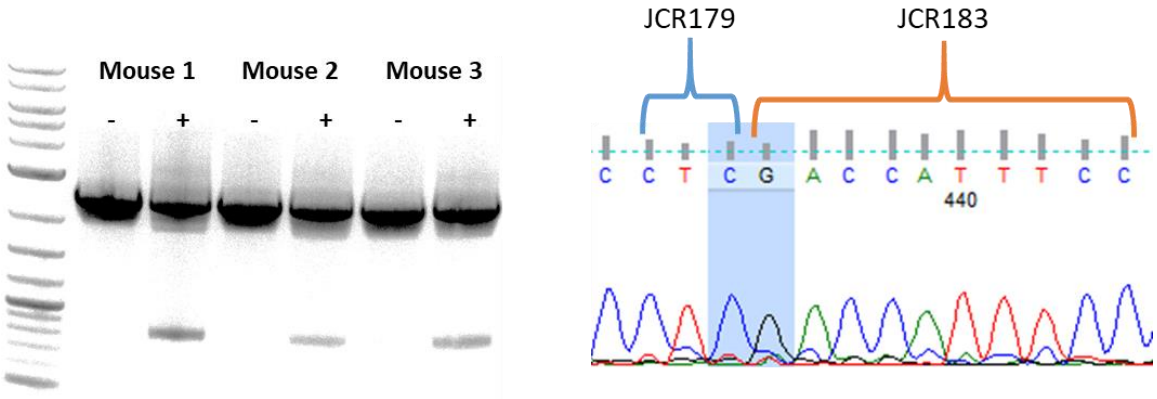

Figure 38: PCR amplification of gDNA extracted from untreated (-) and treated (+) TA muscles showing a smaller band from loss of exon 51 in treated muscles. Sequencing of this band shows the ligation of the gRNA sequences 3 bp upstream of the PAM.

Loss of exon 51 in the gDNA resulted in dystrophin protein restoration observed by IHC and Western blot.

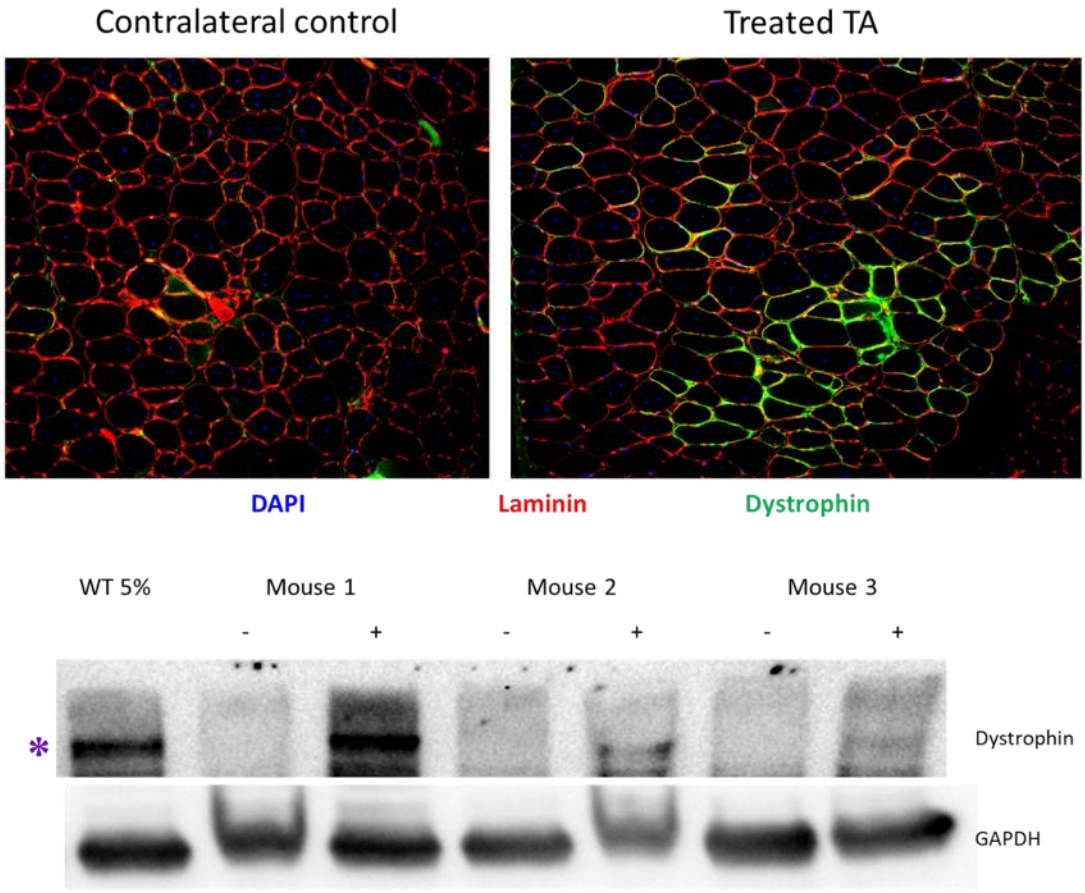

Figure 39: Dystrophin protein expression in treated TA muscles. Top shows dystrophin stained in green present in the treated sample and absent in the contralateral control; bottom shows variable but nonetheless present levels of dystrophin protein detected in only treated samples (+) compared to contralateral control samples (-) by Western blot.

5.4.2 Systemic Administration of AAV Mediated CRISPR-SaCas9 System Demonstrates On-Target Activity

Following systemic administration on-target activity of both gRNAs was measured by deep sequencing at the predicted indel sites in cardiac and various skeletal muscle gDNA from mice treated as adults and neonates.

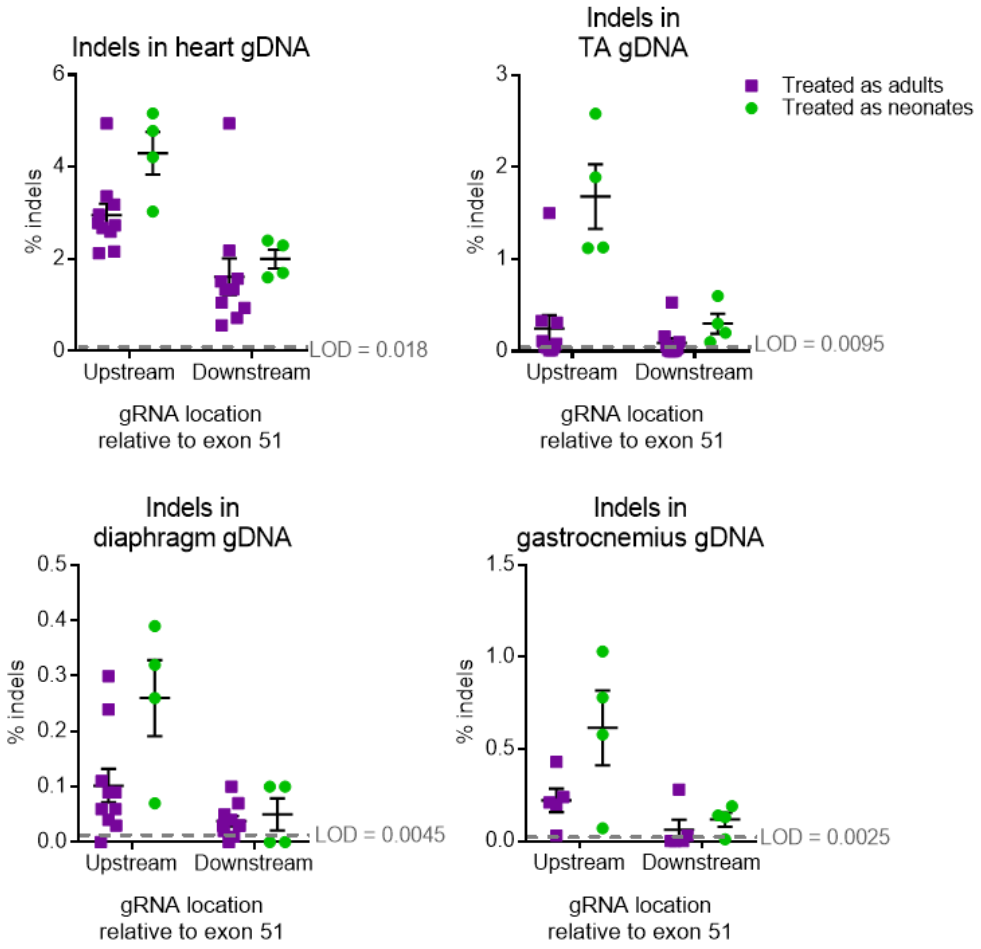

Figure 40: Indels measured by deep sequencing in gDNA extract from heart, TA, diaphragm, and gastrocnemius muscles from mice treated with our CRISPR-SaCas9 system via AAV9 as adults (purple squares) and neonates (green circles).

Traditional deep sequencing for on-target events does not evaluate the efficacy of excision of a region of the genome. Deletion, insertion, and AAV integration events were quantified in the gDNA extracted from hearts and TA muscles from mice treated as adults by linear amplification-mediated high-throughput genome-wide translocation sequencing (LAM-HTGTS)[245].

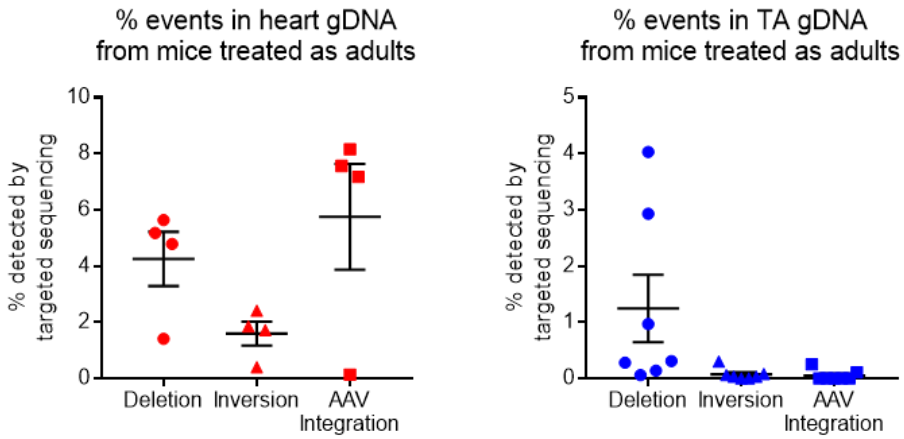

Figure 41: LAM-HTGTS on gDNA from hearts and TA muscles from mice treated as adults showing deletion, inversion, and AAV integration events.

5.4.3 Excision of Exon 51 in the Genome Leads to Loss of Exon 51 in mRNA

Precise edits made in the genome are carried through transcription to the RNA.

These changes are detected in the cDNA by endpoint PCR as well as ddPCR.

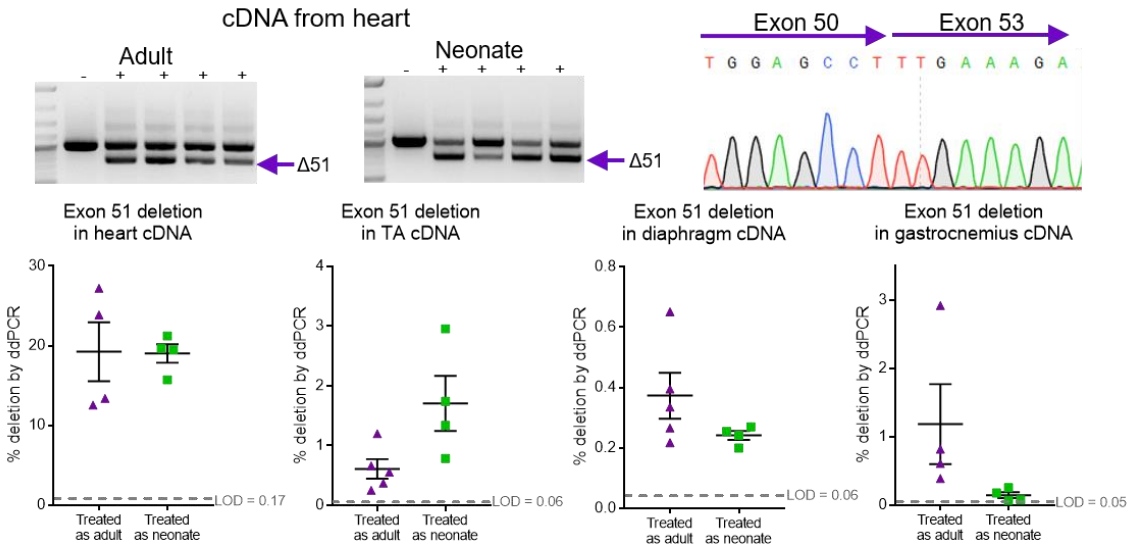

Figure 42: Analysis of loss of exon 51 in mRNA by endpoint PCR and ddPCR. cDNA reverse transcribed from mRNA extracted from heats of mice treated as adults and neonates was PCR amplified and electrophoresed; the loss of exon 51 is observed by the smaller band. Sanger sequencing of this band shows the ligation of exon 50 to exon 53. ddPCR of cDNA from heart, TA, diaphragm, and gastrocnemius muscles shows measurable loss of exon 51 in all samples. (-) is an untreated mouse, LOD is the limit of detection that is defined by the average of untreated samples.

5.4.4 Excision of Exon 51 in the Genome Leads to Dystrophin Protein Expression

Removal of exon 51 in the genome carries through the central dogma and results in changes in protein due to restoring the reading frame. Dystrophin protein expression was assessed by Western blot for dystrophin expression, with GAPDH as an internal loading control, and SaCas9 assessed by the HA tag in protein extracted from hearts.

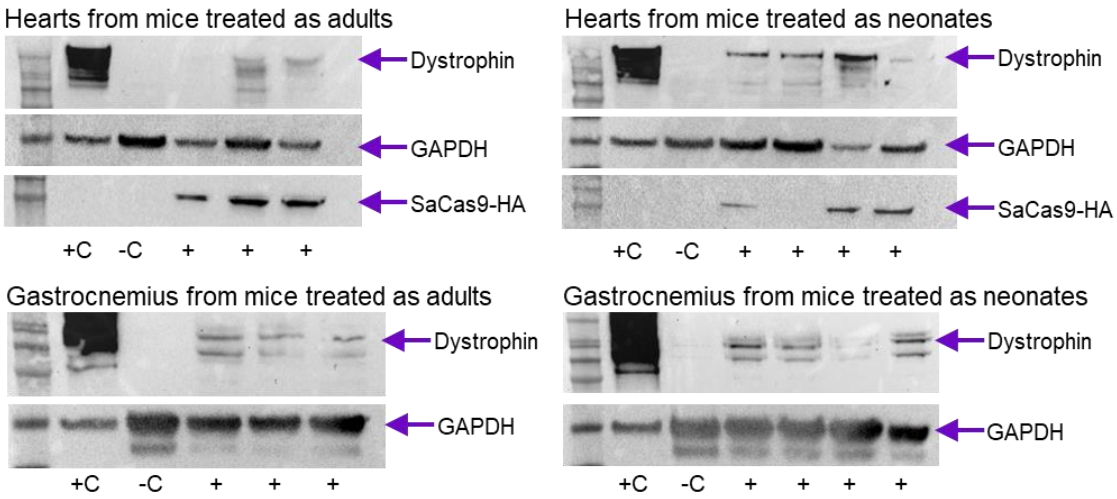

Figure 43: Western blots showing variable levels of dystrophin protein expression in the heart and gastrocnemius muscles from mice treated as adults and neonates. +C is protein from the hDMD/*mdx* mouse, -C is protein from an untreated hDMDΔ52/*mdx* mouse, and + indicates treated mice.

IHC on sections from hearts and TA muscles was also utilized to visualize and qualitatively assess restored dystrophin protein expression.

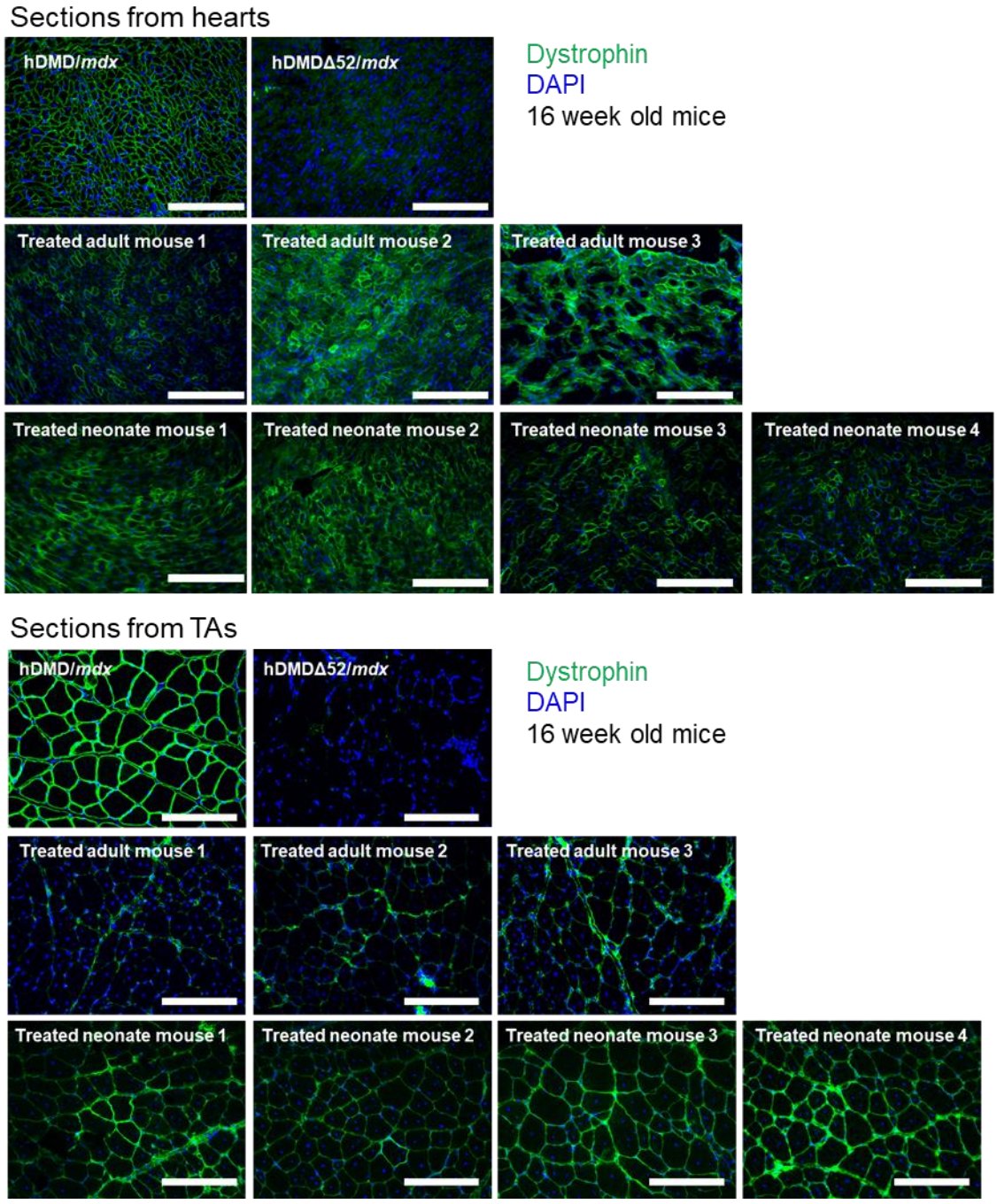

Figure 44: IHC for dystrophin (green) protein expression in sections from heart and TA muscles from mice treated as adults and neonates. hDMD/*mdx* is a positive control, hDMDΔ52/*mdx* is a negative control. Scale bars are 200μm.

5.5 Discussion

5.5.1 Preliminary Study of *In Vivo* Exon 51 Removal by Intramuscular Injection

We showed potential for *in vivo* exon 51 removal from the human *DMD* gene in our hDMDΔ52/*mdx* mouse by intramuscular injection into the TA using AAV8 packaging our CRISPR-SaCas9 system targeted to sequences flanking exon 51. Adult mice were treated and 8 weeks later assessed for gene editing. Here we showed successful removal of exon 51 in the gDNA with the expected edited sequence, ligation of the gRNA sequence in the genome at cut sites 3 bp upstream of the PAM, of the resulting edited genome. Variable levels of dystrophin restoration were observed mouse to mouse by Western blot, and representative IHC indicates sparse, but present, dystrophin protein restoration. This small scale preliminary experiment showed potential for systemic administration of our system for dystrophin restoration.

5.5.2 On-Target Activity of gRNAs *In Vivo* Following Systemic Administration

Indels at the predicted cut site for each gRNA were detected in treated samples via deep sequencing in gDNA extracted from the heart, TA, diaphragm, and gastrocnemius muscles. Mice treated as adults and neonates showed deletion of exon 51 in gDNA from hearts and skeletal muscles by endpoint PCR. Although we observed variable levels of editing with endpoint PCR, the greater sensitivity and reliability of next generation sequencing revealed consistent deletion of exon 51. In particular, linear

amplification-mediated high-throughput genome-wide translocation sequencing demonstrated 4.3% ± 1.0% and 1.2% ± 0.6% deletion of exon 51 in gDNA from heart and TA muscles, respectively, of mice treated at 8 weeks of age (Figure 41). Sequencing of the deletion band from endpoint PCR indicates the majority of the deletion product was the expected ligation of the predicted SaCas9 cut sites three nucleotides upstream of the PAM.

5.5.3 Loss of Exon 51 in cDNA After *In Vivo* Systemic Treatment

PCR amplification of cDNA from hearts also showed a lack of exon 51 in a fraction of alleles in both mice treated as adults and neonates. Sequencing of the deletion band shows the exact junction of exons 50 and 53, indicative of exon 51 removal from the hDMDΔ52/*mdx* mice. Quantification of loss of exon 51 by ddPCR of the cDNA from adults or neonates showed 19.0% ± 1.2% and 19.3% ± 3.7% removal in the heart, 0.6% ± 0.2% and 1.7% ± 0.5% in the TA, 0.2% ± 0.02% and 0.4% ± 0.08% in the diaphragm, and 0.1% ± 0.04% and 1.2% ± 0.6% in the gastrocnemius. While we observe the most robust deletion activity in the heart, it is promising to see activity throughout relevant skeletal muscles.

5.5.4 Restored Dystrophin Protein Expression Following *In Vivo* Systemic Treatment

Western blot of lysates from the heart and gastrocnemius showed variable levels of dystrophin protein restoration. Significant dystrophin restoration was also observed by immunofluorescence staining of histological sections of heart and TA muscles from

mice treated as adults and neonates. The results from mice treated systemically as adults and neonates demonstrates exon 51 excision from the human gene *in vivo*, which leads to variable but nonetheless present levels of restored dystrophin protein expression.

5.5.5 Conclusions

This work shows the potential of NHEJ-mediated targeted gene editing for Duchenne muscular dystrophy. While the *in vivo* editing rates are low, we do see notable dystrophin protein expression. As previously discussed, it is likely we will not need to achieve 100% dystrophin protein expression to see functional benefit[246]. Here we show between 1-2% deletions of exon 51 in the gDNA, which is a promising start but warrants further optimization. Increased gene editing rates should lead to increased dystrophin protein expression, which may translate to functional benefit. Improved phenotype of the treated dystrophic mice needs to be investigated further, as well as immune response to the CRISPR-SaCas9 system. While significant work to push this technology to this clinic remains, this works shows promising potential for use of CRISPR-Cas9 technology to potentially be a permanent treatment for the genetic cause of Duchenne muscular dystrophy.

Chapter 6. Conclusions

6.1 Summary

This dissertation demonstrates and progresses work for a gene editing therapy for DMD. Here we have created and characterized a relevant mouse model for DMD that has the human dystrophin gene mutated to have a DMD genotype, and the mouse displays a mild DMD phenotype. We have created a CRISPR-SaCas9 system and shown on-target efficacy *in vitro* with little off-target concern by deep sequencing, and also packaged this system in AAV and delivered it to mice locally and systemically. Local injections indicated clear deletions of exon 51 in gDNA and restoration of dystrophin protein expression by IHC and Western blot. Systemic injections in neonatal and adult mice showed on-target indel formation and loss of exon 51 in cDNA from various muscles. There was also varied, but present, dystrophin protein restoration by IHC and Western blot. This dissertation capitalized on the rapid advancement of genome engineering tools for therapeutic applications to treat Duchenne muscular dystrophy. Although many other treatments for DMD are further along in development, direct editing of the native locus maintains as much of the natural sequence as possible and is a powerful method to permanently edit the gene and restore dystrophin protein expression. Gene editing offers a promising alternative to transient methods such as oligonucleotides to induce exon skipping and gene transfer of minidystrophin and

microdystrophin. While the system showed proof-of-principle for testing human specific gRNAs in a small animal model, there are still many potential improvements.

6.2 Future Directions

6.2.1 Increased *In Vivo* Editing Efficacy

6.2.1.1 gRNA Design and Assessment for Deletion Efficacy

A significant challenge with creating a CRISPR-Cas9 system is choosing gRNAs. While designing gRNAs in general is not difficult, there is very little clarity about what makes a "good" gRNA. Vague guidelines exist[247], including ranking potential gRNAs based on off-target likelihood as well as targeting all isoforms if applicable, but there is little consensus about what makes an optimal guide for those considerations as well as on-target activity. Particularly, working with newer variants of Cas9, including SaCas9, complicates this problem further as majority of the literature has used SpCas9 and thus many suggestions for "good" gRNA design may only be applicable to SpCas9. For example, gRNA length is still not well understood other than that varying lengths in different genomic contexts seem to have an effect on SaCas9 gRNAs on-target activity, whereas this is largely less of a potent problem for SpCas9 gRNA design. In this work we designed and screened several gRNAs targeted to the intronic region flanking exon 51, but this by no means was a rigorous process. The intronic regions of the *DMD* gene are massive, sometimes even over one hundred of thousand bp, and the few gRNAs screened in Aim 2 certainly do not reflect the vast potential of gRNAs that exist.

Complicating the issue further is the fact that gRNAs that have strong on-target activity individually may not be the best gRNAs to use in a deletion pair. Anecdotally, many lab members have seen gRNAs that have poor or no measurable on-target activity individually measured by the Surveyor assay that when combined with another gRNA still create on-target deletions. Thus, there is still much to learn about gRNA design and testing. To help address this a library screen of gRNAs upstream and downstream of exon 51 should be tested *in vitro* or *in vivo*. The data from this will certainly help discern optimal guides for making deletions of exon 51, and with careful analysis the large data set could be used to help uncover what makes a "good" gRNA overall. While this library screen around exon 51 will be beneficial for this project, gRNAs may very well be quite context dependent and thus further screens in different genomic loci may need to be conducted in order to create a set of guidelines for designing effective gRNAs that would apply in a broad context.

6.2.1.2 Vector Design and AAV Serotype

This work utilized a two-vector system, where each vector contained SaCas9 and one gRNA. Ultimately, we would like to move to a one vector design where both gRNAs and SaCas9 are produced from one virus. One motivating factor to this is temporal considerations. In the current two-vector system it is entirely possible that one gRNA is making a double stranded break whereas the other gRNA may not be available at the same time. In a one vector system all necessary parts for creating the deletion will

be present temporally together. This advantage may help increase our *in vivo* on-target editing rates. Another large motivating factor is forward looking to the clinic. A two-vector system would require two viruses to be produced at GMP quality for every treatment. Reducing this down to one vector may have meaningful impact on the ability to produce enough virus for treatment as well as reduced cost of production, which may lead to reduced cost of treatment for the patient and insurance companies.

Another aspect of vector design is the promoter driving SaCas9. In our current system we are using a constitutive CMV promoter. For clinical translation we likely need to test and potentially switch to muscle-specific promoters. This may enhance on-target editing, but also should reduce the risk of off-target double stranded breaks.

Lastly, our lab has primarily focused on previously-known muscle-tropic AAV serotypes such as AAV8 and AAV9. While our lab is currently not an AAV engineering lab, AAV engineering is a large field that is constantly producing new and exciting engineered AAV variants. Increased transduction of both muscle cells and satellite cells may increase our overall gene editing levels.

6.2.1.3 Dose Escalation Study

This study was completed at small range of viral doses that is consistent with the dose range being tested in clinical trials using AAV9, such as the spinal muscular atrophy type I trial (NCT02122952). While this dose has the most clinical relevance, we are seeing only modest levels of editing. Other groups have shown treated of DMD *in*

vivo in a mouse using doses one to two orders of magnitude higher than what we have typically been injecting. A true dose escalation study ranging across at least two orders of magnitude will help elucidate the required dose to achieve high levels of gene editing.

6.2.1.4 Time Course Study

This study analyzed all treated mice at 16 weeks of age. That is approximately 16 weeks after treatment of neonates and 8 weeks post treatment of adults. While this timepoint may be representative, a time course evaluating gene editing over time would be informative. In particular, as this is a lifelong disease, timepoints when the mice are aged will be extremely valuable. It is thought that these permanent edits CRISPR-Cas9 makes will persist, but proof of this from analyzing mice from 18-24+ month old would be tremendously valuable.

6.2.2 gRNAs Targeted to Create Frameshifts

Deleting an exon using CRISPR-Cas9 is not the only option to treat DMD. Rather, splice acceptors can be targeted to be shifted out of frame using just one gRNA[224]. Splice acceptors can also be altered via base editing[248, 249] so the site is no longer recognized. This work did not explore these methods, but they warrant investigation.

6.2.3 Replace Exon(s)

Rather than create deletions of exons to restore the reading frame, the missing exons in the gene could be put back in by homology directed repair or homology-independent targeted integration[250]. This is perhaps the most desirable gene editing

strategy as it has potential to return the mRNA product and even possibly the genome itself to the wild type version. This method then would not rely on shifting a DMD patient to a BMD genotype, but rather to a genotype with full-length healthy and functional dystrophin. Homology directed repair rates in muscle have been reported to be about an order of magnitude lower than NHEJ rates[44], but this technology is also being actively researched and pushed forward. If rates of exon integration increase to rival that of NHEJ then these methods may be much more favorable for clinical development.

6.2.4 Excise Other Portions of the Dystrophin Gene

The hDMDΔ52/*mdx* mouse is a useful tool for more than assessing deletion of exon 51. Removal of exon 53 also restores the reading frame in this mouse, as well as removal of exons 45-55. The latter is noteworthy as this method could address about 60-65% of DMD patients[5, 226, 227].

6.2.5 Off-Target Analysis

Off-target analysis was done by deep sequencing around predicted sites of off-target activity on HEK29T cell gDNA. There are obvious limitations of probing for off targets *in vivo*, as the work was done in a mouse model that contains primarily the mouse genome, whereas we are interested in human genome off-targets. Off-target analysis could be conducted *in vitro* using a nonbiased method such as digenome-seq[243]

or CIRCLE-seq[244], potentially on gDNA extracted from multiple cell lines including patient cells rather than just a standard cell line such as HEK293T cells.

6.2.6 Safety Profile

While we have shown work regarding the minimizing of off-target DNA breaks, the rest of the safety profile needs to be assessed. A dose much higher than what would be proposed to give to humans needs to be studied. AAV-integration[251] rates at both on and off-target locations needs to be evaluated. The immune response needs to be parsed out with techniques like an ELISA against SaCas9 and ELISPOT.

6.2.7 Satellite Cells

While editing the muscle directly is important to see short term benefit, editing the stem cell population of muscle, called satellite cells, is relevant to maintain any beneficial changes over time. As muscle cells deteriorate due to injury the satellite cells replace the lost muscle cell population. Thus, in a DMD patient, it is vital to achieve editing of the satellite cells such that all the muscle cells created by the satellite cells are not of a DMD genotype. This poses an interesting challenge and dilemma as Cas9 driven by a muscle specific promoter, by definition, should not effectively edit satellite cells. Thus, there will likely need to be studies comparing overall editing as well as editing of satellite cells when SaCas9 is driven by a muscle specific promoter versus a constitutive promoter. Achieving ideal editing rates of both muscle and satellite cells may also

require a combination of viruses driven by different promoters, which would need to be tested at varying ratios *in vivo* in a small animal model.

6.2.8 Mouse Strain and Phenotype Rescue

The hDMDΔ52/*mdx* mouse, like the *mdx* mouse, exhibits a mild dystrophic phenotype. We have done preliminary systemic studies to assess phenotypic rescue after treatment, however results were inconclusive in tests such as overall distance moved, rearing postures, and grip strength in mice treated as adults and neonates. It is difficult to show rescue of a phenotype through *in vivo* tests when the phenotype is quite mild to begin with. One option is to move to *ex vivo* and *in situ* testing of muscle force and fatigue from hindlimbs, as these tests typically have much less mouse to mouse variance than the voluntary *in vivo* tests. Ultimately though we would like to see improvements through *in vivo* tests such as grip strength and distance moved to demonstrate systemic phenotypic rescue rather than only showing improved force in isolated individual muscles. Thus, exacerbating the disease state of our mouse may prove useful. One method for this is to exercise the mice by twice weekly treadmill running. This method has been shown to exacerbate disease pathology[237], and exercising the mice before and/or after our CRISPR-Cas9 treatment may allow us to see more stark differences in treated versus untreated mice. Further, we are currently back breeding our hDMDΔ52/*mdx* mouse onto the utrophin double knockout strain, which displays a severe phenotype that more accurately recapitulates the human disease including

waddling gait, joint contractures, growth retardation, and necrosis of the diaphragm starting at 6 days old[252]. We expect to see a dramatic difference in baseline of untreated hDMD/*mdx* and hDMDΔ52/*mdx* mice compared to hDMDΔ52/*mdx*/utrn mice, and this dramatic starting phenotype leaves a large opportunity to demonstrate statistically significant improvements in phenotype after our CRISPR-SaCas9 treatment.

6.2.9 CRISPR Variants

This dissertation focused exclusively on SaCas9. However, as the rapidly advancing field of gene editing progresses new CRISPR variants and classes are being characterized including *Neisseria meningitidis* (NmCas9)[253], *Francisella novicida* (FnCas9)[254], *Campylobacter jejuni* (CjCas9)[255, 256], CasX and CasY[257], Cpf1[258], C2c1[259], and C2c2[260, 261]. Different CRISPR variants with different PAMs lead to a plethora of gRNAs to choose from, which may be particularly useful for needing to target specific sequences such as splice sites. Further, recent studies highlighting variable but potentially concerning levels of pre-existing immunity to SpCas9[262] and SaCas9[263] may force the therapeutic side of the field to shift away from these popular Cas9 tools.

References

1. Hoffman, EP, Brown, RH, Jr., and Kunkel, LM (1987). Dystrophin: the protein product of the Duchenne muscular dystrophy locus. *Cell* **51**: 919-928.

2. Monaco, AP, Bertelson, CJ, Colletti-Feener, C, and Kunkel, LM (1987). Localization and cloning of Xp21 deletion breakpoints involved in muscular dystrophy. *Human genetics* **75**: 221-227.

3. Mendell, JR, Goemans, N, Lowes, LP, Alfano, LN, Berry, K, Shao, J, *et al.* (2016). Longitudinal effect of eteplirsen versus historical control on ambulation in Duchenne muscular dystrophy. *Annals of neurology* **79**: 257-271.

4. Voit, T, Topaloglu, H, Straub, V, Muntoni, F, Deconinck, N, Campion, G, *et al.* (2014). Safety and efficacy of drisapersen for the treatment of Duchenne muscular dystrophy (DEMAND II): an exploratory, randomised, placebo-controlled phase 2 study. *The Lancet Neurology* **13**: 987-996.

5. Lu, QL, Yokota, T, Takeda, S, Garcia, L, Muntoni, F, and Partridge, T (2011). The Status of Exon Skipping as a Therapeutic Approach to Duchenne Muscular Dystrophy. *Molecular Therapy* **19**: 9-15.

6. Wood, MJA (2010). Toward an Oligonucleotide Therapy for Duchenne Muscular Dystrophy: A Complex Development Challenge. *Sci Transl Med* **2**.

7. Yokota, T, Pistilli, E, Duddy, W, and Nagaraju, K (2007). Potential of oligonucleotide-mediated exon-skipping therapy for Duchenne muscular dystrophy. *Expert opinion on biological therapy* **7**: 831-842.

8. Gussoni, E, Soneoka, Y, Strickland, CD, Buzney, EA, Khan, MK, Flint, AF, *et al.* (1999). Dystrophin expression in the mdx mouse restored by stem cell transplantation. *Nature* **401**: 390-394.

9. Partridge, TA, Grounds, M, and Sloper, JC (1978). Evidence of Fusion between Host and Donor Myoblasts in Skeletal-Muscle Grafts. *Nature* **273**: 306-308.

10. Partridge, TA, Morgan, JE, Coulton, GR, Hoffman, EP, and Kunkel, LM (1989). Conversion of Mdx Myofibers from Dystrophin-Negative to Dystrophin-Positive by Injection of Normal Myoblasts. *Nature* **337**: 176-179.

11. Darabi, R, Arpke, RW, Irion, S, Dimos, JT, Grskovic, M, Kyba, M, *et al.* (2012). Human ES- and iPS-derived myogenic progenitors restore DYSTROPHIN and improve contractility upon transplantation in dystrophic mice. *Cell Stem Cell* **10**: 610-619.

12. Karpati, G, Ajdukovic, D, Arnold, D, Gledhill, RB, Guttmann, R, Holland, P, *et al.* (1993). Myoblast Transfer in Duchenne Muscular-Dystrophy. *Annals of neurology* **34**: 8-17.

13. Tremblay, JP, Malouin, F, Roy, R, Huard, J, Bouchard, JP, Satoh, A, *et al.* (1993). Results of a triple blind clinical study of myoblast transplantations without immunosuppressive treatment in young boys with Duchenne muscular dystrophy. *Cell transplantation* **2**: 99-112.

14. Gussoni, E, Pavlath, GK, Lanctot, AM, Sharma, KR, Miller, RG, Steinman, L, *et al.* (1992). Normal Dystrophin Transcripts Detected in Duchenne Muscular-Dystrophy Patients after Myoblast Transplantation. *Nature* **356**: 435-438.

15. Law, PK, Goodwin, TG, Fang, Q, Duggirala, V, Larkin, C, Florendo, JA, *et al.* (1992). Feasibility, safety, and efficacy of myoblast transfer therapy on Duchenne muscular dystrophy boys. *Cell transplantation* **1**: 235-244.

16. Mendell, JR, Kissel, JT, Amato, AA, King, W, Signore, L, Prior, TW, *et al.* (1995). Myoblast Transfer in the Treatment of Duchennes Muscular-Dystrophy. *New Engl J Med* **333**: 832-838.

17. Baum, C, Kustikova, O, Modlich, U, Li, ZX, and Fehse, B (2006). Mutagenesis and oncogenesis by chromosomal insertion of gene transfer vectors. *Hum Gene Ther* **17**: 253-263.

18. Romero, NB, Braun, S, Benveniste, O, Leturcq, F, Hogrel, JY, Morris, GE, *et al.* (2004). Phase I study of dystrophin Duchenne/Becker plasmid-based gene therapy in muscular dystrophy. *Hum Gene Ther* **15**: 1065-1076.

19. Zhang, GF, Ludtke, JJ, Thioudellet, C, Kleinpeter, P, Antoniou, M, Herweijer, H, *et al.* (2004). Intraarterial delivery of naked plasmid DNA expressing full-length mouse dystrophin in the mdx mouse model of Duchenne muscular dystrophy. *Hum Gene Ther* **15**: 770-782.

20. Bowles, DE, McPhee, SWJ, Li, CW, Gray, SJ, Samulski, JJ, Camp, AS, *et al.* (2012). Phase 1 Gene Therapy for Duchenne Muscular Dystrophy Using a Translational Optimized AAV Vector. *Molecular Therapy* **20**: 443-455.

21. Okada, T, and Takeda, S (2013). Current Challenges and Future Directions in Recombinant AAV-Mediated Gene Therapy of Duchenne Muscular Dystrophy. *Pharmaceuticals* **6**: 813-836.

22. Wang, B, Li, J, Fu, FH, and Xiao, X (2009). Systemic human minidystrophin gene transfer improves functions and life span of dystrophin and dystrophin/utrophin-deficient mice. *J Orthop Res* **27**: 421-426.

23. Wang, B, Li, J, and Xiao, X (2000). Adeno-associated virus vector carrying human minidystrophin genes effectively ameliorates muscular dystrophy in mdx mouse model. *Proc Natl Acad Sci U S A* **97**: 13714-13719.

24. Watchko, J, O'Day, T, Wang, B, Zhou, LQ, Tang, Y, Li, J, *et al.* (2002). Adeno-associated virus vector-mediated minidystrophin gene therapy improves dystrophic muscle contractile function in mdx mice. *Hum Gene Ther* **13**: 1451-1460.

25. Wells, DJ, Wells, KE, Asante, EA, Turner, G, Sunada, Y, Campbell, KP, *et al.* (1995). Expression of Human Full-Length and Minidystrophin in Transgenic Mdx Mice - Implications for Gene-Therapy of Duchenne Muscular-Dystrophy. *Hum Mol Genet* **4**: 1245-1250.

26. Gregorevic, P, Allen, JM, Minami, E, Blankinship, MJ, Haraguchi, M, Meuse, L, *et al.* (2006). rAAV6-microdystrophin preserves muscle function and extends lifespan in severely dystrophic mice. *Nature medicine* **12**: 787-789.

27. Gregorevic, P, Blankinship, MJ, Allen, JM, and Chamberlain, JS (2008). Systemic microdystrophin gene delivery improves skeletal muscle structure and function in old dystrophic mdx mice. *Molecular therapy : the journal of the American Society of Gene Therapy* **16**: 657-664.

28. Liu, MJ, Yue, YP, Harper, SQ, Grange, RW, Chamberlain, JS, and Duan, DS (2005). Adeno-associated virus-mediated microdystrophin expression protects young mdx muscle from contraction-induced injury. *Molecular Therapy* **11**: 245-256.

29. Yoshimura, M, Sakamoto, M, Ikemoto, M, Mochizuki, Y, Yuasa, K, Miyagoe-Suzuki, Y, *et al.* (2004). AAV vector-mediated microdystrophin expression in a relatively small percentage of mdx myofibers improved the mdx phenotype. *Molecular therapy : the journal of the American Society of Gene Therapy* **10**: 821-828.

30. Yue, YP, Li, ZB, Harper, SQ, Davisson, RL, Chamberlain, JS, and Duan, DS (2003). Microdystrophin gene therapy of cardiomyopathy restores dystrophin-glycoprotein complex and improves sarcolemma integrity in the mdx mouse heart. *Circulation* **108**: 1626-1632.

31. Bostick, B, Shin, JH, Yue, Y, Wasala, NB, Lai, Y, and Duan, D (2012). AAV micro-dystrophin gene therapy alleviates stress-induced cardiac death but not myocardial fibrosis in >21-m-old mdx mice, an end-stage model of Duchenne muscular dystrophy cardiomyopathy. *Journal of molecular and cellular cardiology* **53**: 217-222.

32. Bostick, B, Shin, JH, Yue, YP, and Duan, DS (2011). AAV-microdystrophin Therapy Improves Cardiac Performance in Aged Female mdx Mice. *Molecular Therapy* **19**: 1826-1832.

33. Bostick, B, Yue, YP, Lai, Y, Long, C, Li, DJ, and Duan, DS (2008). Adeno-associated virus serotype-9 microdystrophin gene therapy ameliorates electrocardiographic abnormalities in mdx mice. *Hum Gene Ther* **19**: 851-856.

34. Lorain, S, Gross, DA, Goyenvalle, A, Danos, O, Davoust, J, and Garcia, L (2008). Transient immunomodulation allows repeated injections of AAV1 and correction of muscular dystrophy in multiple muscles. *Molecular therapy : the journal of the American Society of Gene Therapy* **16**: 541-547.

35. Mingozzi, F, and High, KA (2011). Therapeutic in vivo gene transfer for genetic disease using AAV: progress and challenges. *Nature reviews Genetics* **12**: 341-355.

36. Wu, Z, Asokan, A, and Samulski, RJ (2006). Adeno-associated virus serotypes: vector toolkit for human gene therapy. *Molecular therapy : the journal of the American Society of Gene Therapy* **14**: 316-327.

37. Katwal, AB, Konkalmatt, PR, Piras, BA, Hazarika, S, Li, SS, John Lye, R, *et al.* (2013). Adeno-associated virus serotype 9 efficiently targets ischemic skeletal muscle following systemic delivery. *Gene Ther* **20**: 930-938.

38. Shen, S, Horowitz, ED, Troupes, AN, Brown, SM, Pulicherla, N, Samulski, RJ, *et al.* (2013). Engraftment of a galactose receptor footprint onto adeno-associated viral capsids improves transduction efficiency. *The Journal of biological chemistry* **288**: 28814-28823.

39. Yang, L, Li, J, and Xiao, X (2011). Directed evolution of adeno-associated virus (AAV) as vector for muscle gene therapy. *Methods in molecular biology* **709**: 127-139.

40. Smalley, E (2017). First AAV gene therapy poised for landmark approval. *Nature biotechnology* **35**: 998-999.

41. t Hoen, PA, de Meijer, EJ, Boer, JM, Vossen, RH, Turk, R, Maatman, RG, *et al.* (2008). Generation and characterization of transgenic mice with the full-length human DMD gene. *The Journal of biological chemistry* **283**: 5899-5907.

42. Ousterout, DG, Kabadi, AM, Thakore, PI, Perez-Pinera, P, Brown, MT, Majoros, WH, *et al.* (2015). Correction of dystrophin expression in cells from Duchenne muscular dystrophy patients through genomic excision of exon 51 by zinc finger nucleases. *Molecular therapy : the journal of the American Society of Gene Therapy* **23**: 523-532.

43. Long, C, Amoasii, L, Mireault, AA, McAnally, JR, Li, H, Sanchez-Ortiz, E, *et al.* (2015). Postnatal genome editing partially restores dystrophin expression in a mouse model of muscular dystrophy. *Science*.

44. Bengtsson, NE, Hall, JK, Odom, GL, Phelps, MP, Andrus, CR, Hawkins, RD, *et al.* (2017). Muscle-specific CRISPR/Cas9 dystrophin gene editing ameliorates pathophysiology in a mouse model for Duchenne muscular dystrophy. *Nature communications* **8**: 14454.

45. Tabebordbar, M, Zhu, K, Cheng, JK, Chew, WL, Widrick, JJ, Yan, WX, *et al.* (2015). In vivo gene editing in dystrophic mouse muscle and muscle stem cells. *Science*.

46. Nelson, CE, Hakim, CH, Ousterout, DG, Thakore, PI, Moreb, EA, Castellanos Rivera, RM, *et al.* (2016). In vivo genome editing improves muscle function in a mouse model of Duchenne muscular dystrophy. *Science* **351**: 403-407.

47. Iyombe-Engembe, JP, Ouellet, DL, Barbeau, X, Rousseau, J, Chapdelaine, P, Lague, P, *et al.* (2016). Efficient Restoration of the Dystrophin Gene Reading Frame and Protein Structure in DMD Myoblasts Using the CinDel Method. *Molecular therapy Nucleic acids* **5**: e283.

48. Ousterout, DG, Kabadi, AM, Thakore, PI, Majoros, WH, Reddy, TE, and Gersbach, CA (2015). Multiplex CRISPR/Cas9-based genome editing for correction of dystrophin mutations that cause Duchenne muscular dystrophy. *Nature communications* **6**: 6244.

49. Ran, FA, Cong, L, Yan, WX, Scott, DA, Gootenberg, JS, Kriz, AJ, *et al.* (2015). In vivo genome editing using Staphylococcus aureus Cas9. *Nature* **520**: 186-191.

50. Bae, S, Park, J, and Kim, JS (2014). Cas-OFFinder: a fast and versatile algorithm that searches for potential off-target sites of Cas9 RNA-guided endonucleases. *Bioinformatics* **30**: 1473-1475.

51. Robinson-Hamm, JN, and Gersbach, CA (2016). Gene therapies that restore dystrophin expression for the treatment of Duchenne muscular dystrophy. *Human genetics* **135**: 1029-1040.

52. Stark, AE (2015). Determinants of the incidence of Duchenne muscular dystrophy. *Ann Transl Med* **3**: 287.

53. Harper, SQ, Hauser, MA, DelloRusso, C, Duan, D, Crawford, RW, Phelps, SF, *et al.* (2002). Modular flexibility of dystrophin: implications for gene therapy of Duchenne muscular dystrophy. *Nature medicine* **8**: 253-261.

54. Darras, BT, Urion, DK, and Ghosh, PS (1993). Dystrophinopathies. In: Adam, MP, *et al.* (eds). *GeneReviews((R))*: Seattle (WA).

55. Cui, CH, Uyama, T, Miyado, K, Terai, M, Kyo, S, Kiyono, T, *et al.* (2007). Menstrual blood-derived cells confer human dystrophin expression in the murine model of Duchenne muscular dystrophy via cell fusion and myogenic transdifferentiation. *Mol Biol Cell* **18**: 1586-1594.

56. Zalaudek, I, Bonelli, RM, Koltringer, P, Reisecker, F, and Wagner, K (1999). Early diagnosis in Duchenne muscular dystrophy. *Lancet* **353**: 1975.

57. D'Amico, A, Catteruccia, M, Baranello, G, Politano, L, Govoni, A, Previtali, SC, *et al.* (2017). Diagnosis of Duchenne Muscular Dystrophy in Italy in the last decade: Critical issues and areas for improvements. *Neuromuscular disorders : NMD* **27**: 447-451.

58. Passamano, L, Taglia, A, Palladino, A, Viggiano, E, D'Ambrosio, P, Scutifero, M, *et al.* (2012). Improvement of survival in Duchenne Muscular Dystrophy: retrospective analysis of 835 patients. *Acta myologica : myopathies and*

cardiomyopathies : official journal of the Mediterranean Society of Myology / edited by the Gaetano Conte Academy for the study of striated muscle diseases **31**: 121-125.

59. Romitti, PA, Zhu, Y, Puzhankara, S, James, KA, Nabukera, SK, Zamba, GK, *et al.* (2015). Prevalence of Duchenne and Becker muscular dystrophies in the United States. *Pediatrics* **135**: 513-521.

60. Mendell, JR, Sahenk, Z, Malik, V, Gomez, AM, Flanigan, KM, Lowes, LP, *et al.* (2015). A phase 1/2a follistatin gene therapy trial for becker muscular dystrophy. *Molecular therapy : the journal of the American Society of Gene Therapy* **23**: 192-201.

61. England, SB, Nicholson, LVB, Johnson, MA, Forrest, SM, Love, DR, Zubrzyckagaarn, EE, *et al.* (1990). Very Mild Muscular-Dystrophy Associated with the Deletion of 46-Percent of Dystrophin. *Nature* **343**: 180-182.

62. Hermans, MC, Pinto, YM, Merkies, IS, de Die-Smulders, CE, Crijns, HJ, and Faber, CG (2010). Hereditary muscular dystrophies and the heart. *Neuromuscular disorders : NMD* **20**: 479-492.

63. Nigro, G, Comi, LI, Politano, L, and Bain, RJI (1990). The Incidence and Evolution of Cardiomyopathy in Duchenne Muscular-Dystrophy. *Int J Cardiol* **26**: 271-277.

64. Muntoni, F, Torelli, S, and Ferlini, A (2003). Dystrophin and mutations: one gene, several proteins, multiple phenotypes. *The Lancet Neurology* **2**: 731-740.

65. Tennyson, CN, Klamut, HJ, and Worton, RG (1995). The Human Dystrophin Gene Requires 16 Hours to Be Transcribed and Is Cotranscriptionally Spliced. *Nat Genet* **9**: 184-190.

66. Davie, AM, and Emery, AEH (1978). Estimation of Proportion of New Mutants among Cases of Duchenne Muscular-Dystrophy. *Journal of medical genetics* **15**: 339-345.

67. Ahn, AH, and Kunkel, LM (1993). The structural and functional diversity of dystrophin. *Nat Genet* **3**: 283-291.

68. Takeshima, Y, Yagi, M, Okizuka, Y, Awano, H, Zhang, Z, Yamauchi, Y, *et al.* (2010). Mutation spectrum of the dystrophin gene in 442 Duchenne/Becker muscular dystrophy cases from one Japanese referral center. *J Hum Genet* **55**: 379-388.

69. Blake, DJ, Weir, A, Newey, SE, and Davies, KE (2002). Function and genetics of dystrophin and dystrophin-related proteins in muscle. *Physiol Rev* **82**: 291-329.

70. Rando, TA (2001). The dystrophin-glycoprotein complex, cellular signaling, and the regulation of cell survival in the muscular dystrophies. *Muscle & nerve* **24**: 1575-1594.

71. Konieczny, P, Swiderski, K, and Chamberlain, JS (2013). Gene and cell-mediated therapies for muscular dystrophy. *Muscle & nerve* **47**: 649-663.

72. Sejerson, T, Bushby, K, and Excellence, T-NENo (2009). Standards of care for Duchenne muscular dystrophy: brief TREAT-NMD recommendations. *Adv Exp Med Biol* **652**: 13-21.

73. Viollet, L, Thrush, PT, Flanigan, KM, Mendell, JR, and Allen, HD (2012). Effects of angiotensin-converting enzyme inhibitors and/or beta blockers on the cardiomyopathy in Duchenne muscular dystrophy. *Am J Cardiol* **110**: 98-102.

74. Jefferies, JL, Eidem, BW, Belmont, JW, Craigen, WJ, Ware, SM, Fernbach, SD, *et al.* (2005). Genetic predictors and remodeling of dilated cardiomyopathy in muscular dystrophy. *Circulation* **112**: 2799-2804.

75. American Academy of Pediatrics Section on, C, and Cardiac, S (2005). Cardiovascular health supervision for individuals affected by Duchenne or Becker muscular dystrophy. *Pediatrics* **116**: 1569-1573.

76. Kinali, M, Messina, S, Mercuri, E, Lehovsky, J, Edge, G, Manzur, AY, *et al.* (2006). Management of scoliosis in Duchenne muscular dystrophy: a large 10-year retrospective study. *Developmental medicine and child neurology* **48**: 513-518.

77. Phillips, MF, Quinlivan, RC, Edwards, RH, and Calverley, PM (2001). Changes in spirometry over time as a prognostic marker in patients with Duchenne muscular dystrophy. *Am J Respir Crit Care Med* **164**: 2191-2194.

78. Eagle, M, Baudouin, SV, Chandler, C, Giddings, DR, Bullock, R, and Bushby, K (2002). Survival in Duchenne muscular dystrophy: improvements in life expectancy since 1967 and the impact of home nocturnal ventilation. *Neuromuscular disorders : NMD* **12**: 926-929.

79. Gomez-Merino, E, and Bach, JR (2002). Duchenne muscular dystrophy: prolongation of life by noninvasive ventilation and mechanically assisted coughing. *Am J Phys Med Rehabil* **81**: 411-415.

80. Bushby, K, Finkel, R, Birnkrant, DJ, Case, LE, Clemens, PR, Cripe, L, *et al.* (2010). Diagnosis and management of Duchenne muscular dystrophy, part 2: implementation of multidisciplinary care. *The Lancet Neurology* **9**: 177-189.

81. Fenichel, GM, Florence, JM, Pestronk, A, Mendell, JR, Moxley, RT, 3rd, Griggs, RC, *et al.* (1991). Long-term benefit from prednisone therapy in Duchenne muscular dystrophy. *Neurology* **41**: 1874-1877.

82. Griggs, RC, Moxley, RT, 3rd, Mendell, JR, Fenichel, GM, Brooke, MH, Pestronk, A, *et al.* (1993). Duchenne dystrophy: randomized, controlled trial of prednisone (18 months) and azathioprine (12 months). *Neurology* **43**: 520-527.

83. Mendell, JR, Moxley, RT, Griggs, RC, Brooke, MH, Fenichel, GM, Miller, JP, *et al.* (1989). Randomized, double-blind six-month trial of prednisone in Duchenne's muscular dystrophy. *The New England journal of medicine* **320**: 1592-1597.

84. Connolly, AM, Schierbecker, J, Renna, R, and Florence, J (2002). High dose weekly oral prednisone improves strength in boys with Duchenne muscular dystrophy. *Neuromuscular disorders : NMD* **12**: 917-925.

85. Bonifati, MD, Ruzza, G, Bonometto, P, Berardinelli, A, Gorni, K, Orcesi, S, *et al.* (2000). A multicenter, double-blind, randomized trial of deflazacort versus prednisone in Duchenne muscular dystrophy. *Muscle & nerve* **23**: 1344-1347.

86. Biggar, WD, Harris, VA, Eliasoph, L, and Alman, B (2006). Long-term benefits of deflazacort treatment for boys with Duchenne muscular dystrophy in their second decade. *Neuromuscular disorders : NMD* **16**: 249-255.

87. McPherron, AC, Lawler, AM, and Lee, SJ (1997). Regulation of skeletal muscle mass in mice by a new TGF-beta superfamily member. *Nature* **387**: 83-90.

88. Whittemore, LA, Song, K, Li, X, Aghajanian, J, Davies, M, Girgenrath, S, *et al.* (2003). Inhibition of myostatin in adult mice increases skeletal muscle mass and strength. *Biochem Biophys Res Commun* **300**: 965-971.

89. Ohsawa, Y, Hagiwara, H, Nakatani, M, Yasue, A, Moriyama, K, Murakami, T, *et al.* (2006). Muscular atrophy of caveolin-3-deficient mice is rescued by myostatin inhibition. *J Clin Invest* **116**: 2924-2934.

90. LeBrasseur, NK, Schelhorn, TM, Bernardo, BL, Cosgrove, PG, Loria, PM, and Brown, TA (2009). Myostatin inhibition enhances the effects of exercise on performance and metabolic outcomes in aged mice. *J Gerontol A Biol Sci Med Sci* **64**: 940-948.

91. St Andre, M, Johnson, M, Bansal, PN, Wellen, J, Robertson, A, Opsahl, A, *et al.* (2017). A mouse anti-myostatin antibody increases muscle mass and improves muscle strength and contractility in the mdx mouse model of Duchenne muscular dystrophy and its humanized equivalent, domagrozumab (PF-06252616), increases muscle volume in cynomolgus monkeys. *Skelet Muscle* **7**: 25.

92. Kirk, S, Oldham, J, Kambadur, R, Sharma, M, Dobbie, P, and Bass, J (2000). Myostatin regulation during skeletal muscle regeneration. *Journal of cellular physiology* **184**: 356-363.

93. Mendias, CL, Lynch, EB, Gumucio, JP, Flood, MD, Rittman, DS, Van Pelt, DW, *et al.* (2015). Changes in skeletal muscle and tendon structure and function following genetic inactivation of myostatin in rats. *J Physiol* **593**: 2037-2052.

94. Qiao, C, Li, J, Zheng, H, Bogan, J, Li, J, Yuan, Z, *et al.* (2009). Hydrodynamic limb vein injection of adeno-associated virus serotype 8 vector carrying canine myostatin propeptide gene into normal dogs enhances muscle growth. *Hum Gene Ther* **20**: 1-10.

95. Bish, LT, Sleeper, MM, Forbes, SC, Morine, KJ, Reynolds, C, Singletary, GE, *et al.* (2011). Long-term systemic myostatin inhibition via liver-targeted gene transfer in golden retriever muscular dystrophy. *Hum Gene Ther* **22**: 1499-1509.

96. Kambadur, R, Sharma, M, Smith, TP, and Bass, JJ (1997). Mutations in myostatin (GDF8) in double-muscled Belgian Blue and Piedmontese cattle. *Genome research* **7**: 910-916.

97. Kota, J, Handy, CR, Haidet, AM, Montgomery, CL, Eagle, A, Rodino-Klapac, LR, *et al.* (2009). Follistatin gene delivery enhances muscle growth and strength in nonhuman primates. *Sci Transl Med* **1**: 6ra15.

98. Bhattacharya, I, Pawlak, S, Marraffino, S, Christensen, J, Sherlock, SP, Alvey, C, *et al.* (2017). Safety, Tolerability, Pharmacokinetics, and Pharmacodynamics of Domagrozumab (PF-06252616), an Antimyostatin Monoclonal Antibody, in Healthy Subjects. *Clin Pharmacol Drug Dev*.

99. Dorchies, OM, Wagner, S, Vuadens, O, Waldhauser, K, Buetler, TM, Kucera, P, *et al.* (2006). Green tea extract and its major polyphenol (-)-epigallocatechin gallate improve muscle function in a mouse model for Duchenne muscular dystrophy. *Am J Physiol Cell Physiol* **290**: C616-625.

100. Evans, NP, Call, JA, Bassaganya-Riera, J, Robertson, JL, and Grange, RW (2010). Green tea extract decreases muscle pathology and NF-kappaB immunostaining in regenerating muscle fibers of mdx mice. *Clin Nutr* **29**: 391-398.

101. Acharyya, S, Villalta, SA, Bakkar, N, Bupha-Intr, T, Janssen, PM, Carathers, M, *et al.* (2007). Interplay of IKK/NF-kappaB signaling in macrophages and myofibers promotes muscle degeneration in Duchenne muscular dystrophy. *J Clin Invest* **117**: 889-901.

102. Islam, MA (2012). Cardiovascular effects of green tea catechins: progress and promise. *Recent Pat Cardiovasc Drug Discov* **7**: 88-99.

103. Xia, B, Hoyte, K, Kammesheidt, A, Deerinck, T, Ellisman, M, and Martin, PT (2002). Overexpression of the CT GalNAc transferase in skeletal muscle alters myofiber growth, neuromuscular structure, and laminin expression. *Dev Biol* **242**: 58-73.

104. Nguyen, HH, Jayasinha, V, Xia, B, Hoyte, K, and Martin, PT (2002). Overexpression of the cytotoxic T cell GalNAc transferase in skeletal muscle inhibits muscular dystrophy in mdx mice. *Proc Natl Acad Sci U S A* **99**: 5616-5621.

105. Yoon, JH, Chandrasekharan, K, Xu, R, Glass, M, Singhal, N, and Martin, PT (2009). The synaptic CT carbohydrate modulates binding and expression of extracellular matrix proteins in skeletal muscle: Partial dependence on utrophin. *Mol Cell Neurosci* **41**: 448-463.

106. Martin, PT, Xu, R, Rodino-Klapac, LR, Oglesbay, E, Camboni, M, Montgomery, CL, *et al.* (2009). Overexpression of Galgt2 in skeletal muscle prevents injury resulting from eccentric contractions in both mdx and wild-type mice. *Am J Physiol Cell Physiol* **296**: C476-488.

107. Chicoine, LG, Rodino-Klapac, LR, Shao, G, Xu, R, Bremer, WG, Camboni, M, *et al.* (2014). Vascular delivery of rAAVrh74.MCK.GALGT2 to the gastrocnemius muscle of the rhesus macaque stimulates the expression of dystrophin and laminin alpha2 surrogates. *Molecular therapy : the journal of the American Society of Gene Therapy* **22**: 713-724.

108. Hoffman, EP, Riddle, V, Siegler, MA, Dickerson, D, Backonja, M, Kramer, WG, *et al.* (2018). Phase 1 trial of vamorolone, a first-in-class steroid, shows

improvements in side effects via biomarkers bridged to clinical outcomes. *Steroids* **134**: 43-52.

109. Raman, SV, Hor, KN, Mazur, W, He, X, Kissel, JT, Smart, S, *et al.* (2017). Eplerenone for early cardiomyopathy in Duchenne muscular dystrophy: results of a two-year open-label extension trial. *Orphanet journal of rare diseases* **12**: 39.

110. Kornegay, JN, Spurney, CF, Nghiem, PP, Brinkmeyer-Langford, CL, Hoffman, EP, and Nagaraju, K (2014). Pharmacologic management of Duchenne muscular dystrophy: target identification and preclinical trials. *ILAR J* **55**: 119-149.

111. Wehling, M, Spencer, MJ, and Tidball, JG (2001). A nitric oxide synthase transgene ameliorates muscular dystrophy in mdx mice. *J Cell Biol* **155**: 123-131.

112. Shin, J, Tajrishi, MM, Ogura, Y, and Kumar, A (2013). Wasting mechanisms in muscular dystrophy. *Int J Biochem Cell Biol* **45**: 2266-2279.

113. Hammers, DW, Sleeper, MM, Forbes, SC, Coker, CC, Jirousek, MR, Zimmer, M, *et al.* (2016). Disease-modifying effects of orally bioavailable NF-kappaB inhibitors in dystrophin-deficient muscle. *JCI Insight* **1**: e90341.

114. Donovan, JM, Zimmer, M, Offman, E, Grant, T, and Jirousek, M (2017). A Novel NF-kappaB Inhibitor, Edasalonexent (CAT-1004), in Development as a Disease-Modifying Treatment for Patients With Duchenne Muscular Dystrophy: Phase 1 Safety, Pharmacokinetics, and Pharmacodynamics in Adult Subjects. *J Clin Pharmacol* **57**: 627-639.

115. Brenman, JE, Chao, DS, Xia, H, Aldape, K, and Bredt, DS (1995). Nitric oxide synthase complexed with dystrophin and absent from skeletal muscle sarcolemma in Duchenne muscular dystrophy. *Cell* **82**: 743-752.

116. Ramachandran, J, Schneider, JS, Crassous, PA, Zheng, RF, Gonzalez, JP, Xie, LH, *et al.* (2013). Nitric oxide signalling pathway in Duchenne muscular dystrophy mice: up-regulation of L-arginine transporters. *Biochem J* **449**: 133-142.

117. Tidball, JG, and Wehling-Henricks, M (2014). Nitric oxide synthase deficiency and the pathophysiology of muscular dystrophy. *J Physiol* **592**: 4627-4638.

118. Kobayashi, YM, Rader, EP, Crawford, RW, Iyengar, NK, Thedens, DR, Faulkner, JA, *et al.* (2008). Sarcolemma-localized nNOS is required to maintain activity after mild exercise. *Nature* **456**: 511-515.

119. Kobayashi, YM, Rader, EP, Crawford, RW, and Campbell, KP (2012). Endpoint measures in the mdx mouse relevant for muscular dystrophy pre-clinical studies. *Neuromuscular disorders : NMD* **22**: 34-42.

120. Nelson, MD, Rader, F, Tang, X, Tavyev, J, Nelson, SF, Miceli, MC, *et al.* (2014). PDE5 inhibition alleviates functional muscle ischemia in boys with Duchenne muscular dystrophy. *Neurology* **82**: 2085-2091.

121. Martin, EA, Barresi, R, Byrne, BJ, Tsimerinov, EI, Scott, BL, Walker, AE, *et al.* (2012). Tadalafil alleviates muscle ischemia in patients with Becker muscular dystrophy. *Sci Transl Med* **4**: 162ra155.

122. Victor, RG, Sweeney, HL, Finkel, R, McDonald, CM, Byrne, B, Eagle, M, *et al.* (2017). A phase 3 randomized placebo-controlled trial of tadalafil for Duchenne muscular dystrophy. *Neurology* **89**: 1811-1820.

123. Percival, JM, Whitehead, NP, Adams, ME, Adamo, CM, Beavo, JA, and Froehner, SC (2012). Sildenafil reduces respiratory muscle weakness and fibrosis in the mdx mouse model of Duchenne muscular dystrophy. *J Pathol* **228**: 77-87.

124. Leung, DG, Herzka, DA, Thompson, WR, He, B, Bibat, G, Tennekoon, G, *et al.* (2014). Sildenafil does not improve cardiomyopathy in Duchenne/Becker muscular dystrophy. *Annals of neurology* **76**: 541-549.

125. Colussi, C, Mozzetta, C, Gurtner, A, Illi, B, Rosati, J, Straino, S, *et al.* (2008). HDAC2 blockade by nitric oxide and histone deacetylase inhibitors reveals a common target in Duchenne muscular dystrophy treatment. *Proc Natl Acad Sci U S A* **105**: 19183-19187.

126. Consalvi, S, Mozzetta, C, Bettica, P, Germani, M, Fiorentini, F, Del Bene, F, *et al.* (2013). Preclinical studies in the mdx mouse model of duchenne muscular dystrophy with the histone deacetylase inhibitor givinostat. *Mol Med* **19**: 79-87.

127. Minetti, GC, Colussi, C, Adami, R, Serra, C, Mozzetta, C, Parente, V, *et al.* (2006). Functional and morphological recovery of dystrophic muscles in mice treated with deacetylase inhibitors. *Nature medicine* **12**: 1147-1150.

128. Bettica, P, Petrini, S, D'Oria, V, D'Amico, A, Catteruccia, M, Pane, M, *et al.* (2016). Histological effects of givinostat in boys with Duchenne muscular dystrophy. *Neuromuscular disorders : NMD* **26**: 643-649.

129. Perkins, KJ, and Davies, KE (2002). The role of utrophin in the potential therapy of Duchenne muscular dystrophy. *Neuromuscular disorders : NMD* **12 Suppl 1**: S78-89.

130. Rybakova, IN, Patel, JR, Davies, KE, Yurchenco, PD, and Ervasti, JM (2002). Utrophin binds laterally along actin filaments and can couple costameric actin with sarcolemma when overexpressed in dystrophin-deficient muscle. *Mol Biol Cell* **13**: 1512-1521.

131. Cerletti, M, Negri, T, Cozzi, F, Colpo, R, Andreetta, F, Croci, D, *et al.* (2003). Dystrophic phenotype of canine X-linked muscular dystrophy is mitigated by adenovirus-mediated utrophin gene transfer. *Gene Ther* **10**: 750-757.

132. Ricotti, V, Ridout, DA, Scott, E, Quinlivan, R, Robb, SA, Manzur, AY, *et al.* (2013). Long-term benefits and adverse effects of intermittent versus daily glucocorticoids in boys with Duchenne muscular dystrophy. *Journal of neurology, neurosurgery, and psychiatry* **84**: 698-705.

133. Fairclough, RJ, Wood, MJ, and Davies, KE (2013). Therapy for Duchenne muscular dystrophy: renewed optimism from genetic approaches. *Nature reviews Genetics* **14**: 373-378.

134. Woodman, KG, Coles, CA, Lamande, SR, and White, JD (2016). Nutraceuticals and Their Potential to Treat Duchenne Muscular Dystrophy: Separating the Credible from the Conjecture. *Nutrients* **8**.

135. Palmieri, B, and Tremblay, JP (2010). Myoblast transplantation: a possible surgical treatment for a severe pediatric disease. *Surg Today* **40**: 902-908.

136. Roy, R, Tremblay, JP, Huard, J, Richards, C, Malouin, F, and Bouchard, JP (1993). Antibody formation after myoblast transplantation in Duchenne-dystrophic patients, donor HLA compatible. *Transplant Proc* **25**: 995-997.

137. Miller, RG, Sharma, KR, Pavlath, GK, Gussoni, E, Mynhier, M, Lanctot, AM, *et al.* (1997). Myoblast implantation in Duchenne muscular dystrophy: the San Francisco study. *Muscle & nerve* **20**: 469-478.

138. Skuk, D, Goulet, M, Roy, B, Chapdelaine, P, Bouchard, JP, Roy, R, *et al.* (2006). Dystrophin expression in muscles of duchenne muscular dystrophy patients after high-density injections of normal myogenic cells. *J Neuropathol Exp Neurol* **65**: 371-386.

139. Emery, AEH, Muntoni, F, and Quinlivan, R (2015). *Duchenne muscular dystrophy*, Oxford University Press, Oxford.

140. Jirka, S, and Aartsma-Rus, A (2015). An update on RNA-targeting therapies for neuromuscular disorders. *Current opinion in neurology* **28**: 515-521.

141. Aartsma-Rus, A, Fokkema, I, Verschuuren, J, Ginjaar, I, van Deutekom, J, van Ommen, GJ, *et al.* (2009). Theoretic applicability of antisense-mediated exon skipping for Duchenne muscular dystrophy mutations. *Human mutation* **30**: 293-299.

142. Mendell, JR, Rodino-Klapac, LR, Sahenk, Z, Roush, K, Bird, L, Lowes, LP, *et al.* (2013). Eteplirsen for the treatment of Duchenne muscular dystrophy. *Annals of neurology* **74**: 637-647.

143. Kole, R, and Krieg, AM (2015). Exon skipping therapy for Duchenne muscular dystrophy. *Advanced drug delivery reviews* **87**: 104-107.

144. Aartsma-Rus, A, Ferlini, A, Goemans, N, Pasmooij, AM, Wells, DJ, Bushby, K, *et al.* (2014). Translational and regulatory challenges for exon skipping therapies. *Hum Gene Ther* **25**: 885-892.

145. McDonald, C, Henricson, E, Abresch, R, Han, J, Nicorici, A, Goude, E, *et al.* (2010). The 6-Minute Walk Test in Duchenne Muscular Dystrophy: Longitudinal Observations. *Neurology* **74**: A219-A219.

146. Crapo, RO, Casaburi, R, Coates, AL, Enright, PL, MacIntyre, NR, McKay, RT, *et al.* (2002). ATS statement: Guidelines for the six-minute walk test. *Am J Resp Crit Care* **166**: 111-117.

147. Vill, K, Ille, L, Schroeder, SA, Blaschek, A, and Muller-Felber, W (2015). Six-minute walk test versus two-minute walk test in children with Duchenne muscular dystrophy: Is more time more information? *Eur J Paediatr Neuro* **19**: 640-646.

148. Mayhew, AG, Cano, SJ, Scott, E, Eagle, M, Bushby, K, Manzur, A, *et al.* (2013). Detecting meaningful change using the North Star Ambulatory Assessment in Duchenne muscular dystrophy. *Developmental medicine and child neurology* **55**: 1046-1052.

149. FDA, US (2016). FDA grants accelerated approval to first drug for Duchenne muscular dystrophy. https://www.fda.gov/NewsEvents/Newsroom/PressAnnouncements/ucm521263.htm.

150. Woodcock, J (2016). Accelerated Approval for NDA 206488. In: Sarepta Therapeutics, I (ed). U.S. FDA: https://www.accessdata.fda.gov/drugsatfda_docs/appletter/2016/206488Orig1s000ltr.pdf. p 11.

151. Carver, MP, Charleston, JS, Shanks, C, Zhang, J, Mense, M, Sharma, AK, *et al.* (2016). Toxicological Characterization of Exon Skipping Phosphorodiamidate Morpholino Oligomers (PMOs) in Non-human Primates. *J Neuromuscul Dis* **3**: 381-393.

152. Nakamura, A (2017). Moving towards successful exon-skipping therapy for Duchenne muscular dystrophy. *J Hum Genet* **62**: 871-876.

153. Goyenvalle, A, Griffith, G, Babbs, A, El Andaloussi, S, Ezzat, K, Avril, A, *et al.* (2015). Functional correction in mouse models of muscular dystrophy using exon-skipping tricyclo-DNA oligomers. *Nature medicine* **21**: 270-275.

154. Wu, B, Moulton, HM, Iversen, PL, Jiang, J, Li, J, Li, J, *et al.* (2008). Effective rescue of dystrophin improves cardiac function in dystrophin-deficient mice by a modified morpholino oligomer. *Proc Natl Acad Sci U S A* **105**: 14814-14819.

155. Goyenvalle, A, Babbs, A, Wright, J, Wilkins, V, Powell, D, Garcia, L, *et al.* (2012). Rescue of severely affected dystrophin/utrophin-deficient mice through scAAV-U7snRNA-mediated exon skipping. *Hum Mol Genet* **21**: 2559-2571.

156. Goyenvalle, A, Vulin, A, Fougerousse, F, Leturcq, F, Kaplan, JC, Garcia, L, *et al.* (2004). Rescue of dystrophic muscle through U7 snRNA-mediated exon skipping. *Science* **306**: 1796-1799.

157. Bish, LT, Sleeper, MM, Forbes, SC, Wang, B, Reynolds, C, Singletary, GE, *et al.* (2012). Long-term restoration of cardiac dystrophin expression in golden retriever muscular dystrophy following rAAV6-mediated exon skipping. *Molecular therapy : the journal of the American Society of Gene Therapy* **20**: 580-589.

158. Le Guiner, C, Montus, M, Servais, L, Cherel, Y, Francois, V, Thibaud, JL, *et al.* (2014). Forelimb treatment in a large cohort of dystrophic dogs supports delivery of a recombinant AAV for exon skipping in Duchenne patients. *Molecular therapy : the journal of the American Society of Gene Therapy* **22**: 1923-1935.

159. Vulin, A, Barthelemy, I, Goyenvalle, A, Thibaud, JL, Beley, C, Griffith, G, *et al.* (2012). Muscle function recovery in golden retriever muscular dystrophy after AAV1-U7 exon skipping. *Molecular therapy : the journal of the American Society of Gene Therapy* **20**: 2120-2133.

160. Mendell, JR, Buzin, CH, Feng, J, Yan, J, Serrano, C, Sangani, DS, *et al.* (2001). Diagnosis of Duchenne dystrophy by enhanced detection of small mutations. *Neurology* **57**: 645-650.

161. Flanigan, KM, von Niederhausern, A, Dunn, DM, Alder, J, Mendell, JR, and Weiss, RB (2003). Rapid direct sequence analysis of the dystrophin gene. *Am J Hum Genet* **72**: 931-939.

162. Barton-Davis, ER, Cordier, L, Shoturma, DI, Leland, SE, and Sweeney, HL (1999). Aminoglycoside antibiotics restore dystrophin function to skeletal muscles of mdx mice. *J Clin Invest* **104**: 375-381.

163. Politano, L, Nigro, G, Nigro, V, Piluso, G, Papparella, S, Paciello, O, *et al.* (2003). Gentamicin administration in Duchenne patients with premature stop codon. Preliminary results. *Acta myologica : myopathies and cardiomyopathies : official journal of the Mediterranean Society of Myology / edited by the Gaetano Conte Academy for the study of striated muscle diseases* **22**: 15-21.

164. Wagner, KR, Hamed, S, Hadley, DW, Gropman, AL, Burstein, AH, Escolar, DM, *et al.* (2001). Gentamicin treatment of Duchenne and Becker muscular dystrophy due to nonsense mutations. *Annals of neurology* **49**: 706-711.

165. Malik, V, Rodino-Klapac, LR, Viollet, L, Wall, C, King, W, Al-Dahhak, R, *et al.* (2010). Gentamicin-induced readthrough of stop codons in Duchenne muscular dystrophy. *Annals of neurology* **67**: 771-780.

166. Shimizu-Motohashi, Y, Miyatake, S, Komaki, H, Takeda, S, and Aoki, Y (2016). Recent advances in innovative therapeutic approaches for Duchenne muscular dystrophy: from discovery to clinical trials. *Am J Transl Res* **8**: 2471-2489.

167. Welch, EM, Barton, ER, Zhuo, J, Tomizawa, Y, Friesen, WJ, Trifillis, P, *et al.* (2007). PTC124 targets genetic disorders caused by nonsense mutations. *Nature* **447**: 87-91.

168. Finkel, RS, Flanigan, KM, Wong, B, Bonnemann, C, Sampson, J, Sweeney, HL, *et al.* (2013). Phase 2a study of ataluren-mediated dystrophin production in patients with nonsense mutation Duchenne muscular dystrophy. *PloS one* **8**: e81302.

169. Bushby, K, Finkel, R, Wong, B, Barohn, R, Campbell, C, Comi, GP, *et al.* (2014). Ataluren treatment of patients with nonsense mutation dystrophinopathy. *Muscle & nerve* **50**: 477-487.

170. McDonald, CM, Campbell, C, Torricelli, RE, Finkel, RS, Flanigan, KM, Goemans, N, *et al.* (2017). Ataluren in patients with nonsense mutation Duchenne muscular dystrophy (ACT DMD): a multicentre, randomised, double-blind, placebo-controlled, phase 3 trial. *Lancet* **390**: 1489-1498.

171. Kayali, R, Ku, JM, Khitrov, G, Jung, ME, Prikhodko, O, and Bertoni, C (2012). Read-through compound 13 restores dystrophin expression and improves muscle function in the mdx mouse model for Duchenne muscular dystrophy. *Hum Mol Genet* **21**: 4007-4020.

172. Zhang, G, Ludtke, JJ, Thioudellet, C, Kleinpeter, P, Antoniou, M, Herweijer, H, *et al.* (2004). Intraarterial delivery of naked plasmid DNA expressing full-length mouse dystrophin in the mdx mouse model of duchenne muscular dystrophy. *Hum Gene Ther* **15**: 770-782.

173. Lostal, W, Kodippili, K, Yue, Y, and Duan, D (2014). Full-length dystrophin reconstitution with adeno-associated viral vectors. *Hum Gene Ther* **25**: 552-562.

174. Wang, Z, Zhu, T, Qiao, C, Zhou, L, Wang, B, Zhang, J, *et al.* (2005). Adeno-associated virus serotype 8 efficiently delivers genes to muscle and heart. *Nature biotechnology* **23**: 321-328.

175. Penaud-Budloo, M, Le Guiner, C, Nowrouzi, A, Toromanoff, A, Cherel, Y, Chenuaud, P, *et al.* (2008). Adeno-associated virus vector genomes persist as episomal chromatin in primate muscle. *Journal of virology* **82**: 7875-7885.

176. Ehrhardt, A, Engler, JA, Xu, H, Cherry, AM, and Kay, MA (2006). Molecular analysis of chromosomal rearrangements in mammalian cells after phiC31-mediated integration. *Hum Gene Ther* **17**: 1077-1094.

177. Wang, B, Li, J, Fu, FH, and Xiao, X (2009). Systemic Human Minidystrophin Gene Transfer Improves Functions and Life Span of Dystrophin and Dystrophin/Utrophin-Deficient Mice. *J Orthop Res* **27**: 421-426.

178. Yue, Y, Li, Z, Harper, SQ, Davisson, RL, Chamberlain, JS, and Duan, D (2003). Microdystrophin gene therapy of cardiomyopathy restores dystrophin-glycoprotein complex and improves sarcolemma integrity in the mdx mouse heart. *Circulation* **108**: 1626-1632.

179. Schinkel, S, Bauer, R, Bekeredjian, R, Stucka, R, Rutschow, D, Lochmuller, H, *et al.* (2012). Long-term preservation of cardiac structure and function after adeno-associated virus serotype 9-mediated microdystrophin gene transfer in mdx mice. *Hum Gene Ther* **23**: 566-575.

180. Mendell, JR, Campbell, K, Rodino-Klapac, L, Sahenk, Z, Shilling, C, Lewis, S, *et al.* (2010). Dystrophin immunity in Duchenne's muscular dystrophy. *The New England journal of medicine* **363**: 1429-1437.

181. Mingozzi, F, and High, KA (2013). Immune responses to AAV vectors: overcoming barriers to successful gene therapy. *Blood* **122**: 23-36.

182. Collins, FS, and McKusick, VA (2001). Implications of the Human Genome Project for medical science. *Jama* **285**: 540-544.

183. Cox, DB, Platt, RJ, and Zhang, F (2015). Therapeutic genome editing: prospects and challenges. *Nature medicine* **21**: 121-131.

184. Doudna, JA (2015). Genomic engineering and the future of medicine. *Jama* **313**: 791-792.

185. High, K, Gregory, PD, and Gersbach, C (2014). CRISPR technology for gene therapy. *Nature medicine* **20**: 476-477.

186. Perez-Pinera, P, Ousterout, DG, and Gersbach, CA (2012). Advances in targeted genome editing. *Current opinion in chemical biology* **16**: 268-277.

187. Prakash, V, Moore, M, and Yanez-Munoz, RJ (2016). Current Progress in Therapeutic Gene Editing for Monogenic Diseases. *Molecular therapy : the journal of the American Society of Gene Therapy*.

188. Carroll, D (2008). Progress and prospects: Zinc-finger nucleases as gene therapy agents. *Gene Ther* **15**: 1463-1468.

189. Gersbach, CA, Gaj, T, and Barbas, CF, 3rd (2014). Synthetic zinc finger proteins: the advent of targeted gene regulation and genome modification technologies. *Accounts of chemical research* **47**: 2309-2318.

190. Gaj, T, Gersbach, CA, and Barbas, CF, 3rd (2013). ZFN, TALEN, and CRISPR/Cas-based methods for genome engineering. *Trends in biotechnology* **31**: 397-405.

191. Joung, JK, and Sander, JD (2013). TALENs: a widely applicable technology for targeted genome editing. *Nature reviews Molecular cell biology* **14**: 49-55.

192. Miller, JC, Tan, S, Qiao, G, Barlow, KA, Wang, J, Xia, DF, *et al.* (2011). A TALE nuclease architecture for efficient genome editing. *Nature biotechnology* **29**: 143-148.

193. Arnould, S, Delenda, C, Grizot, S, Desseaux, C, Paques, F, Silva, GH, *et al.* (2011). The I-CreI meganuclease and its engineered derivatives: applications from cell modification to gene therapy. *Protein engineering, design & selection : PEDS* **24**: 27-31.

194. Silva, G, Poirot, L, Galetto, R, Smith, J, Montoya, G, Duchateau, P, *et al.* (2011). Meganucleases and other tools for targeted genome engineering: perspectives and challenges for gene therapy. *Current gene therapy* **11**: 11-27.

195. Cho, SW, Kim, S, Kim, JM, and Kim, JS (2013). Targeted genome engineering in human cells with the Cas9 RNA-guided endonuclease. *Nature biotechnology* **31**: 230-232.

196. Esvelt, KM, Mali, P, Braff, JL, Moosburner, M, Yaung, SJ, and Church, GM (2013). Orthogonal Cas9 proteins for RNA-guided gene regulation and editing. *Nature methods* **10**: 1116-1121.

197. Li, H, Haurigot, V, Doyon, Y, Li, T, Wong, SY, Bhagwat, AS, *et al.* (2011). In vivo genome editing restores haemostasis in a mouse model of haemophilia. *Nature* **475**: 217-221.

198. Urnov, FD, Rebar, EJ, Holmes, MC, Zhang, HS, and Gregory, PD (2010). Genome editing with engineered zinc finger nucleases. *Nature reviews Genetics* **11**: 636-646.

199. Sebastiano, V, Maeder, ML, Angstman, JF, Haddad, B, Khayter, C, Yeo, DT, *et al.* (2011). In situ genetic correction of the sickle cell anemia mutation in human induced pluripotent stem cells using engineered zinc finger nucleases. *Stem cells* **29**: 1717-1726.

200. Zou, J, Mali, P, Huang, X, Dowey, SN, and Cheng, L (2011). Site-specific gene correction of a point mutation in human iPS cells derived from an adult patient with sickle cell disease. *Blood* **118**: 4599-4608.

201. Barrangou, R, Fremaux, C, Deveau, H, Richards, M, Boyaval, P, Moineau, S, *et al.* (2007). CRISPR provides acquired resistance against viruses in prokaryotes. *Science* **315**: 1709-1712.

202. Bolotin, A, Quinquis, B, Sorokin, A, and Ehrlich, SD (2005). Clustered regularly interspaced short palindrome repeats (CRISPRs) have spacers of extrachromosomal origin. *Microbiology* **151**: 2551-2561.

203. Makarova, KS, Grishin, NV, Shabalina, SA, Wolf, YI, and Koonin, EV (2006). A putative RNA-interference-based immune system in prokaryotes: computational analysis of the predicted enzymatic machinery, functional analogies with eukaryotic RNAi, and hypothetical mechanisms of action. *Biol Direct* **1**: 7.

204. Mojica, FJ, Diez-Villasenor, C, Garcia-Martinez, J, and Soria, E (2005). Intervening sequences of regularly spaced prokaryotic repeats derive from foreign genetic elements. *J Mol Evol* **60**: 174-182.

205. Mojica, FJ, Diez-Villasenor, C, Soria, E, and Juez, G (2000). Biological significance of a family of regularly spaced repeats in the genomes of Archaea, Bacteria and mitochondria. *Mol Microbiol* **36**: 244-246.

206. Jansen, R, Embden, JD, Gaastra, W, and Schouls, LM (2002). Identification of genes that are associated with DNA repeats in prokaryotes. *Mol Microbiol* **43**: 1565-1575.

207. Pourcel, C, Salvignol, G, and Vergnaud, G (2005). CRISPR elements in Yersinia pestis acquire new repeats by preferential uptake of bacteriophage DNA, and provide additional tools for evolutionary studies. *Microbiology* **151**: 653-663.

208. Brouns, SJ, Jore, MM, Lundgren, M, Westra, ER, Slijkhuis, RJ, Snijders, AP, *et al.* (2008). Small CRISPR RNAs guide antiviral defense in prokaryotes. *Science* **321**: 960-964.

209. Deveau, H, Barrangou, R, Garneau, JE, Labonte, J, Fremaux, C, Boyaval, P, *et al.* (2008). Phage response to CRISPR-encoded resistance in Streptococcus thermophilus. *J Bacteriol* **190**: 1390-1400.

210. Sapranauskas, R, Gasiunas, G, Fremaux, C, Barrangou, R, Horvath, P, and Siksnys, V (2011). The Streptococcus thermophilus CRISPR/Cas system provides immunity in Escherichia coli. *Nucleic acids research* **39**: 9275-9282.

211. Jinek, M, Chylinski, K, Fonfara, I, Hauer, M, Doudna, JA, and Charpentier, E (2012). A programmable dual-RNA-guided DNA endonuclease in adaptive bacterial immunity. *Science* **337**: 816-821.

212. Gasiunas, G, Barrangou, R, Horvath, P, and Siksnys, V (2012). Cas9-crRNA ribonucleoprotein complex mediates specific DNA cleavage for adaptive immunity in bacteria. *Proc Natl Acad Sci U S A* **109**: E2579-2586.

213. Jinek, M, East, A, Cheng, A, Lin, S, Ma, EB, and Doudna, J (2013). RNA-programmed genome editing in human cells. *Elife* **2**.

214. Mali, P, Yang, LH, Esvelt, KM, Aach, J, Guell, M, DiCarlo, JE, *et al.* (2013). RNA-Guided Human Genome Engineering via Cas9. *Science* **339**: 823-826.

215. Adli, M (2018). The CRISPR tool kit for genome editing and beyond. *Nature communications* **9**: 1911.

216. Chapdelaine, P, Pichavant, C, Rousseau, J, Paques, F, and Tremblay, JP (2010). Meganucleases can restore the reading frame of a mutated dystrophin. *Gene Ther* **17**: 846-858.

217. Long, C, McAnally, JR, Shelton, JM, Mireault, AA, Bassel-Duby, R, and Olson, EN (2014). Prevention of muscular dystrophy in mice by CRISPR/Cas9-mediated editing of germline DNA. *Science* **345**: 1184-1188.

218. Nelson, CE, Hakim, CH, Ousterout, DG, Thakore, PI, Moreb, EA, Rivera, RM, *et al.* (2015). In vivo genome editing improves muscle function in a mouse model of Duchenne muscular dystrophy. *Science*.

219. Tabebordbar, M, Zhu, K, Cheng, JKW, Chew, WL, Widrick, JJ, Yan, WX, *et al.* (2016). In vivo gene editing in dystrophic mouse muscle and muscle stem cells. *Science* **351**: 407-411.

220. Xu, L, Park, KH, Zhao, L, Xu, J, El Refaey, M, Gao, Y, *et al.* (2015). CRISPR-mediated genome editing restores dystrophin expression and function in mdx mice. *Molecular therapy : the journal of the American Society of Gene Therapy*.

221. Ousterout, DG, Perez-Pinera, P, Thakore, PI, Kabadi, AM, Brown, MT, Qin, X, *et al.* (2013). Reading frame correction by targeted genome editing restores dystrophin expression in cells from Duchenne muscular dystrophy patients. *Molecular therapy : the journal of the American Society of Gene Therapy* **21**: 1718-1726.

222. Young, CS, Hicks, MR, Ermolova, NV, Nakano, H, Jan, M, Younesi, S, *et al.* (2016). A Single CRISPR-Cas9 Deletion Strategy that Targets the Majority of DMD Patients Restores Dystrophin Function in hiPSC-Derived Muscle Cells. *Cell Stem Cell* **18**: 533-540.

223. Young, CS, Mokhonova, E, Quinonez, M, Pyle, AD, and Spencer, MJ (2017). Creation of a Novel Humanized Dystrophic Mouse Model of Duchenne Muscular Dystrophy and Application of a CRISPR/Cas9 Gene Editing Therapy. *J Neuromuscul Dis* **4**: 139-145.

224. Long, C, Li, H, Tiburcy, M, Rodriguez-Caycedo, C, Kyrychenko, V, Zhou, H, *et al.* (2018). Correction of diverse muscular dystrophy mutations in human engineered heart muscle by single-site genome editing. *Sci Adv* **4**: eaap9004.

225. Helderman-van den Enden, AT, Straathof, CS, Aartsma-Rus, A, den Dunnen, JT, Verbist, BM, Bakker, E, *et al.* (2010). Becker muscular dystrophy patients with deletions around exon 51; a promising outlook for exon skipping therapy in Duchenne patients. *Neuromuscular disorders : NMD* **20**: 251-254.

226. Aoki, Y, Yokota, T, Nagata, T, Nakamura, A, Tanihata, J, Saito, T, *et al.* (2012). Bodywide skipping of exons 45-55 in dystrophic mdx52 mice by systemic antisense delivery. *Proc Natl Acad Sci U S A* **109**: 13763-13768.

227. Flanigan, KM, Dunn, DM, von Niederhausern, A, Soltanzadeh, P, Gappmaier, E, Howard, MT, *et al.* (2009). Mutational spectrum of DMD mutations in dystrophinopathy patients: application of modern diagnostic techniques to a large cohort. *Human mutation* **30**: 1657-1666.

228. Popplewell, L, Koo, T, Leclerc, X, Duclert, A, Mamchaoui, K, Gouble, A, *et al.* (2013). Gene correction of a duchenne muscular dystrophy mutation by meganuclease-enhanced exon knock-in. *Hum Gene Ther* **24**: 692-701.

229. Muntoni, F, and Wells, D (2007). Genetic treatments in muscular dystrophies. *Current opinion in neurology* **20**: 590-594.

230. Veltrop, M, van Vliet, L, Hulsker, M, Claassens, J, Brouwers, C, Breukel, C, *et al.* (2018). A dystrophic Duchenne mouse model for testing human antisense oligonucleotides. *PloS one* **13**: e0193289.

231. Shrock, E, and Guell, M (2017). CRISPR in Animals and Animal Models. *Prog Mol Biol Transl Sci* **152**: 95-114.

232. Emes, RD, Goodstadt, L, Winter, EE, and Ponting, CP (2003). Comparison of the genomes of human and mouse lays the foundation of genome zoology. *Hum Mol Genet* **12**: 701-709.

233. Rhesus Macaque Genome, S, Analysis, C, Gibbs, RA, Rogers, J, Katze, MG, Bumgarner, R, *et al.* (2007). Evolutionary and biomedical insights from the rhesus macaque genome. *Science* **316**: 222-234.

234. Hsu, PD, Scott, DA, Weinstein, JA, Ran, FA, Konermann, S, Agarwala, V, *et al.* (2013). DNA targeting specificity of RNA-guided Cas9 nucleases. *Nature biotechnology* **31**: 827-832.

235. Guschin, DY, Waite, AJ, Katibah, GE, Miller, JC, Holmes, MC, and Rebar, EJ (2010). A rapid and general assay for monitoring endogenous gene modification. *Methods in molecular biology* **649**: 247-256.

236. Lefaucheur, JP, Pastoret, C, and Sebille, A (1995). Phenotype of dystrophinopathy in old mdx mice. *Anat Rec* **242**: 70-76.

237. Aartsma-Rus, A, and van Putten, M (2014). Assessing functional performance in the mdx mouse model. *J Vis Exp*.

238. Dow, LE (2015). Modeling Disease In Vivo With CRISPR/Cas9. *Trends Mol Med* **21**: 609-621.

239. Grieger, JC, and Samulski, RJ (2005). Packaging capacity of adeno-associated virus serotypes: impact of larger genomes on infectivity and postentry steps. *Journal of virology* **79**: 9933-9944.

240. Friedland, AE, Baral, R, Singhal, P, Loveluck, K, Shen, S, Sanchez, M, *et al.* (2015). Characterization of Staphylococcus aureus Cas9: a smaller Cas9 for all-in-one adeno-associated virus delivery and paired nickase applications. *Genome biology* **16**: 257.

241. Pinello, L, Canver, MC, Hoban, MD, Orkin, SH, Kohn, DB, Bauer, DE, *et al.* (2016). Analyzing CRISPR genome-editing experiments with CRISPResso. *Nature biotechnology* **34**: 695-697.

242. Thorley, M, Duguez, S, Mazza, EMC, Valsoni, S, Bigot, A, Mamchaoui, K, *et al.* (2016). Skeletal muscle characteristics are preserved in hTERT/cdk4 human myogenic cell lines. *Skelet Muscle* **6**: 43.

243. Kim, D, Bae, S, Park, J, Kim, E, Kim, S, Yu, HR, *et al.* (2015). Digenome-seq: genome-wide profiling of CRISPR-Cas9 off-target effects in human cells. *Nature methods* **12**: 237-243, 231 p following 243.

244. Tsai, SQ, Nguyen, NT, Malagon-Lopez, J, Topkar, VV, Aryee, MJ, and Joung, JK (2017). CIRCLE-seq: a highly sensitive in vitro screen for genome-wide CRISPR-Cas9 nuclease off-targets. *Nature methods* **14**: 607-614.

245. Hu, J, Meyers, RM, Dong, J, Panchakshari, RA, Alt, FW, and Frock, RL (2016). Detecting DNA double-stranded breaks in mammalian genomes by linear amplification-mediated high-throughput genome-wide translocation sequencing. *Nat Protoc* **11**: 853-871.

246. Godfrey, C, Muses, S, McClorey, G, Wells, KE, Coursindel, T, Terry, RL, *et al.* (2015). How much dystrophin is enough: the physiological consequences of different levels of dystrophin in the mdx mouse. *Hum Mol Genet* **24**: 4225-4237.

247. Mohr, SE, Hu, Y, Ewen-Campen, B, Housden, BE, Viswanatha, R, and Perrimon, N (2016). CRISPR guide RNA design for research applications. *FEBS J* **283**: 3232-3238.

248. Gaudelli, NM, Komor, AC, Rees, HA, Packer, MS, Badran, AH, Bryson, DI, *et al.* (2017). Programmable base editing of A*T to G*C in genomic DNA without DNA cleavage. *Nature* **551**: 464-471.

249. Komor, AC, Kim, YB, Packer, MS, Zuris, JA, and Liu, DR (2016). Programmable editing of a target base in genomic DNA without double-stranded DNA cleavage. *Nature* **533**: 420-424.

250. Suzuki, K, Tsunekawa, Y, Hernandez-Benitez, R, Wu, J, Zhu, J, Kim, EJ, *et al.* (2016). In vivo genome editing via CRISPR/Cas9 mediated homology-independent targeted integration. *Nature* **540**: 144-149.

251. Deyle, DR, and Russell, DW (2009). Adeno-associated virus vector integration. *Curr Opin Mol Ther* **11**: 442-447.

252. Deconinck, AE, Rafael, JA, Skinner, JA, Brown, SC, Potter, AC, Metzinger, L, *et al.* (1997). Utrophin-dystrophin-deficient mice as a model for Duchenne muscular dystrophy. *Cell* **90**: 717-727.

253. Lee, CM, Cradick, TJ, and Bao, G (2016). The Neisseria meningitidis CRISPR-Cas9 System Enables Specific Genome Editing in Mammalian Cells. *Molecular therapy : the journal of the American Society of Gene Therapy* **24**: 645-654.

254. Hirano, H, Gootenberg, JS, Horii, T, Abudayyeh, OO, Kimura, M, Hsu, PD, *et al.* (2016). Structure and Engineering of Francisella novicida Cas9. *Cell* **164**: 950-961.

255. Kim, E, Koo, T, Park, SW, Kim, D, Kim, K, Cho, HY, *et al.* (2017). In vivo genome editing with a small Cas9 orthologue derived from Campylobacter jejuni. *Nature communications* **8**: 14500.

256. Yamada, M, Watanabe, Y, Gootenberg, JS, Hirano, H, Ran, FA, Nakane, T, *et al.* (2017). Crystal Structure of the Minimal Cas9 from Campylobacter jejuni Reveals the Molecular Diversity in the CRISPR-Cas9 Systems. *Molecular cell* **65**: 1109-1121 e1103.

257. Burstein, D, Harrington, LB, Strutt, SC, Probst, AJ, Anantharaman, K, Thomas, BC, *et al.* (2017). New CRISPR-Cas systems from uncultivated microbes. *Nature* **542**: 237-241.

258. Zetsche, B, Gootenberg, JS, Abudayyeh, OO, Slaymaker, IM, Makarova, KS, Essletzbichler, P, *et al.* (2015). Cpf1 Is a Single RNA-Guided Endonuclease of a Class 2 CRISPR-Cas System. *Cell* **163**: 759-771.

259. Shmakov, S, Abudayyeh, OO, Makarova, KS, Wolf, YI, Gootenberg, JS, Semenova, E, *et al.* (2015). Discovery and Functional Characterization of Diverse Class 2 CRISPR-Cas Systems. *Molecular cell* **60**: 385-397.

260. Murovec, J, Pirc, Z, and Yang, B (2017). New variants of CRISPR RNA-guided genome editing enzymes. *Plant Biotechnol J* **15**: 917-926.

261. Abudayyeh, OO, Gootenberg, JS, Konermann, S, Joung, J, Slaymaker, IM, Cox, DB, *et al.* (2016). C2c2 is a single-component programmable RNA-guided RNA-targeting CRISPR effector. *Science* **353**: aaf5573.

262. Mortensen, R, Nissen, TN, Blauenfeldt, T, Christensen, JP, Andersen, P, and Dietrich, J (2015). Adaptive Immunity against Streptococcus pyogenes in Adults Involves Increased IFN-gamma and IgG3 Responses Compared with Children. *J Immunol* **195**: 1657-1664.

263. Colque-Navarro, P, Jacobsson, G, Andersson, R, Flock, JI, and Mollby, R (2010). Levels of antibody against 11 Staphylococcus aureus antigens in a healthy population. *Clin Vaccine Immunol* **17**: 1117-1123.

Biography

Jacqueline Robinson-Hamm was born in Federal Way, WA on 18 July 1991. She attended the University of Washington and received her Bachelor of Science in Bioengineering with Honors in June 2013. She later attended Duke University where she earned her Master of Science in Biomedical Engineering in December of 2017.

She has been supported by the National Science Foundation Graduate Research Fellows Program from August 2013 until July 2016 and the American Heart Association Mid-Atlantic Affiliate Pre-Doctoral Fellowship from January 2017 until the end of her doctoral training in July 2018. She attended the American Society of Gene and Cell Therapy annual meeting in May of 2016, 2017, and 2018, where she was awarded a travel award in 2016 and 2017 and the Excellence in Research Award in 2017.

Articles:

Robinson-Hamm JN, Nelson CN, Gemberling M, Gough V, Oliver ML, Castellanos Rivera RM, Aartsma-Rus A, Asokan A, Gersbach CA. Dystrophin restoration in a humanized mouse model of Duchenne muscular dystrophy by gene editing with S. aureus Cas9. In review.

Nelson CN, **Robinson-Hamm JN**, Gersbach, CA. Genome Engineering: A new Approach for Gene Therapy in Neuromuscular Disorders. *Nature Reviews Neurology* 2017 Nov;13(11):647-661.

Huang J, Chen M, Whitley MJ, Kuo HC, Xu ES, Walens A, Mowery YM, Van Mater D, Eward WC, Cardona DM, Luo L, Ma Y, Lopez OM, Nelson CE, **Robinson-Hamm JN**, Reddy A, Dave SS, Gersbach CA, Dodd RD, Kirsch DG. Generation and comparison of CRISPR-Cas9 and Cre-mediated genetically engineered mouse models of sarcoma. *Nat Commun* 2017 Jul 10;8:15999.

Robinson-Hamm JN, and Gersbach CA. Gene therapies that restore dystrophin expression for the treatment of Duchenne muscular dystrophy. *Hum Genet*. 2016 Sept;135(9): 1029—40.

Nowakowski SG and Kolwicz SC Jr, Korte FS, Luo C, **Robinson-Hamm J**, Brozovich FV, Weiss RS, Tian R, Murry CE, Regnier M. Transgenic overexpression of ribonucleotide reductase improves cardiac performance. *Proc. Natl. Acad. Sci. U.S.A*. 2013 Apr 9;110(15):6187-92.